Physiological Investigations into Environmental Stress Response in the Hydrothermal Vent Polychaete Paralvinella sulfincola

Professor Peter Girguis Geoffrey Dilly

Physiological Investigations into Environmental Stress Response in the Hydrothermal Vent Polychaete *Paralvinella sulfincola*

Abstract

The most universal abiotic influence is temperature, and thus, thermotolerance, adaptations and response to thermal variation, is a fundamental factor shaping evolution. Prokaryotic life may have an upper thermal limit near 150°C; however, eukaryotic survival is limited to 50°C – the thermal maximum for sustained biosynthesis and homeostasis. My research focuses on understanding the physiological and biochemical factors that limit eukaryotic thermotolerance, by studying an organism near the upper limit of all eukaryotes: *Paralvinella sulfincola*.

P. sulfincola, a hydrothermal vent polychaete, has the broadest known thermal range of any metazoan: (5-48 °C). This species, along with the mesotolerant congener with *Paralvinella palmiformis*, is found at vents along the Juan de Fuca Ridge, Washington, USA. Making an ideal study system, both species are found in similar habitats, genetically comparable, and amenable to recovery and shipboard experimentation. Here, I present data from a series of high pressure *in vivo* experiments that investigate stress response to variations in temperature, pH, sulfide concentration, and duration. Field work was coupled with a suite of biomolecular techniques including pyrosequencing, comparative proteomics, enzyme assays, and quantitative PCR.

From this research, the first to quantify global protein and antioxidant responses to temperature in an extremely thermotolerant eukaryote, three primary conclusions can be reached. 1) Pronounced thermal tolerance in *P. sulfincola* is likely enabled by its constitutive expression of heat shock proteins and limited by its ability to quickly and appropriately respond to the

commensurate increase in oxidative stress. 2) Thermal tolerance limits are likely negatively affected by synergistic multistress effects. 3) Antioxidant gene expression response differs significantly between chronically and acutely stressed treatments, supporting the theory that oxidative stress is limiting in this system.

Table of Contents **Page #**

Acknowledgements

I would like to acknowledge a large number of people who helped me along this journey both professionally and personally. Thank you to all the wonderful members of the Girguis lab who I had the pleasure and privilege to work with over the years. Additionally I'd like to thank the crews of the Atlantis and Alvin, as well as staff at the Harvard Proteomic Facility, Joint Genome Institute, and the Pacific Northwest National Labs for their collection assistance and ongoing collaborations. A huge thank you to my committee members – Gonzalo Giribet, Colleen Cavanaugh, and John Wakeley – who guided my path and kept me away from many missteps. My friends and family have been there through it all, with friendly ears and keen eyes, keeping me sane and my grammar correct – I cannot thank them enough. A special thanks to caffeine and chicken nachos – without which I probably would not have made it. Christine – you have been there for me through all the long days and nights with unending support – a thousand thank yous would not be enough, but it is a start.

Dedication

This dissertation is dedicated to my mom and dad. If it was not for your unwavering support in me and my passion for marine biology over my entire life, this would simply never have been possible. Thank you.

List of Figures

List of Tables

Figure and table numbers are numbered according to their order within a chapter. For example, the third figure in the second chapter is labeled **Figure 2.3**.

Chapter 1

Introduction

Perhaps the most ubiquitous environmental factor influencing organisms is temperature. Temperature widely influences biological functions including metabolic rates (1-3) and enzymatic structure and activity (4-5), thereby inducing significant changes in gene and protein expression (6-7). Prokaryotic life may have an upper thermal limit near 150°C (8-9), and a hyperthermophilic methanogen has already been shown to survive at 122°C (10). However, no eukaryote comes close to this temperature. Sustained metazoan thermal tolerance is predicted to be between 45 and 47°C – the upper limit for biosynthesis and homeostasis (11). Naturally, a question arises from this observation. What are the primary causes that significantly limit thermal tolerance in metazoan life? While this may seem at first to be a simplistic inquiry, it has proven to be a complex and enduring question. More than fifteen hundred papers examining organismal thermal tolerance have been published over the last sixty years. Despite this plethora of research, we have not been able to resolve what ultimately limits thermal tolerance of metazoans.

Over the past century of research, investigators have employed a variety of metrics and techniques to characterize thermal tolerance. Dominant among these are lethal dosage studies (e.g. LD_{50}, the temperature at which 50% of the population dies) and critical thermal maxima (CT_{Max} – the temperature for a given species above which most individuals exhibit physiological dysfunction including impaired locomotion, subjecting the animal to likely death) (12). Over this time we have learned a great deal about organismal tolerance ranges, enzymatic thermal limits,

and the roles of heat shock proteins (HSPs), oxidant scavengers, and ATP-regulators in mitigating the damaging effects of thermal stress (6, 13-15).

It has been difficult to determine the upper thermal limit of life (or the CT_{Max}) largely due to methodological differences (for review: (12)). Investigators have used numerous behavioral proxies to determine the CT_{Max}, such as loss of righting response (LRR) and the onset of spasms (OS), (16). The far greater heat capacity of water (~25x) presents another issue when comparing terrestrial and aquatic organisms. Moreover, behavior modification (e.g. escape) exhibited by many organisms for thermal stress avoidance complicates the identification of physiological maximums (17-18). The determination of CT_{Max} does not require the investigators to consider how the organism responds biochemically to thermal stress. Indeed, the definition of CT_{Max} does not include an assessment of physiological poise or even duration of exposure, but only the lethal maximum temperature. Thus, upon completion of the experiment (death), it is impractical to assess the biochemical response of the organism.

To understand the physiological and biochemical responses to thermal stress, an alternate approach is being more widely used – the chronic lethal maximum (CL_{Max}, first described in (19)). The CL_{Max} is defined as the temperature at which an organism can no longer withstand sustained exposure (as determined by physiological metrics such as oxygen consumption), even while acclimating slowly to increasing thermal regimes. This differs from the CT_{Max} because it includes the element of time, affording investigators the opportunity to study the underlying physiological and biochemical responses (including acclimation and adaptation) to thermal stress over time.

To date, we have surprisingly little information on the biochemical mechanisms that confer (or limit) thermal tolerance in all metazoans, including the most thermotolerant metazoans. It has been suggested that mitochondrial dysfunction and nuclear membrane instability are possible modes of failure at high temperatures (9), though unicellular eukaryotic fungi such as *Thermomyces lanuginosus* grow at 60-62°C (20-21), thus calling this hypothesis into question. It

is likely that there are additional limiting factors responsible for constraining thermal tolerance below 60°C in organisms with complex multicellular structure, e.g. structural integrity or functional organization (11). As such, it is still unclear as to which mechanisms limit metazoan thermotolerance to regimes at least 10°C lower than *T. lanuginosus*. A small number of studies have examined global changes in gene or protein expression in response to thermal stress, such as studies of intertidal eelgrass (7), killifish (22), cattle (6), and marine mussels (23). These studies have yielded interesting transcriptional patterns in these organisms during thermal exposure, such as the role of oxidant-scavenging systems. Notably, none of these organisms are exceptionally thermotolerant.

To better understand the physiological and biochemical factors that limit metazoan thermotolerance, one must conduct systems-level experiments using an organism that A) is among the most thermotolerant of metazoans, B) is amenable to laboratory experimentation and maintenance, and C) has a body of genomic or transcriptomic data that can serve as a frame of reference for detailed gene and protein expression studies. Candidates include *Cataglyphis sp.* and other desert ant species, which have been shown to have a CT_{Max} between 52-55 °C (24). However, their short-burst scavenging behavior plays heavily into their thermal tolerance. Also, as mentioned previously, in aerial systems the rate of heat transfer is much lower than in aquatic systems, making it difficult to ascertain whether the organism is in thermal equilibrium with the environment. The thermophilic aquatic ostracod *Potamocypris sp.* is another candidate, but experiments have demonstrated a 50% loss at 50°C after one hour of exposure (25). Additionally, there is no genomic or transcriptomic data available for either of these species. The ideal environment to study extreme metazoan thermal tolerance is one where extreme temperatures have strongly selected for this capacity – hydrothermal vents.

The discovery of deep-sea hydrothermal vents in 1977 redefined our notions about life on earth. These underwater hot springs discharge chemically altered seawater at temperatures up to 350°C through fissures in the earth's crust (26). Heavy metals, reduced sulfur compounds, and

even radioactive material is entrained in the vent fluid and released into the surrounding environment through cracks and chimneys. Vent fluid is anaerobic and the pH has been measured as low as 2.8 (27). There is tremendous flux with water temperatures varying from 2°C in surrounding seawater to more than 400°C from the vent chimneys over the span of inches. Arguably, the sharp and dynamic thermal and chemical gradients make deep-sea hydrothermal vents among the most physiologically challenging of environments (28).

Thus, the opportunity to study extreme thermal tolerance presents itself at these deep-sea hydrothermal vents. Two of the most thermotolerant animals known are indigenous to this habitat: polychaete worms *Alvinella pompejana* (29) on the East Pacific Rise and *Paralvinella sulfincola* (30) on the Juan de Fuca Ridge. *In situ* temperatures of the substratum directly under live worms has been recorded at 81°C for *A. pompejana* (31) and at 88.5 and 110°C for *P. sulfincola* (32-33). These data suggest that these organisms can survive brief exposure to high temperature. Subsequent laboratory studies of *P. sulfincola* have shown that it has the largest known experimentally demonstrated thermal range of any metazoan (5-48°C) with individuals surviving >15 minutes at 55°C (34-35). *P. sulfincola*, unlike *A. pompejana* (36), can be readily kept in the laboratory for weeks and is amenable to recovery and experimentation. Previous *in vitro* studies of *A. pompejana* enzymes and transport proteins suggested that key proteins are not thermally stable in vitro (37); similar studies of *P. sulfincola* have examined the effect of elevated temperature on sulfide toxicity and respiratory pathways (38-39). However, to date, no broad-scale thermal response studies have been completed on either of these extremely thermotolerant metazoans.

Furthermore, hydrothermal vents provide an opportunity to examine multi-stressor effects. Multiple stressor experiments are becoming increasing relevant because of the effects that climate change will have on marine organismal physiology. Not only will animals need to respond to increasing temperature, they will experience ocean acidification – decreasing pH as CO_2 input increases (40-41). Because *P. sulfincola* face a number of concurrent physiological

challenges at vents (i.e. low pH, high sulfide, high temperature, etc.), they must cope with multiple stress factors simultaneously. This allows us to investigate if individual effects of each factor work synergistically to cause emergent stresses (e.g. lowering the pH alters the dominant species of sulfide from HS^- in ambient seawater to the more permeable H_2S). *Paralvinella sulfincola* must therefore sustain thermal tolerance, intracellular pH via acid-base regulation, and sulfide detoxification pathways to maintain or regain homeostasis during periods of multi-stress.

The habitat that *Paralvinella sulfincola* lives in, Juan de Fuca Ridge off the coast of Washington state, also hosts a mesotolerant congener, *Paralvinella palmiformis.* This polychaete, with an upper thermal limit of approximately 40°C (34), is also abundant and readily amenable to *in vivo* shipboard experimentation. Its genetic similarity to *P. sulfincola* is such that tandem mass spectroscopy can identify an equivalent number of proteins in both species. Thus, *P. palmiformis* provides an ideal control to evaluating specific biomolecular aspects that confer extreme thermotolerance to *P. sulfincola.*

The overarching goal of this thesis is three-fold: A) to identify the factor(s) that confer extreme thermal tolerance in the polychaete *P. sulfincola* as compared to the mesotolerant congener *P. palmiformis*, B) to determine the independent and combinatory effects of thermal, pH, and sulfide stresses on aerobic respiration rate, and C) to report responses to both acute and sustained thermal stress. I have pursued these goals with an array of high-pressure aquaria that enabled me to maintain organisms at *in situ* temperatures and pressures. I have conducted *in vivo* experiments in which the worms were exposed to a variety of thermal and temporal condition sets, concurrently monitoring their aerobic respiration rates using a real-time oxygen probe. In addition, I have conducted a series of experiments combining elements of elevated temperature, H_2S, and low pH. I have combined the following chapters will detail our findings for each of these investigations.

Chapter two is entitled “Exploring the limit of metazoan thermal tolerance via comparative proteomics: Thermally induced expression shifts in two hydrothermal vent

polychaetes". Quantitative comparative global proteomics coupled with antioxidant enzymatic assays were employed to establish the responses to sustained thermal treatments in *P. sulfincola* and *P. palmiformis.* Briefly, each species was subjected to a sustained exposure to three temperatures spanning an experimentally-determined thermal range. In conjunction with the DOE-Joint Genome Institute (Walnut Creek, CA), a *P. sulfincola* transcriptome was built using pyrosequencing. This database informed our tandem mass spectrometry data, allowing us to observe differences in protein expression between thermal treatments. I determined that, among other responses, proteins involved in the creation and recycling of the antioxidant glutathione (GSH) were differentially expressed in *P. sulfincola*. These data were then coupled with GSH enzyme assays to determine the level and ratio (reduced v. oxidized) of the antioxidant.

Chapter three, entitled "Understanding the independent and combined effects of temperature, pH, and sulfide concentration on respiration of the hydrothermal vent polychaete *Paralvinella sulfincola*", examines the effect of environmental stresses on real-time respiration measurements taken during *in vivo* experimental treatments of *P. sulfincola*. A series of sustained tolerance experiments combining varying levels of temperature, pH, and sulfide concentration were conducted in high pressure aquaria. *P. sulfincola* aerobic respiration rate (a proxy for physiological stress) was measured in real time using a dissolved oxygen probe response to each treatment. These data are combined with *in vitro* measurements of intracellular pH buffering capacity, unbound internal sulfide concentrations, and rate calculations from previous studies to investigate the causes of physiological stress in a multivariable treatment.

Chapter four, entitled "Differential expression of antioxidant genes during thermal stress in *Paralvinella sulfincola*", explores the gene response using the sensitive method quantitative PCR. Unlike the previous chapters, worms for this experiment were sampled at multiple time points to observe acute changes in gene expression to thermal stress. Worms were maintained at two experimental treatments – one (45°C) below the sustainable thermal limit, CL_{Max}, and one (50°C) below the acute tolerance limit, CT_{Max}. This allows for a comparison of gene responses

that likely correspond to chronic and acute survival respectively. Informed by the findings of chapter two, I chose to examine the response of a suite of antioxidant genes – glutathione peroxidase, glutathione reductase, superoxide dismutase, and catalase. The expression levels of these genes in the experimental treatments are normalized first to an internal reference gene (β-Actin) and to the expression of an untreated control maintained at 30°C.

Paralvinella sulfincola are an ideal species to investigate questions pertaining to environmental stress because they live at one of the most dynamic environments, subjected to some of the most variable condition sets on the planet. These organisms have one of largest thermal ranges of any known metazoan, including a CL_{Max} at or even slightly above the limit predicted by Pörtner (11). In addition they must withstand wide fluctuations in sulfide concentration and pH, among other factors. The goal of my research on *P. sulfincola* has been to understand their response to these environmental stresses and their ultimate physiological boundaries. And thus, I hope these experiments will provide new insight into what constraints ultimately limit all metazoan thermal survival.

REFERENCES

1. Ege R, Krogh A. On the Relation between the Temperature and the Respiratory Exchange in Fishes. Internationale Revue der Hydrobiologie Leipzig. 1914;7:(48-55).

2. Braby CE, Somero GN. Following the heart: temperature and salinity effects on heart rate in native and invasive species of blue mussels (genus *Mytilus*). J Exp Biol. 2006;209(13):2554-66.

3. Portner HO, Bennett AF, Bozinovic F, Clarke A, Lardies MA, Lucassen M, et al. Trade-offs in thermal adaptation: the need for a molecular to ecological integration. Physiol Biochem Zool. 2006 Mar-Apr;79(2):295-313.

4. Cowan DA. Thermophilic proteins: stability and function in aqueous and organic solvents. Comp Biochem Physiol A Physiol. 1997 Nov;118(3):429-38.

5. Daniel RM, Danson MJ, Eisenthal R, Lee CK, Peterson ME. The effect of temperature on enzyme activity: new insights and their implications. Extremophiles. 2008 Jan;12(1):51-9.

6. Collier RJ, Collier JL, Rhoads RP, Baumgard LH. Invited review: genes involved in the bovine heat stress response. J Dairy Sci. 2008 Feb;91(2):445-54.

7. Reusch TB, Veron AS, Preuss C, Weiner J, Wissler L, Beck A, et al. Comparative analysis of expressed sequence tag (EST) libraries in the seagrass *Zostera marina* subjected to temperature stress. Mar Biotechnol (NY). 2008 May-Jun;10(3):297-309.

8. Deming JW, Baross JA. Deep-sea smokers: windows to a subsurface biosphere? Geochim Cosmochim Acta. 1993 Jul;57(14):3219-30.

9. Hochachka PW, Somero GN. Biochemical adaptation: mechanism and process in physiological evolution: Oxford University Press, USA; 2002.

10. Takai K, Nakamura K, Toki T, Tsunogai U, Miyazaki M, Miyazaki J, et al. Cell proliferation at 122 degrees C and isotopically heavy CH4 production by a hyperthermophilic methanogen under high-pressure cultivation. Proc Natl Acad Sci U S A. 2008 Aug 5;105(31):10949-54.

11. Pörtner H. Climate change and temperature-dependent biogeography: oxygen limitation of thermal tolerance in animals. Naturwissenschaften. 2001;88(4):137-46.

12. Lutterschmidt WI, Hutchison VH. The critical thermal maximum: history and critique. Canadian Journal of Zoology. 1997;75(10):1561-74.

13. Horowitz M. From molecular and cellular to integrative heat defense during exposure to chronic heat. Comp Biochem Physiol A Mol Integr Physiol. 2002 Mar;131(3):475-83.

14. Lesser MP. Oxidative stress in marine environments: biochemistry and physiological ecology. Annu Rev Physiol. 2006;68:253-78.

15. Frederich M, O'Rourke MR, Furey NB, Jost JA. AMP-activated protein kinase (AMPK) in the rock crab, *Cancer irroratus*: an early indicator of temperature stress. J Exp Biol. 2009 Mar;212(Pt 5):722-30.

16. Lighton JRB, Turner RJ. Thermolimit respirometry: an objective assessment of critical thermal maxima in two sympatric desert harvester ants, *Pogonomyrmex rugosus* and *P. californicus*. J Exp Biol. 2004;207(11):1903-13.

17. Hendersen RW, Graham JA. Avoidance of heat by rats: Effects of thermal context on rapidity of extinction. Learning and Motivation. 1979;10(3):351-63.

18. Wittenburg N, Baumeister R. Thermal avoidance in *Caenorhabditis elegans*: an approach to the study of nociception. Proc Natl Acad Sci U S A. 1999 Aug 31;96(18):10477-82.

19. Beitinger TL, Bennett WA, McCauley RW. Temperature tolerances of North American freshwater fishes exposed to dynamic changes in temperature. Environmental Biology of Fishes. 2000;58(3):237-75.

20. Cooney D, Emerson R. Thermophilic fungi: WH Freeman San Francisco, CA; 1964.

21. Brock T, Libraries UoW--M. Thermophilic microorganisms and life at high temperatures: Springer-Verlag New York; 1978.

22. Podrabsky JE, Somero GN. Changes in gene expression associated with acclimation to constant temperatures and fluctuating daily temperatures in an annual killifish *Austrofundulus limnaeus*. J Exp Biol. 2004;207(13):2237-54.

23. Boutet I, Jollivet D, Shillito B, Moraga D, Tanguy A. Molecular identification of differentially regulated genes in the hydrothermal-vent species *Bathymodiolus thermophilus* and *Paralvinella pandorae* in response to temperature. BMC Genomics. 2009;10:222.

24. Gehring W, Wehner R. Heat shock protein synthesis and thermotolerance in *Cataglyphis*, an ant from the Sahara desert. Proceedings of the National Academy of Sciences of the United States of America. 1995;92(7):2994.

25. Wickstrom C, Castenholz R. Thermophilic ostracod: aquatic metazoan with the highest known temperature tolerance. Science. 1973;181(4104):1063.

26. Urabe T, Baker ET, Ishibashi J, Feely RA, Marumo K, Massoth GJ, et al. The effect of magmatic activity on hydrothermal venting along the superfast-spreading East pacific rise. Science. 1995 Aug 25;269(5227):1092-5.

27. Douville E, Charlou J, Oelkers E, Bienvenu P, Jove Colon C, Donval J, et al. The Rainbow vent fluids (36 14'N, MAR): the influence of ultramafic rocks and phase separation on trace metal content in Mid-Atlantic Ridge hydrothermal fluids. Chemical Geology. 2002;184(1-2):37-48.

28. Lowell RP, Rona PA, Von Herzen RP. Seafloor hydrothermal systems. Journal of geophysical research. 1995;100(B1):327-52.

29. Desbruyeres D, Laubier L. *Alvinella pompejana* gen. sp. nov., Ampharetidae aberrant des sources hydrothermales de la ride Est-Pacifique. Oceanologica Acta. 1980;3(3):267-74.

30. Desbruyeres D, Laubier L. New species of Alvinellidae (Polychaeta) from the north Fiji back-arc basin hydrothermal vents (southwestern Pacific). Proceedings of the Biological Society of Washington. 1993;106(2):225-36.

31. Cary SC, Shank T, Stein J. Worms bask in extreme temperatures. Nature (London). 1998;391(6667):545-6.

32. Sarrazin J, JUNIPER K. The use of video imagery to gather biological information at deep-sea hydrothermal vents. Cahiers de biologie marine. 1998;39(3-4):255-8.

33. Sarrazin J, Levesque C, Juniper S, Tivey M. Mosaic community dynamics on Juan de Fuca Ridge sulphide edifices: substratum, temperature and implications for trophic structure. CBM-Cahiers de Biologie Marine. 2002;43(3-4):275-9.

34. Lee RW. Thermal tolerances of deep-sea hydrothermal vent animals from the Northeast Pacific. Biol Bull. 2003 Oct;205(2):98-101.

35. Girguis PR, Lee RW. Thermal preference and tolerance of alvinellids. Science. 2006 Apr 14;312(5771):231.

36. Cottin D, Ravaux J, Leger N, Halary S, Toullec JY, Sarradin PM, et al. Thermal biology of the deep-sea vent annelid Paralvinella grasslei: in vivo studies. J Exp Biol. 2008 Jul;211(Pt 14):2196-204.

37. Chevaldonné P, Fisher C, Childress J, Desbruyères D, Jollivet D, Zal F, et al. Thermotolerance and the'Pompeii worms'. Marine Ecology Progress Series. 2000;208:293-5.

38. Yancey PH, Ishikawa J, Meyer B, Girguis PR, Lee RW. Thiotaurine and hypotaurine contents in hydrothermal-vent polychaetes without thiotrophic endosymbionts: correlation With sulfide exposure. J Exp Zool A Ecol Genet Physiol. 2009 Jul 1;311(6):439-47.

39. Rinke C, Lee RW. Pathways, activities and thermal stability of anaerobic and aerobic enzymes in thermophilic vent paralvinellid worms. Marine Ecology Progress Series. 2009;382:99-112.

40. O'Donnell MJ, Hammond LTM, Hofmann GE. Predicted impact of ocean acidification on a marine invertebrate: elevated CO2 alters response to thermal stress in sea urchin larvae. Marine Biology. 2009;156(3):439-46.

41. Anthony K, Kline D, Diaz-Pulido G, Dove S, Hoegh-Guldberg O. Ocean acidification causes bleaching and productivity loss in coral reef builders. Proceedings of the National Academy of Sciences. 2008;105(45):17442.

Chapter 2

Exploring the limit of metazoan thermal tolerance via comparative proteomics: Thermally induced expression shifts in two hydrothermal vent polychaetes

Abstract

Eukaryotic thermotolerance is challenged at deep-sea hydrothermal vents, where temperatures can reach 300 °C. *Paralvinella sulfincola*, an extremely thermotolerant vent polychaete, and *P. palmiformis*, a congener with a more modest thermal tolerance, both flourish at vents along the Juan de Fuca Ridge, Washington, USA. We conducted a series of shipboard, high-pressure, thermotolerance experiments on both species to examine the physiological adaptations that confer pronounced thermotolerance. Quantitative proteomics, a deeply sequenced EST library, and glutathione (GSH, an antioxidant) assays revealed that *P. sulfincola* exhibited an upregulation in the synthesis and recycling of GSH with increasing temperature, downregulated NADH and succinate dehydrogenases (key enzymes in oxidative phosphorylation) with increasing temperature, but maintained elevated levels of heat shock proteins (HSPs) across treatments. In contrast, *P. palmiformis* exhibited more typical responses to increasing temperatures, e.g. increasing HSPs at higher temperatures. These data, among the first to quantify global protein and antioxidant responses to temperature in an extremely thermotolerant eukaryote, suggest that *P. sulfincola's* pronounced thermal tolerance is largely due to its capacity to mitigate oxidative stress via increased synthesis of antioxidants and decreased flux through the mitochondrial electron transport chain. Ultimately oxidative stress may be the key factor in limiting all metazoan thermotolerance.

Introduction

Physiological adaptations to thermal stress are ubiquitous among all organisms. While prokaryotes have a known upper thermal limit of at least 122 °C (1), metazoans have a much lower thermal tolerance, with 45 to 47 °C as the currently accepted upper limit of homeostasis (2). Mitochondrial dysfunction and membrane instability have been suggested as possible modes of physiological failure in eukaryotes at higher temperatures (3), though unicellular eukaryotic fungi such as *Thermomyces lanuginosus* are known to grow at 60-62 °C (4). Other recent studies have suggested that oxygen transport and aerobic respiration impose a physiological limit with increasing temperature, as mitochondrial activity has been observed to decline at higher temperatures in some mesotolerant metazoans (5-7). Additional limiting constraints on thermotolerance may exist in organisms with complex multicellular structure, e.g., structural integrity or functional organization (2).

There have been many studies to date on metazoan thermotolerance (for reviews see: (8-9)). A few have focused on the most highly thermotolerant animals such as desert ants and hot spring ostracods (10-11), and largely examined the response to acute thermal tolerance. Little research has focused on physiological or biochemical responses to chronic exposure. Recently, some studies have employed proteomics to examine responses to thermal stress in mesotolerant animals (6, 12); however, there remains a paucity of biomolecular data for extremely thermotolerant metazoans. Thus, it remains to be determined how highly thermotolerant organisms respond to chronic thermal exposure, and which physiological or biochemical adaptations enable them to ameliorate the aforementioned issues that arise at higher temperatures.

Deep-sea hydrothermal vents are ideal habitats to address such questions, as these environments are home to some of the most thermotolerant animals known including the polychaetes *Alvinella pompejana* and *Paralvinella sulfincola*. *In situ* temperatures of the substratum directly under live worms have been recorded at 81 °C for *A. pompejana* (13). *In vitro* research on *Alvinella pompejana* has suggested key enzymes may not be thermally stable at very

high temperature (14). Because *A. pompejana* are not easily amenable to *in vivo* experimentation (15), *P. sulfincola* are a suitable choice to study thermal stress response research. The polychaete *Paralvinella sulfincola* lives on hydrothermal sulfides in the Northwest Pacific. *In situ* temperature measurements of the substratum directly beneath *P. sulfincola* have been recorded at 88.5°C (16), while *in vivo* laboratory studies of *P. sulfincola* have demonstrated experimentally the broadest known sustained tolerance range in metazoans (5-48 °C) (17-18) and **Figure 2.1**. *Paralvinella sulfincola* and *Paralvinella palmiformis* (a close congener with a reduced thermal scope – **Figure 2.1**) have broad overlap in environmental habitat but significantly different thermal tolerance ranges. Both are amenable to *in vivo* recovery and laboratory experimentation which affords the unique opportunity to elucidate the biochemical responses of meso- and thermotolerant metazoans in a phylogenetic context. Here we present data from a series of *in vivo* laboratory experiments, in which we examined quantitative changes in protein expression of the two congeners over a series of temperatures that span their thermal range. The highest thermal exposures neared each species' respective ultimate incipient lethal temperature (UILT, defined here as the temperature beyond which 50% of the population cannot survive indefinitely (19-20)).

The data shown here reveal statistically significant differences in protein abundance and upregulation, as well as antioxidant abundance, between these two congeners across their thermal ranges and at their respective UILTs. The results of this study add empirical evidence to the theory that oxidative stress may be the primary stressor at the upper temperature limits of eukaryotic life. In concert, the use of experimental treatments and global protein analyses links physiological and biomolecular data to provide broader understanding of the underlying limits of thermal tolerance in all metazoans.

Results and Discussion

These data reveal that *P. sulfincola* maintains elevated expression of HSPs across its thermal range. Moreover, *P. sulfincola* -operating near the UILT of all known metazoan life-

Figure 2.1: *P. sulfincola* and *P. palmiformis* chronic thermal range

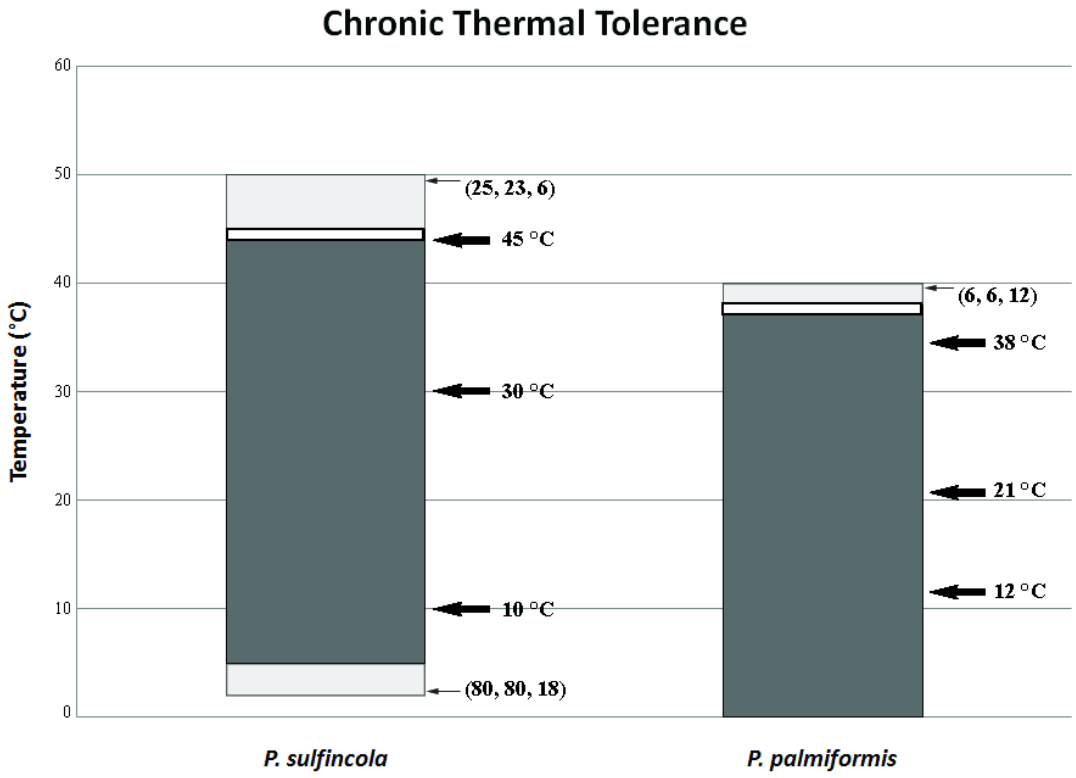

The Ultimate Incipient Lethal Temperature (UILT) is represented by a white band. The dark grey box represents an LD_0 for at least 12 hours of treatment. The light grey box represents a transition from LD_0 to LD_{100} for less than 12 hours of maintenance. At thermal boundaries, parentheses represent (Number experimented, Number dead, Duration in hours of experiment) i.e. 23 of 25 *P. sulfincola* were dead at 6 hours at 50°C. Note that no *P. sulfincola* death was observed at 10 hours at 2°C, but all worms died after 8 hours at 0°C. No lower LD_0 was determined for *P. palmiformis*, as all 10 maintained at 0°C for 17 hours survived. Proteomic treatments were chosen from across the chronic ranges for both species, representing a high, medium, and low temperature sample, represented by the large black arrows.

upregulate mechanisms that mitigate oxidative stress, and upregulates proteins that shift metabolic emphasis away from aerobic processes. *P. palmiformis* exhibited responses to temperature that are more similar to those observed in previous studies of mesotolerant organisms, including increased representation of heat shock proteins and other systems only upon exposure to the highest thermal regimes. The combined use of shipboard experimentation at relevant conditions along with global comparative proteomics, based on a *de novo* sequenced *P. sulfincola* transcriptome (see methods), allows a broad, agnostic depiction of changes in protein expression in relation to increasing temperature. The quantitative protein profiles, along with the results of the glutathione antioxidant assays, collectively suggest that *P. sulfincola* encounters pronounced oxidative stress near its UILT. In response, it employs a suite of mechanisms to mitigate the impact–and reduce the production- of oxygen radicals via antioxidants and a concomitant decrease in oxidative phosphorylation. While we cannot infer metabolic flux from these data (discussed below), the observed systemic differences elucidate those physiological and biochemical processes most responsive to thermal stress. The data suggest that the upper temperature limits of metazoan life may indeed be governed by the ability of the organism to mitigate oxidative stress by managing antioxidant production and vital energy yielding metabolic pathways. The sections below discuss in greater detail the observed differences in protein and antioxidant expression between these two sister taxa. Unless otherwise stated, all results correspond solely to comparative proteomics, not to our sequenced nucleotide transcriptome.

Differences in Expression of Molecular Chaperones

Historically, molecular chaperones such as heat shock proteins (HSPs) have been regarded as conferring sustained thermal tolerance by allowing organisms to minimize protein dysfunction at elevated temperature. Chaperones catalyze nascent protein folding in the endoplasmic reticulum (ER), bind to and prevent or reform misfolded proteins, initiate proteolytic degradation, and conduct a host of additional house-keeping functions (21-22). Many chaperones are constitutively expressed under normal conditions; however, a large portion of chaperones are

up-regulated during periods of cellular stress (23). *P. sulfincola* exhibited elevated levels of major chaperones, even among likely inducible forms, over all treatments (**Figure 2.2**), while *P. palmiformis* exhibits higher chaperone production near the UILT. While the metabolic costs associated with maintaining this state are unconstrained, these data suggest that *P. sulfincola* may be better poised to withstand acute periods of thermal stress, consistent with observations of their habitat (discussed in detail below).

A total of 27 chaperones and co-chaperones were included in our analysis, representing members of all detected heat shock proteins **Table 2.1**. In the following section, see **Table 2.1** for log fold changes of chaperone levels.

Heat shock protein 70 (HSP70)

The 70 KDa heat shock proteins (HSP70 family) are the first characterized and best understood chaperones. HSP70 are well conserved across domains of life, broadly found among prokaryotes and eukaryotes (22). Multiple isoforms in the family are constitutive, while others are induced by heat stress (23-24). In *P. sulfincola*, a HSP70 known as GRP75 exhibited the highest abundance of all molecular chaperones across all *P. sulfincola* treatments. GRP75 is homologous to the human HSPA9, a constitutive mitochondrial HSP (25). In *P. palmiformis*, there was a moderate increase in expression of GRP75 at 38°C relative to the cooler thermal regimes. A number of co-chaperones that interact with HSP70 family were also observed in all proteomes, and though their expression varied the overall trend for both species was a slight increase in the high treatments. Moreover, three HSP70 sequences with human homologs were observed in the *P. sulfincola* EST library (HSPA5, HSPA8, and HSPA9). No homologs to the inducible human HSP70 forms (HSPA1A, HSPA1B, or HSPA6) were identified in our nucleotide transcriptome and therefore are absent from the quantitative proteomic analyses. However, when peptide MSMS spectra were compared against the broader NCBI non-redundant protein database, *P. sulfincola* sequences homologous to inducible HSP70s were detected, and their relative proportion to total protein remains consistent with constitutive HSP70 proteins. Together these

Figure 2.2: Molecular chaperones

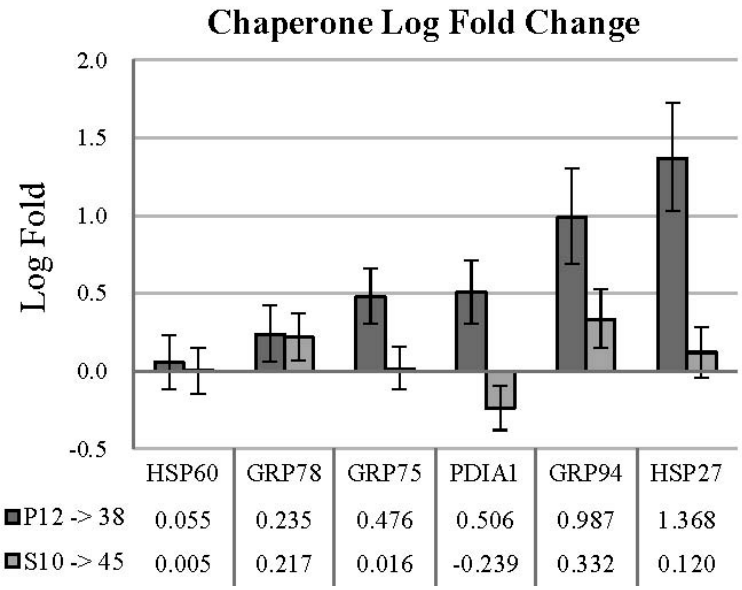

Differences in expression between *P. sulfincola* and *P. palmiformis* in log fold-change for six major molecular chaperones across their thermal range. S10 →45 = difference from *P. sulfincola* maintained at 10°C to 45°C; P12 →38 = difference from *P. palmiformis* maintained at 12°C to 38°C. Stars (*) indicate that the log change is > 0.90 in our Bayesian analysis, indicating a significant change with temperature. We assumed a binomial likelihood for the data and a Beta (0.5,0.5) prior for each treatment. Monte Carlo sampling from the resulting posterior distributions within each treatment was used to estimate the posterior distributions of log-fold changes between treatments. We report the medians and 95% credible intervals (bars) of the posterior distributions of log-fold change between treatments.

Table 2.1: Shifts in *Paralvinella* protein abundance during thermal exposure

a) Chaperones

Name	EST	Log Δ *P.p.* 12→21	Log Δ *P.p.* 12→38	Log Δ *P.s.* 10→30	Log Δ *P.s.* 10→45	Count *P.p* 12	Count *P.p* 21	Count *P.p* 38	Count *P.s.* 10	Count *P.s.* 30	Count *P.s.* 45
HSP70											
GRP78	i04331	0.33	0.46	-0.01	0.32	357	425	443	328	318	408
HSC70	i22380	0.00	0.42	-1.75	-0.71	0	0	1	7	0	3
GRP75	i09313	-0.22	0.83	0.71	0.04	353	286	568	420	672	428
DNAJA1	c14926	0.00	0.00	0.74	2.29	0	0	0	0	2	12
DNAJB5	i03361	-2.13	-0.91	-0.01	0.31	11	0	4	7	7	10
DNAJC20	i17021	0.00	0.74	-0.37	0.10	0	0	2	5	3	5
GRPEL1	i13564	-1.50	0.21	0.43	0.12	23	6	24	27	36	29
HIP	i18335	-2.52	-1.79	1.26	1.70	16	0	2	1	7	11
APG-2	i11168	0.10	1.11	-0.21	0.59	54	56	109	67	56	101
HSPBP1	i04669	-3.57	-1.83	0.57	1.32	36	0	7	7	12	23
BAG4	i16944	0.00	3.12	0.53	0.33	0	0	23	10	15	13
HSP90											
GRP94	i07201	1.13	1.55	-0.01	0.48	111	233	297	203	197	284
HOP	c23313	0.15	0.98	-0.21	0.98	18	19	35	19	16	41
P23	c15040	0.00	2.32	-0.86	-0.33	0	0	12	27	13	20
FKBP52	i04887	0.00	4.06	2.66	3.92	0	0	47	2	31	79
CDC37	i21647	-0.91	-2.66	0.20	0.57	25	11	1	12	14	19
AHA1	i01111	0.00	0.00	0.00	3.58	0	0	0	0	0	33
Other HSPs											
HSP60	i07506	0.18	0.23	0.19	0.02	396	425	419	403	451	405
HSP10	i01229	-0.38	-0.02	-0.19	0.11	43	31	38	46	39	49
HSP27	c31626	-0.11	2.09	0.02	0.18	79	70	313	317	314	358
HSP67Bb	i14733	0.72	2.80	-0.12	-0.82	2	6	32	42	38	23
ER Chaperones											
PDIA1	i05791	-0.15	0.87	-0.21	-0.33	267	228	442	468	395	370
PDIA4	i23366	0.00	2.81	1.74	2.00	0	0	18	1	11	14
PDIA6	i06115	0.23	0.44	1.08	1.43	29	33	37	21	46	60
ERP29	i01807	0.00	3.00	1.10	2.45	0	0	21	4	11	33
FKBP2	i22810	0.16	2.76	-0.13	0.02	2	3	31	18	16	18
CYPB	i05697	-0.16	-0.96	0.88	1.39	79	67	35	10	20	30

b) GSH Pathway

#	Name	EST	Log Δ *P.p.* 12→21	Log Δ *P.p.* 12→38	Log Δ *P.s.* 10→30	Log Δ *P.s.* 10→45	Count *P.p* 12	Count *P.p* 21	Count *P.p* 38	Count *P.s.* 10	Count *P.s.* 30	Count *P.s.* 45
1	SelD	i23688	-1.05	-0.90	3.46	4.41	59	28	31	0	10	20
2	MAT2	c06576	0.40	0.23	1.85	0.49	27	36	32	30	112	43
3	AHCY	i00806	-0.26	-0.08	-0.46	-0.31	63	53	60	79	57	63
4	CBS	i03712 i04188	0.00	7.12	4.46	7.33	0	0	138	0	21	159
5	GCS-Cat	i11155	0.00	0.00	1.00	0.00	0	0	0	0	1	0
5	GCS-Reg	i22617	0.00	3.81	1.69	2.22	0	0	13	2	10	15
6	GPx-3	c29428	0.00	4.64	2.74	1.97	0	0	24	4	30	17
6	PHGPx	i06856	-0.88	-2.25	0.62	0.32	165	89	34	31	49	40
6	GPx-5	i04359	0.00	0.00	-2.21	-2.21	0	0	0	4	0	0
7	GSR	i20935	-0.80	-7.05	1.58	5.09	131	75	0	0	2	33
8	GST-103	i18172	3.90	2.32	-2.71	-1.64	0	14	4	12	1	3
8	GST-13	i12666	0.00	1.58	1.00	2.67	0	0	2	0	1	5
8	GST-3	i12479 i03342	-1.70	0.62	-0.44	-1.59	2	0	4	8	6	2
8	GST-5	i16274	-0.04	-1.47	0.04	0.31	66	64	23	35	36	44
8	GST-7	i11846	0.00	0.00	-1.14	-1.14	0	0	0	1	0	0
8	GST-Z1	i13023	-0.09	0.48	-0.47	-0.26	38	36	54	65	47	55
8	GST-μ1	i13308	1.43	2.24	0.63	1.14	5	14	25	24	38	55
8	GST-σ	i06157	0.00	4.70	-0.27	0.22	0	0	25	34	28	40

Key enzymes of *P. sulfincola* and *P. palmiformis* discussed in the text. EST refers to the (i) isotig or (c) contig identifier for each enzyme. Log change refers to the shift in abundance between treatments, i.e. (log Δ *P.p* – 12 → 21 = protein log fold change between *P. palmiformis* treatments 12°C and 21°C). Counts are combined between all three technical replicates and normalized to treatment library sizes. Red boxes indicate a significant (Pr(DE) >0.9) increase in protein abundance; Blue boxes indicate a significant (Pr(DE) >0.9) decrease in protein abundance. **Table 2.1a** lists chaperones; **Table 2.1b** lists glutathione pathways.

data underscore the importance of HSP70 proteins in thermal tolerance of both species, and the continued elevated expression in *P. sulfincola* suggest that HSP70 proteins may be kept abundant to cope with the rapid changes in temperature typically encountered by this species, which may be required to ensure physiological function near an organism's UILT.

HSP90

Although less well characterized than the HSP70 family, HSP90s are known as abundant flexible dimer ATPases that bind to a variety of cellular proteins (clients) including steroid hormone receptors, transcription factors, and protein kinases (26-27). While representatives of all known HSP90s were found in our EST database, only GRP94 was detected in the proteome. GRP94 is a luminal protein associated with the endoplasmic reticulum (28). The *P. sulfincola* proteome suggests constitutive expression of GRP94 (Probability of differential expression - Pr(DE) 0.11) across all treatments. In *P. palmiformis*, GRP94 expression likely increased with temperature (12°C → 38°C - log 1.55, Pr(DE) 0.66). Co-chaperones such as HOP, FKBP52 and others known to play a regulatory role with cytosolic HSP90s were observed in both *P. sulfincola* and *palmiformis* proteomes. Notably, FKBP52 exhibited a highly significant increase with temperature in both worms (Pr(DE) 1.00). HOP, which modulates HSP70/90 interactions, was moderately upregulated with temperature in both *P. sulfincola* and *P. palmiformis* at their highest treatments (*P.s.* 10°C → 45°C - log 0.98, Pr(DE) 0.82; *P.p.* 12°C → 38°C - log 0.98, Pr(DE) 0.51). The HSP90 inhibitor CDC37 remained constant in *P. sulfincola* and significantly decreased in *P. palmiformis* in higher thermal regimes. Conversely, the HSP90 activator AHA1 was substantially upregulated at 45°C in *P. sulfincola* (10°C → 45°C - log 3.58, Pr(DE) 1.00) but was not detected in *P. palmiformis*. The patterns observed here suggest that HSP90 is constitutively express in *P. sulfincola*, but activity is regulated in both species through the regulation of activators and inhibitors. These observations are also consistent with the aforementioned hypothesis that *P. sulfincola* maintains a biochemical poise to cope with acute temperature fluctuations.

HSP 60 and HSP27

HSP60 is a *mitochondrial* molecular chaperone known to confer thermal tolerance in eukaryotes (29). Our analysis revealed that HSP60 was the most consistently expressed heat shock protein, with high abundance across all treatments in both species. This trend was mirrored in the HSP60 co-chaperone, HSP10, which assists HSP60 in protein folding during periods of stress (30). These findings support the hypothesis that both species maintain pools of HSP60 and HSP10 to mitigate thermal damage to mitochondrial proteins. In contrast, the small 27kDa heat shock protein (sHSP), found throughout cellular compartments and the cytosol, responds to not only thermal, but also oxidative stress by binding to damaged or misfolded proteins and forming reservoirs for other chaperones to correctly refold or initiate proteolytic degradation (31). It is also known to upregulate key enzymes in the glutathione pathway (31-32). HSP27 remained abundantly expressed across all treatments in *P. sulfincola.* However, HSP27 increased only at the highest temperature in *P. palmiformis* (12°C → 38°C - log 2.09, Pr(DE) 1.00). It is posited that the differences observed between expression levels of HSP27 relate to oxidative stress response and the glutathione pathway (discussed in detail below).

Foldases

Foldases are enzymes that catalyze rate-limiting steps in protein folding, many of which play a key role in the cellular "unfolded protein response" (a stress response to an accumulation of unfolded and misfolded proteins in the endoplasmic reticulum, which aims to restore normal function by halting protein translation and signaling the production of molecular chaperones involved in protein folding; (33)). A number of foldases important to the UPR were detected within the *P. sulfincola* EST library, and our proteomic analysis identified a subset of foldases with significant abundance in both Paralvinellid species. Of note, the foldase PDIA1 exhibited high constitutive abundance in both species. PDIA1 is a protein-thiol oxidoreductase that catalyzes both protein isomerization and oxidation. This multifunctional enzyme has roles as both a chaperone and a foldase, has been demonstrated to respond to heat shock, and is not specifically

restricted to the ER (33-34). We observed high constitutive levels of PDIAI in *P. sulfincola* (somewhat higher at 10°C over 45°C) but significant expression increase with temperature in *P. palmiformis*, reinforcing the pattern of differential response observed between these two organisms in relation to thermal stress.

While the data on chaperones demonstrate that *P. sulfincola* maintains elevated expression of chaperones across all thermal regimes, we posit that the representation and abundance of chaperones does not itself explain the observed thermotolerance. Indeed, the representation of chaperones between these two closely related species was (proportionally) equivalent at their respective highest thermal treatments, and if HSP production alone was the key factor in conferring extreme thermotolerance, then *P. palmiformis* would likely have a greater thermal tolerance similar to *P. sulfincola* (with a UILT above 38°C). We therefore further posit that elevated HSP abundances in *P. sulfincola* are more likely a reflection of its ecological niche *in situ*, enabling it to survive acute, rapid shifts in temperatures caused by its proximity to hot vent fluid.

Response to Oxidative Stress

The largest shifts in protein expression observed in both species are related to the mitigation of oxidative stress. Reactive oxygen species include the superoxide radical ($O_2^{\bullet-}$), the hydroxyl radical ($HO^{\bullet}$), and uncharged hydrogen peroxide (H_2O_2), (35). Unchecked, ROS can oxidize and cause major damage to proteins, lipids, and nucleic acids. Under normative conditions, mitochondria consume more than 90% of all cellular O_2, consequently producing the majority of ROS (36). In mitochondria, superoxide ($O_2^{\bullet-}$) is generated in complexes I/III during respiration, and other ROS in outer and inner membranes (for review see (37-38)). While cells can cope with modest ROS production during nominal aerobic respiration, there is a marked increase in oxidative stress during periods of thermal stress in eukaryotes (5, 39-40). Elevated temperatures increase the metabolic demand of tissues and induce a state of functional tissue hypoxia (41). Subsequently, increased mitochondrial respiration rates further increase

endogenous ROS, as electrons pass approximately twice as fast through the electron transport chain (ETC) for every 10°C rise (5-6, 36, 38, 40).

Superoxide dismutase (SOD, EC 1.15.1.1, ,) is responsible for catalyzing the reduction of $O_2^{\bullet-}$ to H_2O_2. The two forms of this metalloprotein differ by their catalytic metal – Copper/Zinc and Manganese (35). Cu/Zn SOD (isotig03775) is primarily found in the cytosol, and Mn SOD (isotig06674) in the mitochondria. *Paralvinella sulfincola* showed no differential regulation of either form of SOD, but *P. palmiformis* demonstrated significant increases in both Mn SOD (Pr(DE) 0.997) and Cu/Zn SOD (Pr(DE) 0.999). It is important to note, while significant, there were very few counts of either SOD in *P. palmiformis.*

In *P. sulfincola,* however, the production of glutathione does appear to play a prominent role in mitigating ROS. Glutathione (L-γ-glutamyl-L-cysteinylglycine, or GSH) is a tripeptide thiol that is the primary nonprotein antioxidant in metazoans. Found up to mM concentrations in mammals, GSH mitigates oxidative stress by chemically reducing hydrogen peroxide (and other toxic compounds (37, 42)). The enzyme glutathione peroxidase (GPx, 1.11.1.9) catalyzes this reduction, yielding glutathione disulfide (GSSG). GSSG is reverted back to GSH by glutathione reductase (GSR, EC 1.8.1.7). Regulation of GSH metabolism and cycling serves as an indicator of cellular oxidative stress levels (42). As cysteine is the required peptide for *de novo* GSH synthesis, and the rare amino acid selenocysteine is required for the synthesis of glutathione peroxidase, increases in cysteine and in particular selenocysteine are good indicators for increases in GSH cycling. See **Table 2.1b** for log fold changes of enzyme levels.

Figure 2.3 depicts key steps and significant changes over temperature in the synthesis of glutathione, the redox cycle of GSH and GSSG, and the catalyzing enzymes glutathione peroxidase (GPx) and glutathione reductase (GSR) in *P. sulfincola* and *P. palmiformis*. Notably, cystathionine beta-synthase (CBS, EC 4.2.1.22), central to both cysteine and selenocysteine synthesis, exhibited the single largest fold increase with temperature of all proteins assayed in *P. sulfincola* and nearly so for *P. palmiformis* (*P.s.* 10°C → 45°C - log 5.74, Pr(DE) 1.00; *P.p.* 12°C

Figure 2.3: Glutathione pathway in *Paralvinella* with responses to thermal exposure

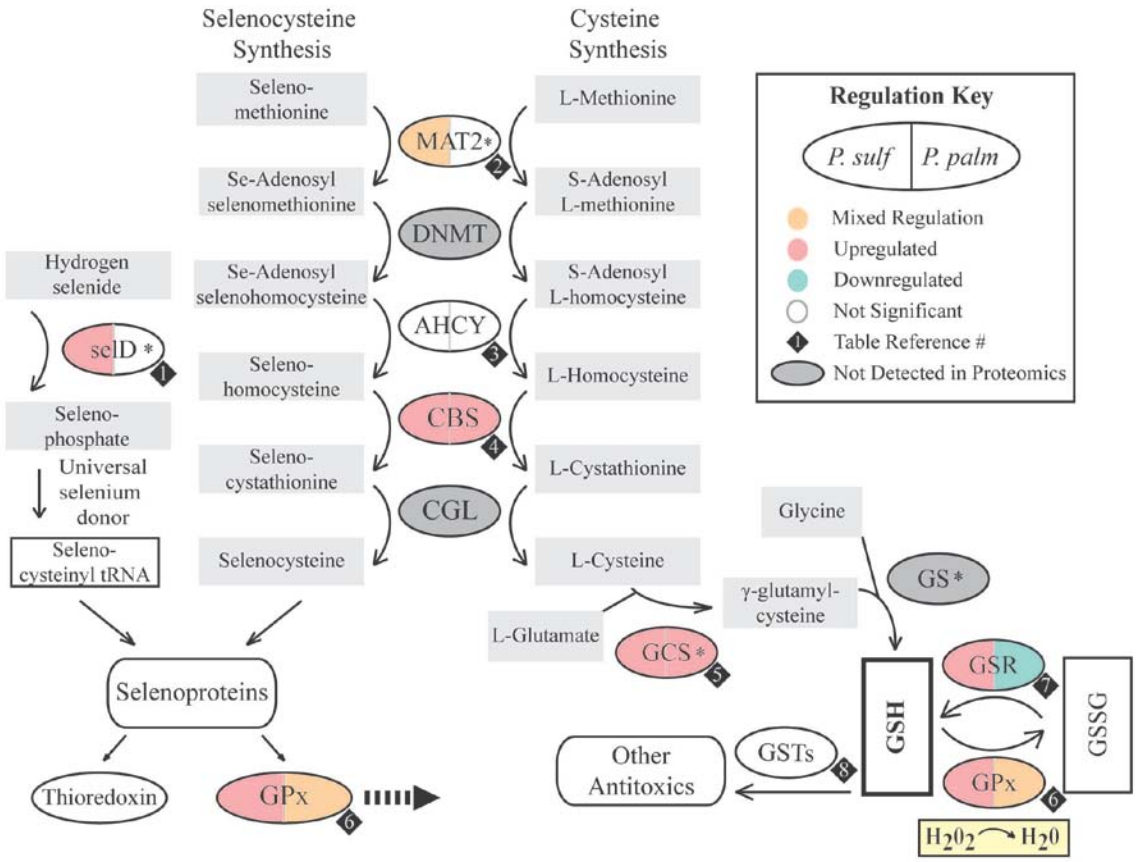

Synthesis pathways of the antioxidant glutathione (GSH) and its catalyzing enzyme Glutathione peroxidase (GPx). Ovals represent enzymes; grey rectangles indicate substrates. Grey ovals represent proteins only observed in the *P. sulfincola* EST database. Color indicates significance and direction of regulation. Asterisks indicate ATP-dependent enzymatic steps. Numbers in diamonds correspond to protein count rows in Table 1b. DNMT is found in cysteine pathway only; at present, the specific seleno-methyltransferase for Paralvinellids is unknown. Some reaction cofactors omitted for simplicity. Abbreviations: AHCY, Adenosylhomocysteinase A; CBS, Cystathionine β-synthase; CGL, Cystathionine γ-synthase; DNMT, DNA (cytosine-5-)-methyltransferase; GPx, Glutathione Peroxidase; GS, Glutathione synthetase; GSH, Glutathione; GSSH, glutathione disulfide; GSR, Glutathione reductase; GSTs, Glutathione sulfur transferases; MAT2, Methionine adenosyltransferase; SelD, Selenide water dikinase.

→ 38°C - log 5.55, Pr(DE) 1.00). Two ATP-dependent rate-limiting steps within the glutathione pathway were detected in our *P. sulfincola* and *P. palmiformis* proteomes: selenide water dikinase (selD, EC 2.7.9.3), and gamma-glutamylcysteine synthetase (GCS, EC 6.3.2.2) (**Figure 2.3**). SelD, essential for *de novo* synthesis of selenoproteins, increased in *P. sulfincola* at 30°C and 45°C, though *P. palmiformis* demonstrated no discernable differential expression. GCS, the rate-limiting step in the production of GSH and subject to feedback inhibition (42), showed a steady increase in expression with temperature in *P. sulfincola*. In *P. palmiformis*, however, GCS was not detected until 38°C treatment, producing a significant correlation with temperature (12°C → 38°C - log 3.81). In concert these data suggest that GSH is being synthesized at higher rates in response to increasing thermal stress in both species.

The catalyst enzyme glutathione peroxidase 3 (GPx-3, cytosolic) showed significant increases in expression at both the medium and high temperature treatments in *P. sulfincola*, as well as at the highest treatment in *P. palmiformis*. Phospholipid hydroperoxide glutathione peroxidase (GPx-4, membrane bound in mitochondria) remained fairly constant in *P. sulfincola* treatments, but exhibits a significant decrease with temperature in *P. palmiformis*. Regulation of GSR also appears to differ dramatically between the species – *P. sulfincola* significantly increases its GSR protein abundance while *P. palmiformis* significantly decreases. These data suggest that *P. sulfincola* is successfully catalyzing and recycling the thiol in the mitochondria. We also hypothesize that the differences here may be indicative of mitochondrial dysfunction and uncoupling in *P. palmiformis*, possibly due to lipid peroxidation from increasing ROS activity, as has previously been observed in cold-water marine mollusks exposed to heat stress and functional hypoxia (5, 36).

To further investigate the effect of thermal and oxidative stress on the pool of GSH, total GSH (GSHt) levels and GSH/GSSG ratios were measured for medium and high temperature treatments in both species (**Figure 2.4**). Notably, GSHt concentrations in *P. sulfincola* were about half those observed in *P. palmiformis.* However, in higher thermal treatments, *P. palmiformis*

Figure 2.4: Glutathione pool and reduced:oxidized ratio analysis

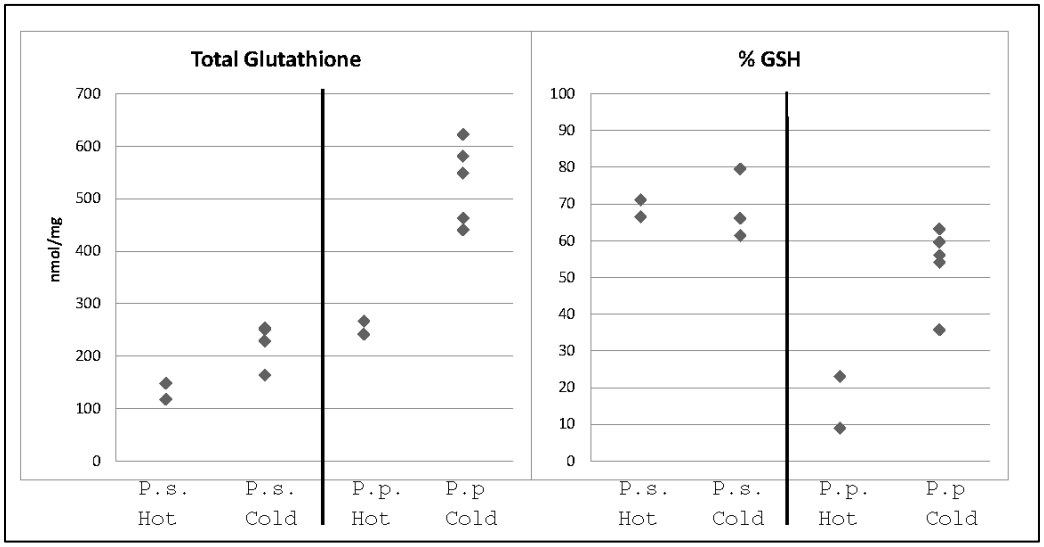

14 samples were analyzed for GSHt: *P. sulfincola* 45°C (2), *P. sulfincola* 30°C (4), *P. palmiformis* 38°C (2), *P. palmiformis* 21°C (6). The GSH/GSSG (reduced:oxidized forms) ratio for each sample except one *P. palmiformis* at 21°C was also determined. A) GSHt (nmol/mg) B) % reduced GSH.

exhibited a 2-fold decrease in the pool of GSHt. A far less pronounced decrease was observed in *P. sulfincola*. In *P. palmiformis* the GSH/GSSG ratio exhibited more than a 3-fold drop at higher thermal treatments, indicating that *P. palmiformis* were not able to recycle glutathione effectively at 38°C. No GSH/GSSG ratio differences were observed among *P. sulfincola* thermal treatments. These trends suggest that *P. sulfincola* may be able to better sustain GSH recycling even near its UILT – allowing it to maintain functionality even under periods of high oxidative stress (though there was insufficient sample to statistically test these results).

Oxidative Stress and Oxidative Phosphorylation

In eukaryotes, oxidative phosphorylation within the ETC is responsible for the majority of ATP production as well as ROS formation. Previous research has indicated that elevated temperature can lead to local tissue hypoxia (41) and increased metabolic demand which leads to a proliferation of endogenous ROS production. Thus, organisms able to reduce mitochondrial respiration respond more readily to increases in oxidative stress.

P. sulfincola exhibited a significant reduction across subunits of NADH dehydrogenase (10°C → 45°C - log -2.01) and succinate dehydrogenase (10°C → 45°C - log -1.00), both of which are involved in the mitochondrial ETC . Indeed, a large portion of ROS is generated by NADH dehydrogenase (complex I). While succinate dehydrogenase (complex II) is not known to contribute directly ROS formation under normative conditions, it does provide electrons to complex III which does produce ROS. The decrease in NADH dehydrogenase was less pronounced in *P. palmiformis* (12°C → 38°C - log -0.48). Surprisingly, *P. palmiformis* increased succinate dehydrogenase with temperature (12°C → 38°C - log 1.53). This contrasts previous findings on a heat sensitive mussel species, *Mytilus trossulus*, which reduced production of NADH dehydrogenase more than its thermotolerant congener, *Mytilus galloprovincialis* (6). These data suggest that *P. sulfincola*, unlike its cooler adapted congener, may be actively repressing ROS formation at high temperatures by lessening endogenous generation *via* the ETC.

Global proteome responses and emerging hypotheses

The quantitative global protein analyses revealed hundreds of differentially expressed proteins in each treatment. Previous efforts have attempted to ally either transcriptomic or proteomic data to metabolic rate, but have met with limited success (43-44). This is attributable to the complexity of regulating biological systems, all of which collude to govern net flux. Nevertheless, changes in metabolic pathways provide a general means of assessing organismal response to thermal stress. To that end, iPath (45) was used to map significant (PP <0.05) changes in global protein abundance within 139 KEGG metabolic pathways. This technique reveals significant, broad and complex differences in protein expression between species and among treatments. What is immediately evident is that the level of protein upregulation for *P. palmiformis* 21°→ 38°C is significantly higher than in other comparisons. One explanation for this phenomenon is that the treatment may have surpassed the range *P. palmiformis* is able to metabolically regulate, and may be experiencing metabolic disorder. **Figure 2.5** highlights two specific pathways (TCA cycle and the pentose phosphate pathway) known to respond to thermal stress (6, 12). At their respective highest thermal exposures in the TCA cycle (the key pathway in aerobic respiration), *P. sulfincola* and *P. palmiformis* exhibited opposing patterns, with *P. sulfincola* decreasing and *P. palmiformis* increasing expression of enzymes respectively. In the pentose phosphate pathway (which shunts glucose from glycolysis to produce pentose), *P. sulfincola* and *P. palmiformis* again exhibited opposing patterns of expression, exhibiting increased and decreased enzymes respectively. These data demonstrate that enzymes within these pathways exhibit sensitivity to changes in temperature, though the precise influence of these changes on pathway regulation and flux remains to be determined. These observed trends in the two aforementioned pathways are consistent with a decreased emphasis on aerobic respiration (TCA cycle) and the need for reducing equivalents to maintain sufficient GSH for antioxidant activity (pentose can be made into glucose 6-phosphate to produce NADPH, a reducing equivalent, used by GSR to recycle oxidized GSH (46)). Further targeted studies may reveal

Figure 2.5: Highlighted shifts in TCA cycle and Pentose Phosphate Pathway

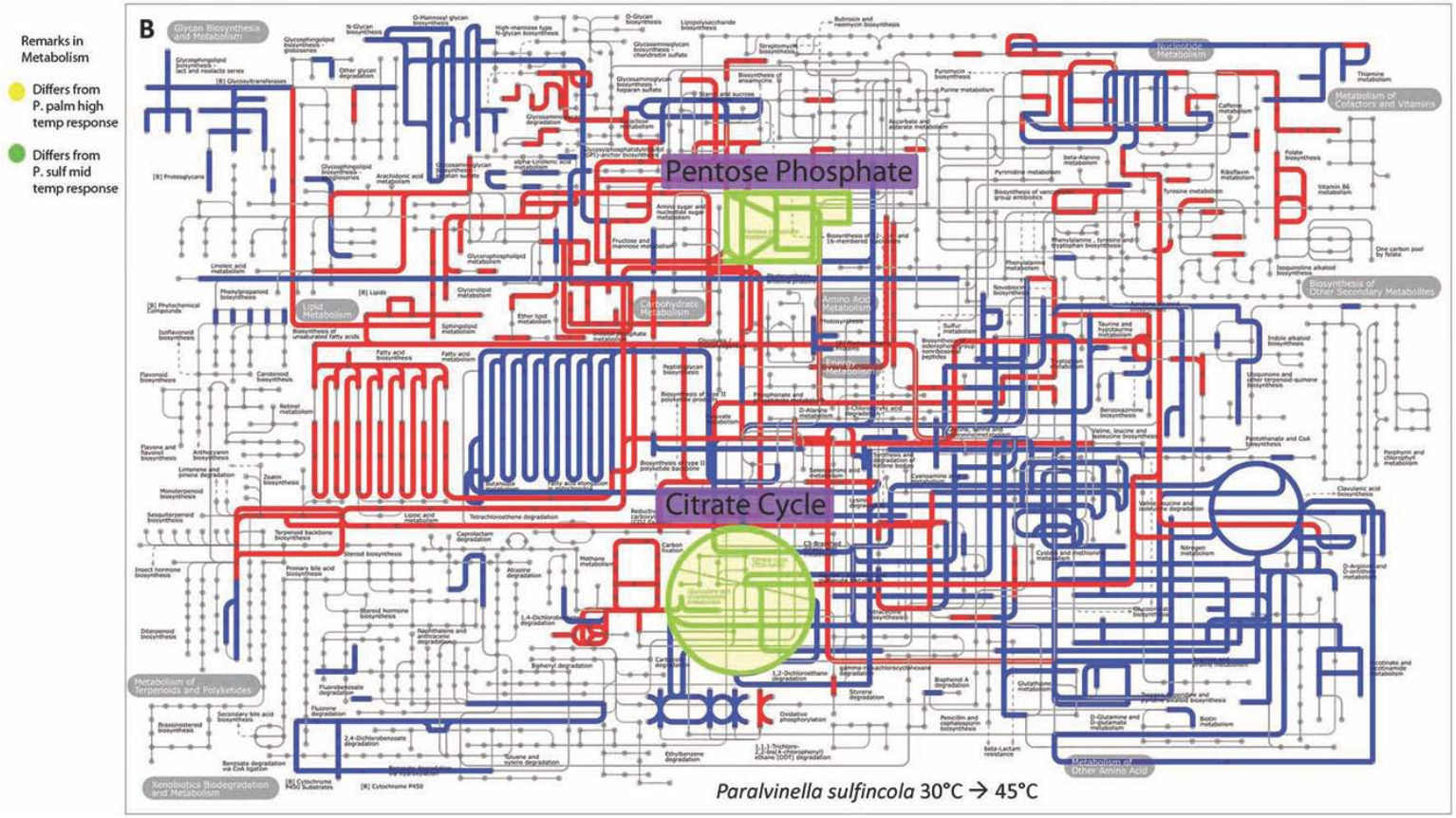

This graph depicts the number of metabolic pathways in *P. sulfincola* 30°C → 45°C that are downregulated (blue), upregulated (red), or not significantly shifted (grey). Additionally, two pathways (TCA cycle and Pentose Phosphate Pathway) that show differential regulation from other treatment types are highlighted in relation to S1a (green) and S1d (yellow).

correlations between flux rates and protein counts, helping our understanding of the effects of thermal stress on metabolic processes.

Conclusions

Based on the proteomic and antioxidant data presented here, we conclude that *P. sulfincola* maintains a pool of heat shock proteins (both canonical constitutive and inducible forms) to cope with rapid, frequent exposure to high temperatures. This lack of induction may be similar to the case of HSP70 in some Antarctic notothenioid fish which also maintain constant levels of the chaperone to prevent protein misfolding at low temperature (47). This is not to imply that *P. palmiformis* is incapable of mitigating rapid thermal responses – *P. palmiformis*, like other comparatively mesotolerant vent endemics *Paralvinella grasslei* (15) and *Rimicaris exoculata* (48), exhibited significant increases in major molecular chaperones with increasing temperature. However *P. sulfincola's* habitat, which is in close proximity to extremely high temperature fluids, has selected for the capacity to more rapidly respond to thermal fluctuations.

Notably, enzymes and pathways associated with the production of antioxidants showed the most pronounced response to thermal exposure in both *P. sulfincola* and *P. palmiformis*. While both species showed increased expression of proteins vital to the creation of the antioxidant GSH, only *P. sulfincola* increased enzymes responsible for reducing GSSG. Increasing the *de novo* synthesis of GSH from the cysteine pathway (and the catalytic enzyme GPx through increases in selenocysteine) at elevated temperatures underscores this pathway's relevance in oxidative scavenging. Increased production of GSR, necessary for recycling GSSG further demonstrates that *P. sulfincola* maintains a sufficient pool of GSH to mitigate oxidative stress. Finally, the concurrent decreases in *P. sulfincola* enzymes associated with oxidative phosphorylation within the ETC may reduce the rate of oxidative radical formation at high temperature.

We posit that *P. sulfincola's* pronounced thermotolerance is enabled primarily by adaptations to mitigate oxidative stress, which include increasing activity of antioxidant systems and decreasing aerobic metabolism. We further suggest these patterns demonstrate that managing ROS, resulting from increased mitochondrial aerobic respiration at elevated temperatures, is a very high priority for thermotolerant organisms. Considering that all metazoans are ultimately dependent on mitochondrial aerobic respiration, ROS may effectively limit them to cooler thermal regimes than thermophilic bacteria and archaea (the most thermophilic prokaryotes are anaerobes, and exhibit a striking antioxidant response when exposed to modest amounts of oxygen (49)). Although oxidative stress has been implicated in previous studies on mesophilic eukaryotes (2, 5-6, 41), this is the first study to empirically derive this link between the UILT and ROS production in one of the most thermotolerant metazoans on the planet, suggesting that oxidative stress -not temperature itself- may limit metazoan thermal tolerance.

Materials and Methods

Animal collection and experimental apparatus

Paralvinella sulfincola and *Paralvinella palmiformis* "palm worms" were collected from hydrothermal vents in the Main Endeavour field located along the Juan de Fuca Ridge (47°57'N, 129°5'W) at a depth of 2,200m during the R/V *Atlantis* cruise 15-34 in July 2008. Organisms were collected by the DSRV *Alvin* on dives #4409-4423, using either a multi-chamber suction sampler or an insulated sample recovery box. Upon recovery at 1 atm, animals were transferred to a 4°C cold room and visually sorted based on segment number and gill morphology. Aggregations of mucus and minerals were removed from the animals before transfer into a flow-through high pressure aquaria system.

High-pressure aquaria system

Moderate and high temperature incubations were conducted in a newly designed high pressure aquaria system (**Figure 2.6**). *Paralvinella sulfincola* low temperature incubations (10°C)

Figure 2.6: High pressure respirometry system

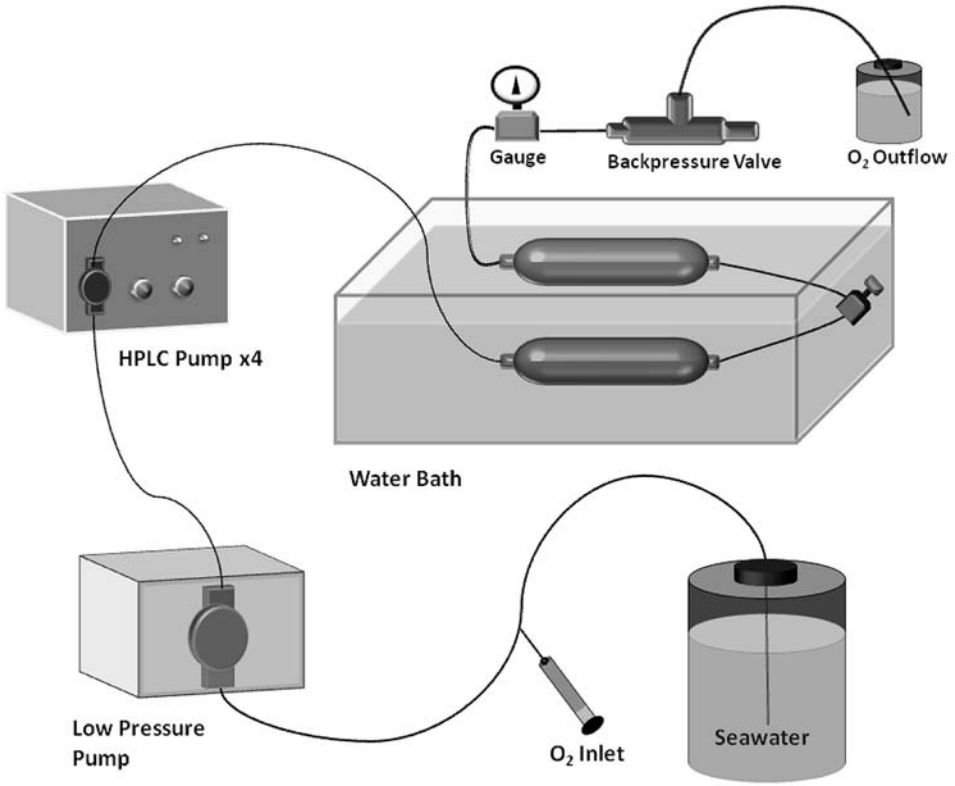

Filtered seawater is drawn from a reservoir using a low pressure pump and fed into four high pressure liquid chromatography pumps. These pumps pressurize the seawater to 20.6MPa (204 atm) and irrigate the Teflon-lined stainless steel chambers at 10 $mL \bullet min^{-1}$. Pressure is measured using a gauge and manually adjusted via a backpressure valve. Isothermal temperatures are maintained by submerging the chambers in large water baths. Discrete dissolved oxygen measurements are taken at the inlet and outlet of the system to determine respiration rates.

were performed in 30-mL flow-through aluminum pressure chambers with 10 mL/min flow rate (as in (18)). *Paralvinella palmiformis* low temperature incubations (12°C) were conducted in a 500 cm^3 titanium flow-through system with 50 mL/min flow rate (50). Dissolved oxygen concentration was measured at the inlet and outlet of each system using a polarigraphic oxygen electrode (limits of detection ca. 1 μM; YSI Inc) to verify that oxygen was always greater than 25 μM, which would not be limiting based on known hemoglobin oxygen binding affinities of alvinellids (51). Dissolved oxygen at air-saturation levels is likely higher in our system than the organism would see at high temperature on the vent, as temperature and oxygen concentration are frequently inversely related at vents. However phosphatase 2A inhibitor (PP2A), the protein identified as overexpressing in *Alvinella pompejana* during hyperoxic treatment (52), was not differentially regulated in our dataset *P. sulfincola* Pr(DE) 0.066, *P. palmiformis* Pr(DE) 0.191.

Experimental design

Though critical thermal maxima (CT_{max}) of both species and thermal preference of *P. sulfincola* were previously examined (17-18), we augmented these data to better establish the chronic thermal tolerance of *P. sulfincola and P. palmiformis* (**Figure 2.1**). A total of 85 *P. sulfincola* and 108 *P. palmiformis* were utilized in this study. Chronic thermal tolerance was defined as a lack of temperature induced mortality over 12 hours of sustained exposure. On occasion, <5% of individuals died during treatments, which upon further inspection we attributed to recovery and handling error. Based on these data, three temperatures were chosen that span the chronic thermal tolerance range of each species (*P. sulfincola* = 10°C, 30°C, and 45°C; *P. palmiformis* = 12°C, 21°C, and 38°C; **Figure 2.1**). At each treatment, six to nine worms were maintained at constant pressure and temperature for >12 hours for global protein expression analysis. To minimize the effects of collection and handling, worms were first acclimated in each system at room temperature (21°C) for a period of twelve hours prior to experimentation. At the conclusion of each trial, the chambers were quickly depressurized; worm health was assessed by looking for signs of embolisms, motor dysfunction or other physiological damage that might have

arisen from thermal exposure or other experimental handling. Healthy worms were selected, and their branchiae and body tissues were separated and flash frozen in liquid nitrogen for subsequent protein extraction.

Transcriptome Sequencing and Analysis

A *Paralvinella sulfincola* expressed sequence tag (EST) library was sequenced and built by the Joint Genome Institute (Walnut Creek, CA). Briefly, mRNA was purified from total RNA isolated at two different temperature conditions for two tissue types (body and gill). cDNA from each was generated using an oligodT primer followed by template switching (Clontech, Mountain View, CA) and subsequently normalized using the provided protocol of the Evrogen Normalization kit (Evrogen, Moscow, Russia). The normalized cDNA was used to build a library with the construction protocol provided in the 454 Flx Titanium Roche kit (Roche, Branford, CT) and then sequenced. Four EST libraries consisting of 2,593,853 reads were filtered and screened for quality and contamination to produce a filtered $_{set}$ of 2,382,211 reads. These reads were then assembled using Newbler (v2.3-PreRelease-6/30/2009), which resulted in 80748 raw contigs. These sequences were combined to create 24,821 isotigs with 19,036 remaining contigs. A cutoff minimum length of 350 base pairs further trimmed the final count to 24,702 sequences (24,164 isotigs and 538 contigs).The average length of this library is 1,290 bp/sequence and the GC content average is 0.40. The sequences were aligned using BlastX with the Swissprot database. 12,562 of the translated sequences had a known BlastX match and 7,002 unique proteins were identified. Longest ORF translations were used as the reference library for all subsequent MS/MS oligopeptide spectra.

Protein extraction

Gill branchiae from three *P. sulfincola* and three *P. palmiformis* per treatment were excised, weighed on an electronic balance (Mettler Toledo, Columbus, OH), and placed into heat-sterilized 0.5 mL glass micropestles (Wheaton, Millville, NJ) containing 24 uL of 20mM Tris pH 7.5 buffer and 6 uL Protease Inhibitor Cocktail (PIC) (Sigma-Aldrich, St. Louis, MO). Tissue was

homogenized until complete dissociation and centrifuged at 1000x g for 5 minutes. For protein extraction, 0.5 mg gill branchiae were used in a modified Laemmli protein boil protocol (53). A Tris/PIC mixture at 1:1v/v and 1:20 2-mercaptoethanol/ Laemmli Buffer were added, and the solution was heated at 95°C for 10 minutes. All extractions were loaded in separate lanes onto 4-20% precast Precise Protein Gels (Pierce Inc) with blank lanes between samples. The gels were bathed in a Tris-HEPES-SDS buffer solution and electrophoresed for 45 minutes at 100V. Band size and run length were assessed by including 10uL of BenchMark Pre-Stained Protein Ladder 10-190 kDa (Invitrogen, Carlsbad, CA). After electrophoresis, gels were rinsed and stained for three hours using the colloidal commassie blue dye Novex (Invitrogen, Carlsbad, CA) according to the manufacturer's instructions. Gels were visualized using a digital gel imaging system - Kodak Gel Logic 100- (Kodak, Rochester, NY) and sub-sectioned into six fragments according to protein size. The three biological replicates from each treatment were pooled into one sample per fragment; total gel surface area did not exceed $1cm^2$. The pooled gel sub-sections were then washed with 1 mL of 50% acetonitrile and frozen at -20°C prior to analysis.

Protein analyses by tandem mass spectrometry

A total of 36 pooled samples (2 species incubated at 3 temperatures fractionated into 6 equal sections) were reduced, carboxyamidomethylated, and digested with trypsin. Resulting peptides from each sample were analyzed over 3 technical replicates using microcapillary reverse-phase HPLC directly coupled to the nano-electrospray ionization source of a ThermoFisher LTQ-Orbitrap XL (replicate 1) or LTQ-Orbitrap Velos (replicates 2 and 3) hybrid mass spectrometer (μLC/MS/MS). The Orbitrap repetitively surveyed *m*/*z* range from 395-1600, while data-dependent MS/MS spectra on the 20 most abundant ions in each survey scan were acquired in the linear ion trap. MS/MS spectra were acquired with a relative collision energy of 30%, 2.5-Da isolation width, and recurring ions dynamically excluded for 60s. Preliminary evaluation of peptide-spectrum matches (PSMs) was facilitated using the SEQUEST algorithm with a 30 ppm mass tolerance against the *P. sulfincola* EST library and NCBI nr databases. PSMs

were accepted with mass error <3.0 ppm and score thresholds to attain an estimated false discovery rate of ~1% using a reverse decoy database strategy and a custom version of the Harvard Proteomics Browser Suite (ThermoFisher Scientific, San Jose, CA). A total of 172,122 peptide spectra were identified with an average of 14.6 amino acids/sequence, with MS/MS spectra populating 1296 referenced proteins.

Glutathione Measurements

Total GSH and GSSG levels were measured using the Glutathione Assay Kit (Cayman Chem, Ann Arbor, MI) as per the manufacturer's instructions. Spectrophotometric readings were taken kinetically for 30 minutes using a Spectramax Plus^{384} (Molecular Devices, Sunnyvale, CA). Internal standards were run with total GSH and GSSG experimental treatments, and standard curves were built from the endpoint readings.

Data Analysis and Statistics

BaySeq (54) was used to determine statistically significant relative changes over experimental treatments. Peptide spectral counts were modeled using a negative binomial distribution to account for potential overdispersion among treatment replicates. The empirical Bayesian method used in baySeq is useful for count data with few replicates per treatment, an issue that frequently arises in high-throughput sequencing studies. By borrowing information on replicate variance among peptides over the entire dataset, the method employed in baySeq better calibrates replicate variance for individual peptides than can be achieved through alternative, more standard methods of modeling overdispersed count data. Using a likelihood cutoff of 0.9, Bayesian analysis revealed 428 differentially expressed proteins in *Paralvinella palmiformis* and 214 differentially expressed proteins in *Paralvinella sulfincola*. We use the convention of a 0.9 likelihood cutoff throughout the analysis as in significance indicator, but it is important to note that Bayesian methodology allows for the comparison of relative likelihoods that we explore within the context of each protein family. Additionally, metabolic enzyme regulation was examined *via* pathway analysis. The R package ShotgunFunctionalizeR (Version: 1.0-3, Date:

2009-10-09) was used after assigning Enzyme Commission (EC) numbers to sequences using KEGG assignments and the R package BioIDMapper (Version: 2.1, Date: 2010-01-16). To assess statistical support for metabolic pathway-level expression differences, ortholog data were combined into KEGG pathways using in-house scripts. We assumed a binomial distribution in this case, and Monte Carlo methods were used to determine the posterior probability of differential expression, point estimates of pathway abundance and 95% credible intervals for these estimates. Methods for iPath described in (45).

REFERENCES

1. Takai K, Nakamura K, Toki T, Tsunogai U, Miyazaki M, Miyazaki J, et al. Cell proliferation at 122 degrees C and isotopically heavy CH4 production by a hyperthermophilic methanogen under high-pressure cultivation. Proc Natl Acad Sci U S A. 2008 Aug 5;105(31):10949-54.

2. Pörtner H. Climate change and temperature-dependent biogeography: oxygen limitation of thermal tolerance in animals. Naturwissenschaften. 2001;88(4):137-46.

3. O'Brien J, Dahlhoff E, Somero G. Thermal resistance of mitochondrial respiration: hydrophobic interactions of membrane proteins may limit thermal resistance. Physiological zoology. 1991;64(6):1509-26.

4. Brock T, Libraries UoWM. Thermophilic microorganisms and life at high temperatures: Springer-Verlag New York; 1978.

5. Abele D, Heise K, Portner H, Puntarulo S. Temperature-dependence of mitochondrial function and production of reactive oxygen species in the intertidal mud clam *Mya arenaria*. J Exp Biol. 2002;205(13):1831-41.

6. Tomanek L, Zuzow MJ. The proteomic response of the mussel congeners *Mytilus galloprovincialis* and *M. trossulus* to acute heat stress: implications for thermal tolerance limits and metabolic costs of thermal stress. J Exp Biol. 2010 Oct 15;213(Pt 20):3559-74.

7. Portner HO, Knust R. Climate change affects marine fishes through the oxygen limitation of thermal tolerance. Science. 2007 Jan 5;315(5808):95-7.

8. Portner HO, Bennett AF, Bozinovic F, Clarke A, Lardies MA, Lucassen M, et al. Trade-offs in thermal adaptation: the need for a molecular to ecological integration. Physiol Biochem Zool. 2006 Mar-Apr;79(2):295-313.

9. Somero GN. Comparative physiology: a "crystal ball" for predicting consequences of global change. Am J Physiol Regul Integr Comp Physiol. 2011 Jul;301(1):R1-14.

10. Gehring W, Wehner R. Heat shock protein synthesis and thermotolerance in *Cataglyphis*, an ant from the Sahara desert. Proceedings of the National Academy of Sciences of the United States of America. 1995;92(7):2994.

11. Wickstrom C, Castenholz R. Thermophilic ostracod: aquatic metazoan with the highest known temperature tolerance. Science. 1973;181(4104):1063.

12. Nguyen TT, Michaud D, Cloutier C. A proteomic analysis of the aphid *Macrosiphum euphorbiae* under heat and radiation stress. Insect Biochem Mol Biol. 2009 Jan;39(1):20-30.

13. Cary SC, Shank T, Stein J. Worms bask in extreme temperatures. Nature (London). 1998;391(6667):545-6.

14. Chevaldonné P, Fisher C, Childress J, Desbruyères D, Jollivet D, Zal F, et al. Thermotolerance and the'Pompeii worms'. Marine Ecology Progress Series. 2000;208:293-5.

15. Cottin D, Ravaux J, Leger N, Halary S, Toullec JY, Sarradin PM, et al. Thermal biology of the deep-sea vent annelid *Paralvinella grasslei*: in vivo studies. J Exp Biol. 2008 Jul;211(Pt 14):2196-204.

16. Sarrazin J, Levesque C, Juniper S, Tivey M. Mosaic community dynamics on Juan de Fuca Ridge sulphide edifices: substratum, temperature and implications for trophic structure. CBM-Cahiers de Biologie Marine. 2002;43(3-4):275-9.

17. Girguis PR, Lee RW. Thermal preference and tolerance of alvinellids. Science. 2006 Apr 14;312(5771):231.

18. Lee RW. Thermal tolerances of deep-sea hydrothermal vent animals from the Northeast Pacific. Biol Bull. 2003 Oct;205(2):98-101.

19. Selong JH, McMahon TE, Zale AV, Barrows FT. Effect of temperature on growth and survival of bull trout, with application of an improved method for determining thermal tolerance in fishes. Transactions of the American Fisheries Society. 2001;130(6):1026-37.

20. Kilgour DM, McCauley RW. Reconciling the two methods of measuring upper lethal temperatures in fishes. Environmental Biology of Fishes. 1986;17(4):281-90.

21. Arndt V, Rogon C, Hohfeld J. To be, or not to be--molecular chaperones in protein degradation. Cell Mol Life Sci. 2007 Oct;64(19-20):2525-41.

22. Mayer MP, Bukau B. Hsp70 chaperones: cellular functions and molecular mechanism. Cell Mol Life Sci. 2005 Mar;62(6):670-84.

23. Feder ME, Hofmann GE. Heat-shock proteins, molecular chaperones, and the stress response: evolutionary and ecological physiology. Annu Rev Physiol. 1999;61:243-82.

24. Parsell DA, Lindquist S. The function of heat-shock proteins in stress tolerance: degradation and reactivation of damaged proteins. Annu Rev Genet. 1993;27:437-96.

25. Vos MJ, Hageman J, Carra S, Kampinga HH. Structural and functional diversities between members of the human HSPB, HSPH, HSPA, and DNAJ chaperone families. Biochemistry. 2008 Jul 8;47(27):7001-11.

26. Terasawa K, Minami M, Minami Y. Constantly updated knowledge of Hsp90. J Biochem. 2005 Apr;137(4):443-7.

27. Wandinger SK, Richter K, Buchner J. The Hsp90 chaperone machinery. J Biol Chem. 2008 Jul 4;283(27):18473-7.

28. Eletto D, Dersh D, Argon Y. GRP94 in ER quality control and stress responses. Semin Cell Dev Biol. 2010 Jul;21(5):479-85.

29. Martin J, Horwich AL, Hartl FU. Prevention of protein denaturation under heat stress by the chaperonin Hsp60. Science. 1992 Nov 6;258(5084):995-8.

30. Höhfeld J, Hartl FU. Role of the chaperonin cofactor Hsp10 in protein folding and sorting in yeast mitochondria. The Journal of cell biology. 1994;126(2):305.

31. Arrigo AP, Virot S, Chaufour S, Firdaus W, Kretz-Remy C, Diaz-Latoud C. Hsp27 consolidates intracellular redox homeostasis by upholding glutathione in its reduced form and by decreasing iron intracellular levels. Antioxid Redox Signal. 2005 Mar-Apr;7(3-4):414-22.

32. Arrigo AP. Hsp27: novel regulator of intracellular redox state. IUBMB Life. 2001 Dec;52(6):303-7.

33. Schroder M, Kaufman RJ. ER stress and the unfolded protein response. Mutat Res. 2005 Jan 6;569(1-2):29-63.

34. Noiva R. Protein disulfide isomerase: the multifunctional redox chaperone of the endoplasmic reticulum. Semin Cell Dev Biol. 1999 Oct;10(5):481-93.

35. Lesser MP. Oxidative stress in marine environments: biochemistry and physiological ecology. Annu Rev Physiol. 2006;68:253-78.

36. Abele D, Puntarulo S. Formation of reactive species and induction of antioxidant defence systems in polar and temperate marine invertebrates and fish. Comp Biochem Physiol A Mol Integr Physiol. 2004 Aug;138(4):405-15.

37. Andreyev AY, Kushnareva YE, Starkov AA. Mitochondrial metabolism of reactive oxygen species. Biochemistry (Mosc). 2005 Feb;70(2):200-14.

38. Starkov AA. Protein-mediated energy-dissipating pathways in mitochondria. Chem Biol Interact. 2006 May 15;161(1):57-68.

39. Heise K, Puntarulo S, Portner HO, Abele D. Production of reactive oxygen species by isolated mitochondria of the Antarctic bivalve *Laternula elliptica* (King and Broderip) under heat stress. Comp Biochem Physiol C Toxicol Pharmacol. 2003 Jan;134(1):79-90.

40. Keller M, Sommer AM, Portner HO, Abele D. Seasonality of energetic functioning and production of reactive oxygen species by lugworm (*Arenicola marina*) mitochondria exposed to acute temperature changes. J Exp Biol. 2004 Jun;207(Pt 14):2529-38.

41. Portner HO. Climate variations and the physiological basis of temperature dependent biogeography: systemic to molecular hierarchy of thermal tolerance in animals. Comp Biochem Physiol A Mol Integr Physiol. 2002 Aug;132(4):739-61.

42. Pastore A, Federici G, Bertini E, Piemonte F. Analysis of glutathione: implication in redox and detoxification. Clin Chim Acta. 2003 Jul 1;333(1):19-39.

43. Fraenkel DG. The top genes: on the distance from transcript to function in yeast glycolysis. Curr Opin Microbiol. 2003 Apr;6(2):198-201.

44. Williams TC, Poolman MG, Howden AJ, Schwarzlander M, Fell DA, Ratcliffe RG, et al. A genome-scale metabolic model accurately predicts fluxes in central carbon metabolism under stress conditions. Plant Physiol. 2010 Sep;154(1):311-23.

45. Letunic I, Yamada T, Kanehisa M, Bork P. iPath: interactive exploration of biochemical pathways and networks. Trends Biochem Sci. 2008 Mar;33(3):101-3.

46. Go YM, Jones DP. Redox compartmentalization in eukaryotic cells. Biochim Biophys Acta. 2008 Nov;1780(11):1273-90.

47. Clark MS, Peck LS. HSP70 heat shock proteins and environmental stress in Antarctic marine organisms: a mini-review. Marine Genomics. 2009;2(1):11-8.

48. Ravaux J, Gaill F, Bris NL, Sarradin PM, Jollivet D, Shillito B. Heat-shock response and temperature resistance in the deep-sea vent shrimp *Rimicaris exoculata*. J Exp Biol. 2003;206(14):2345.

49. Kawakami R, Sakuraba H, Kamohara S, Goda S, Kawarabayasi Y, Ohshima T. Oxidative stress response in an anaerobic hyperthermophilic archaeon: presence of a functional peroxiredoxin in *Pyrococcus horikoshii*. Journal of biochemistry. 2004;136(4):541.

50. Henry M, Childress J, Figueroa D. Metabolic rates and thermal tolerances of chemoautotrophic symbioses from Lau Basin hydrothermal vents and their implications for species distributions. Deep Sea Research Part I: Oceanographic Research Papers. 2008;55(5):679-95.

51. Hourdez S, Lallier F. Adaptations to hypoxia in hydrothermal-vent and cold-seep invertebrates. Reviews in Environmental Science and Biotechnology. 2007;6(1):143-59.

52. Mary J, Rogniaux H, Rees JF, Zal F. Response of *Alvinella pompejana* to variable oxygen stress: a proteomic approach. Proteomics. 2010;10(12):2250-8.

53. Laemmli U. Cleavage of structural proteins during the assembly of the head of bacteriophage T4. Nature. 1970;227(5259):680-5.

54. Hardcastle T, Kelly K. baySeq: Empirical Bayesian methods for identifying differential expression in sequence count data. BMC bioinformatics. 2010;11(1):422.

Chapter 3

Understanding the independent and combined effects of temperature, pH, and sulfide concentration on respiration of the hydrothermal vent polychaete *Paralvinella sulfincola*

Abstract

Abiotic influences often co-vary in dynamic environments but most physiological stress studies focus on response to only one variable. At hydrothermal vents, organisms must adapt to changes in temperature, pH, and sulfide concentration, as well as many other factors. This study is the first to examine the synergistic effects of sulfide, pH, and thermal stresses on the highly thermotolerant hydrothermal vent annelid, *Paralvinella sulfincola.* A series of sustained stress tolerance experiments were conducted, with each varying levels of temperature (30°C and 45°C), pH (6.0 and 8.0), and sulfide concentration (0μM and 250 μM) either unaccompanied and in concert. Using a dissolved oxygen probe, we concurrently measured real-time aerobic respiration rates of *P. sulfincola* exposed for each treatment in high pressure aquaria. These data were combined with subsequent *in vitro* measurements on treated worms of intracellular pH buffering capacity and unbound internal sulfide concentrations, as well as comparisons to rate calculations from previous literature.

We determined that lowered pH and increased sulfide had, separately, the effect of increasing aerobic metabolic demand by ~3x within the animal. However, for *P. sulfincola* exposed to both influences simultaneously, we recorded a 20x increase in metabolic demand. We posit that this synergistic effect when pH is lowered in the presence of high levels of sulfide is due to two causes – 1) at lower pH, sulfide is found in the more membrane permeable and toxic

H_2S species, and 2) the sulfide detoxification pathway causes an increase in intracellular H^+ equivalents which the organism must expend energy to equilibrate. These findings are timely and applicable, as current climate change models show that most marine organisms in the near future will face a multistressor system of elevated CO_2 and elevated temperature coupled with a lower pH, known as ocean acidification.

Introduction

The maintenance of homeostasis is required for sustained biological function, yet most organisms chronically face environmental perturbations that challenge this equilibrium. Stressors of homeostasis include both biotic (i.e. predation, feeding, and competition) and abiotic stresses (i.e. thermal, chemical, and physical changes in the environment). As "open, modulated systems", organisms cannot perpetually insulate themselves from variations in environmental conditions. Rather, organisms must acclimate in response to perturbations (and, over evolutionary time, adapt to cope with significant, chronic environmental changes).

Organisms living in highly dynamic environments must rapidly adapt to environmental variations. Hydrothermal vents are renowned for their extremely dynamic physical and geochemical conditions, and animals living near hydrothermal vents endure wide fluctuations in temperature, pH, and sulfide, as well as other environmental stressors (1). Endemic to the Juan de Fuca Ridge, a vent system in the northeast Pacific, the polychaete *Paralvinella sulfincola* (Desbruyères and Laubier 1993- Tunnicliffe et al 1993) (2) lives closest to the dynamic vent effluent. Among *P. sulfincola*, environmental conditions range from 3°C to 89°C (3), 0 to 300μM sulfide and, due to the acidity of vent effluent, a range of pH (4). Previous research has shown they can tolerate sustained thermal regimes from 4°C to over 55°C, depending on duration of exposure (5-6). While temperature tolerance of alvinellids has received much attention (4, 7-9), little is known about their response to changes in sulfide or pH, and no *in vivo* studies to date have examined these factors. In other vent organisms, experiments have shown that perturbations

to pH and sulfide can adversely affect organismal function, even resulting in death (10). In sulfidic mudflats, experiments involving the worm *Urechis caupo* has established that simultaneous increases in environmental stressors can induce responses that are more than the sum of their individual effects (11-12), a so called multi-stressor response. Recently, because of the combination of ocean acidification and global warming tied to increasing levels of pCO_2, new studies of multistressor effects are beginning to examine the effects of thermal tolerance and hypercapnia on marine organisms such as the ophiuroid *Ophionereis schayeri* (13-14).

Given the environment of *Paralvinella sulfincola*, thermal tolerance, maintenance of intracellular pH via acid-base regulation, and sulfide detoxification are essential to maintain or regain homeostasis during periods of stress. Each of these environmental factors can affect a variety of systems within an organism. Thermal stress increases the rate of formation of reactive oxygen species (ROS) (15-16) and can lead to membrane instability (17-18). Decreasing pH can lead to shifts in the bicarbonate buffering system and ultimately hypoxia, and metabolic acidosis and depression (13, 19). Sulfide can bind to and inhibit cytochrome *c* oxidase (COX) (20-22) as well as cause an increase in ROS damage (23). Applied together, these stresses may act in concert to exacerbate the challenge to homeostasis through a multiple-stress event as described above. Furthermore, emergent stresses can occur when multiple conditions are met. For example, sulfide exists in three charge states: $H_2S \Leftrightarrow HS^- \Leftrightarrow S^{2-}$. The pKa_1 ($H_2S \Leftrightarrow HS^-$) is 7.2 (21, 24). Between 7.2 and pKa_2 ($HS^- \Leftrightarrow S^{2-}$, 11.7), the dominant chemical species is HS^-. Below 7.2, the predominant state shifts to H_2S which is more permeable to tissue membranes, causing greater damage (11, 25). Thus, when the pH of the vent fluid drops in the presence of sulfide, organisms face increased sulfide permeability and toxicity.

To effectively assess the impact of these key environmental stressors, we conducted a series of experiments on *P. sulfincola* in which we studied the independent and interconnected effects of decreasing pH, increasing sulfide concentrations, and increasing temperature on aerobic respiration (measured here as oxygen consumption rate). To better understand the combined

effects of pH and sulfide on oxygen respiration, we developed a conceptual model to predict the flux of hydrogen ions, the speciation of sulfide (H_2S or HS^-), and the subsequent flux of these two sulfide species across the epithelia. Our model also examines and estimates the increase in oxygen consumption required to maintain intracellular pH, as well as to detoxify sulfide. While we hypothesize that respiration rate will increase in response to temperature as has been shown for many invertebrates(26), we further hypothesize that the decreases in pH and increases in sulfide will each, independently result in increased oxygen uptake due to A) increased respiration for the generation of ATP to eliminate proton equivalents and B) increased oxygen uptake to oxidize sulfide to less reactive, less toxic sulfur species. We also hypothesize that the increase in oxygen during simultaneous decreases in pH and increases in sulfide due to the increased proportion of the sulfide species H_2S, which is more membrane permeable and more reactive.

Methods

Animal Collection and Weighing

Paralvinella sulfincola were collected from hydrothermal vents in the Main Endeavour field located along the Juan de Fuca Ridge (47°57'N, 129°5'W) at a depth of 2,200m during the R/V *Atlantis* cruise 15-67 in July 2010. Organisms were collected by the DSRV *Alvin* on dives #4621-4626, using either a multi-chamber suction sampler or an insulated sample recovery box. Upon recovery, animals were visually sorted based on segment number and gill morphology. Aggregations of mucus and minerals were removed from the animals before the animals were placed on a motion compensated shipboard balance for weighing. *P. sulfincola* wet weights were recorded in aggregate for the total biomass of each chamber for per-gram respiration rate calculations.

System Design

Our high pressure respirometry system is modified from the one described in chapter 2. Modifications to the system include the addition of a sulfide delivery system, which enabled

anaerobic sulfidic seawater to be supplied to the vessels for sulfide exposure experiments. Specifically, a 2L polycarbonate vessel was filled with anaerobic seawater in which sodium sulfide salts were dissolved to achieve a concentration of 2.5 mM. The vessel headspace was flushed with nitrogen gas to reduce abiotic sulfide oxidation. A peristaltic pump (Cole Parmer Inc) was equipped with norprene tubing™, and used to deliver this concentrated stock at $1/10^{th}$ speed into the seawater stream, to achieve a final concentration of 250 μM sulfide in the vessels during sulfide treatments. For low pH treatments, 6N HCl was titrated into a 50L 0.2micron filtered seawater reservoir and adjusted to achieve a pH of 6.0 using a handheld pH electrode (Hanna Inc). As before, high pressure pumps irrigated the pressure vessels with seawater of known chemical compositions at a rate of 10 $mL \bullet min^{-1}$. In addition, vessel effluents (post-depressurization via backpressure valves) were directed to a 6-stream selector valve (or SSV, VICI inc. Houston, TX). The SSV was programmed to direct each vessel effluent stream and the pre-vessel stream in series to a Fiber Optic Oxygen Sensor System equipped with a ¼" O.D. optrode probe tip (dO-2000, Golden Scientific, Temecula, CA). The probe tip was housed within a ¼" compression fitting (JACO Inc), and was used to measure dissolved oxygen concentrations in each vessel effluent, as well as the reservoir. Measurements of each channel were recorded every 10 seconds for the duration of ten minutes, using the dO400 v2.0 software and a laptop computer.

Experimental Design and Conditions

This experiment tested the *in vivo* response of *Paralvinella sulfincola* to three independent variables (temperature, sulfide concentration, and pH) by continuously measuring the rate of oxygen respiration throughout the duration of a series of treatment combinations. To test the independent and combinatory effects of these three variables, we designed 7 total treatments, as shown in **Table 3.1**.

Table 3.1: Experimental Design

	pH 8	pH 6
0μM H2S	30°C (4)	30°C (2) 45°C (2)
250μM H2S	30°C (2) 45°C (2)	30°C (2) 45°C (2)

Displayed are the seven treatments performed during this experiment, varying the temperature, pH, and sulfide concentration. The numbers in ( ) are replicate counts.

Five to six pre-weighed *P. sulfincola* were placed into each stainless-steel chamber in our high pressure incubation system and acclimated at pressure overnight (27.5 MPa, 0 μM sulfide, pH 8.0, 21 °C). After the acclimation period, the system was set for a condition described in **Table 1**. Two chambers (10-12 worms) were used per replicate, and four chambers were used per treatment (20-24 worms). Subsampling occurred over a standard time series (2, 4, 6, 10 hours). Concurrent real-time oxygen measurements were recorded as described above. All experiments were concluded at the 10 hour sample point. After *P. sulfincola* were removed from the chambers, they were assessed for viability by looking for movement, and then each individual was quickly flash-frozen for further laboratory assays.

*Intracellular buffering capacity (**β**)*

Total non-bicarbonate buffering was assayed using methods modified from Castellini and Somero (1981) and Seibel et al (1997) (27-28). Frozen treated worms were weighed and then homogenized on ice in 0.5mL normal saline solution (0.9% NaCl) using an eppendorf tube and a Teflon micropestle. 9.5 mL of saline solution was added, and the homogenate was placed on a stir plate. PH of the homogenate was assessed using a S47 SevenMulti pH Meter (Mettler-Toledo, Columbus, OH). If the initial pH was greater than 6.0, the sample was acified using HCl (0.1N) to bring the homogenate to pH 6. Next, a Teflon coated stirbar continually stirred the homogenate during titration with NaOH (0.1N, 2.0 μL). The assay was conducted at 21 °C, over the range of

pH 6.0 to 7.0 with a Distritip™ repeat pipetor. Buffering capacity of each sample was determined based on the slope of the titration from pH 6.0 to pH 7.0. A total of 15 worms were assayed, with five worms representing each of three treatments (30°C, pH 8.0, 0 μM H_2S; 30°C, pH 6.0, H_2S 250μM; 45°C, pH 6.0, H_2S 250μM as well as untreated worms used as control).

Unbound Sulfide Concentration

To measure unbound sulfide in the worm tissues and fluids, we developed a protocol wherein we anaerobically homogenized *P. sulfincola*, filtered out the remaining particulate material, and "trapped" any sulfide in the effluent using 27% zinc acetate solution (which rapidly binds to free sulfide to yield zinc sulfide, which is then quantified using the methods described in Cline (1969) (29). Specifically, experimentally treated frozen animals were weighed and placed in a rigid aluminum anaerobic chamber (Coy Inc, Grass Lake, MI) Previous experiments have demonstrated no significant loss of unbound sulfide due to freezing and thawing (30). Each *P. sulfincola* was homogenized in 300μL anaerobic distilled water using sterile Kontes micropestles (Kimble Chase, Vineland, NJ). The resulting homogenates were placed into microscale desalting spin filters (Microcon 10 kD, Millipore Inc, Billerica, MA) centrifuged at 14000 x g for 30 min inside the anaerobic chamber. When necessary, additional volumes of 50-100 μL of anaerobic distilled water was added to the spin filters to increase sulfide recovery. Samples were continually centrifuged until all liquid had passed through the spin filters. Prior to the spin filtration, we placed 20 μL of 27% Zinc Acetate to trap any free sulfide as a zinc sulfide precipitate at the bottom of each centrifuge tube, The samples were then removed from the chamber, and sulfide was quantified as described in Cline (1969) (29). The samples were run in tandem with a standard curve. The standard curve used *P. sulfincola* maintained for 30 hours at 12 °C in 0 ppm sulfide spiked with a known dilution series of sulfide ($R^2 = 0.9753$), normalizing the effect of tissue constituents on apparent sulfide concentrations**.** All experimental and standard curve readings were taken on a Spectramax Plus 384 UV visible spectrophotometer (Molecular Devices, Sunnyvale, CA) at 670nm using a 96 well optical microtiter dish. A total of twelve experimental

samples are included, representing four individuals from each of three conditions: (45°C, pH 8.0, H_2S 250µM; 30°C, pH 6.0, H_2S 250µM; 45°C, pH 6.0, H_2S 250µM) in addition to untreated worms collected for the standard curve. To determine whether the concentration of unbound sulfide differed significantly between treatments, a standard ANOVA was performed (p <0.05).

Results

Respiration Rates

We report the aerobic respiration rate (µmol O_2 *g^{-1} * h^{-1}) of *P. sulfincola* (wet weight) under varying conditions in **Table 3.2**. Not all of the replicates were continued for the duration of the experiment, as samples were limited and we culled animals at regular intervals for further biochemical analysis. Our pH 6 and 250µM sulfide data is truncated because of an instrument interruption during the first 12 cycles of that experiment. Notably, there were no measureable differences in oxygen consumption rates in vessels run without worms across all experiments, suggesting that endogenous free-living microbial oxygen demand did not contribute to the observed patterns.

Independent effects of decreasing pH and increasing sulfide on oxygen uptake

P. sulfincola maintained at "normative conditions" (defined here as 30°C, 0µM H_2S, pH 8) showed mean respiration rates of 1.13 ± 0.82 µmol O_2•g^{-1}•h^{-1}. These respiration rates establish the baseline value from which we examine shifts due to the aforementioned environmental stressors. After 12 hours exposure to a lower pH 6.0 in the absence of sulfide, mean respiration rates reach 3.46 ± 0.90 µmol O_2•g^{-1}•h^{-1}, exhibiting an increase of 2.33 µmol O_2•g^{-1}•h^{-1}. Exposure to elevated sulfide (250 µmol seawater concentration) at pH 8.0 exhibited a mean oxygen uptake rate of 3.39 ± 0.29 (µmol O_2 *g^{-1} * h^{-1}) at 30°C, revealing a differential increase of 2.26 µmol O_2•g^{-1}•h^{-1} upon exposure to sulfide. Similar patterns were observed at 45°C, with a mean oxygen uptake rate of 6.56 ± 1.84 (µmol O_2 *g^{-1} * h^{-1}). We attribute the additional average increase of

Table 3.2- Oxygen Respiration Rate (µmol O_2 *g^{-1} * h^{-1})

Time (hr)	30°C, 0µM H_2S, pH 8				30°C, 0µM H_2S, pH 6		45°C, 0µM H_2S, pH 6		30°C, 250µM H_2S, pH 8		45°C, 250µM H_2S, pH 8		30°C, 250µM H_2S, pH 6		45°C, 250µM H_2S, pH 6	
	1	2	3	4	1	2	1	2	1	2	1	2	1	2	1	2
0	0.110	-0.045	0.192	0.391	--	--	--	--	--	--	--	--	2.480	1.784	1.995	2.308
1.75	1.335	1.467	0.645	0.781	--	--	--	--	--	--	--	--	0.663	1.773	5.465	8.914
4.75	--	0.981	1.896	2.784	--	--	--	--	0.835	0.206	1.652	-3.180	13.398	8.145	**17.330**	**28.929**
7.75	--	--	1.436	1.813	2.657	2.374	1.738	3.279	2.537	3.406	5.404	4.165	--	10.285	**28.589**	**23.971**
10	--	--	1.951	--	--	3.198	2.716	4.456	3.187	3.590	5.257	7.863	--	23.498	**36.162**	**41.026**

This table shows measured per-gram oxygen respiration rates under each of our treatments. The light grey shaded titles represent either sulfide or pH treatment. Dark grey titles represent combined pH and sulfide treatments. Replicate experiments are numbered. Marker "--" represents no data collected at this time point in the replicate. Samples in bold are those that exceed the theoretical value of 16.02 µmol O_2 *g^{-1} * h^{-1} calculated to be the cumulative effect of each stressor on the high temperature combined experiment.

3.17 μmol O_2 *g^{-1} * h^{-1} in response was to the commonly observed increase in metabolic rate observed in poikilotherms - commonly known as Q_{10} effect of temperature (31).

Combined effect of decreasing pH and increasing sulfide on oxygen uptake

If each environmental stressor exerted a separate, independent effect on aerobic respiration, oxygen uptake rates at 45°C, 250 μM H_2S, pH 6 should approximate the cumulative differential effects of independently elevating sulfide concentrations and temperatures, and decreasing pH. If we assume additive properties of pH and sulfide, as well as an accepted annelid Q_{10} standard value of 2 (32), we would expect to see:

$$\text{Resp. rate}_{(\text{stress})} = (\text{Resp. rate}_{(\text{cntrl})} + \Delta\,\text{rate}_{(\text{pH})} + \Delta\,\text{rate}_{(\text{H2S})}) * \Delta Q_{10\,(30 \rightarrow 45°C)} \quad [0a]$$

$$\text{Resp. rate}_{(\text{stress})} = (1.13 + 2.33 + 2.26)*2.8 = 16.02\ (\mu\text{mol } O_2 \bullet g^{-1} \bullet h^{-1}) \quad [0b]$$

This calculation predicts approximately a 15-fold increase in respiration, yielding a rate of ~ 16.02 μmol $O_2 \bullet g^{-1} \bullet h^{-1}$. However, at 45°C, 250 μM H_2S, pH 6, we empirically observed markedly higher rates, averaging 38.60 ± 3.44 μmol $O_2 \bullet g^{-1} \bullet h^{-1}$ after 12 hours. Respiration rates over time for each of the four combined stressor trials are shown in **Figure 3.1,** which uses a power fit trendline to assign a best-fit curve to each replicate. This method allows us to smooth out artifacts of the sampling procedure associated with our system which were are currently addressing. **Figure 3.1** demonstrates that our theoretical high temperature respiration rate, 16.02 μmol $O_2 \bullet g^{-1} \bullet h^{-1}$, is surpassed between 2-3 hours for the two high temperature replicates.

Sulfide Binding Capacity

Sulfide binding by extracellular hemoglobins was first described in the siboglonid vent tubeworm *Riftia pachyptila*, involves a tightly-bound zinc ring, which has a high affinity for binding sulfide (33-34). Like siboglonids, paralvinellids have the ability to bind free sulfide with extracellular hemoglobins (30) . To estimate the total sulfide binding capacity of *P. sulfincola*, and to subsequently calculate the time it would take to saturate this capacity, we referred to (30), wherein the authors examined sulfide binding by paralvinellids (by *P. palmiformis* in particular, a

Figure 3.1: Respiration Rate Power Curves for High Sulfide, Low pH, and Combined Treatments

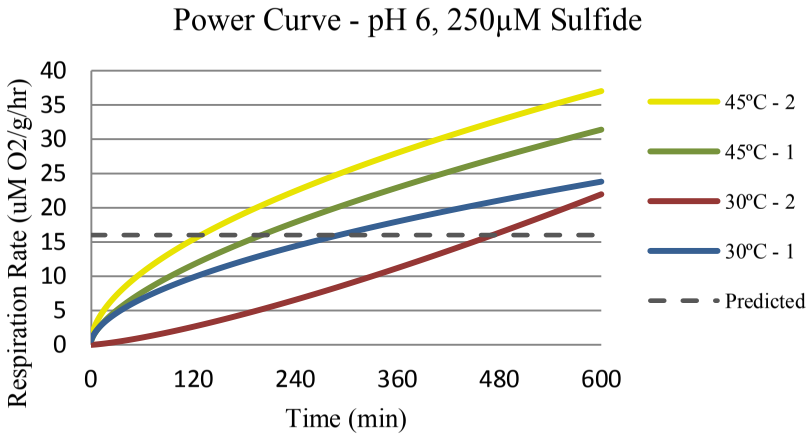

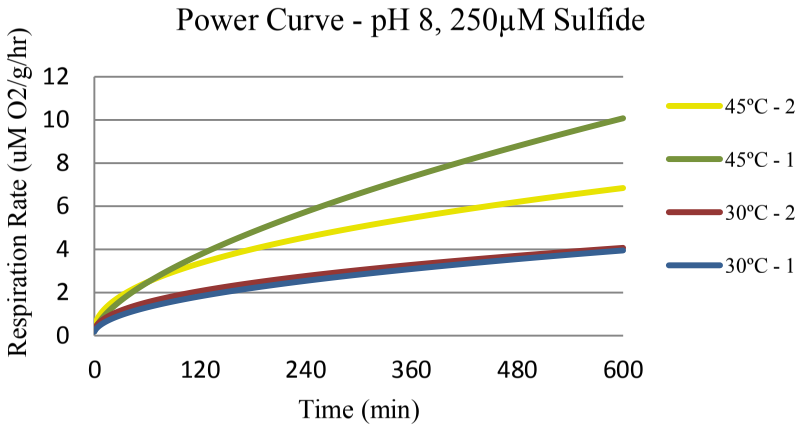

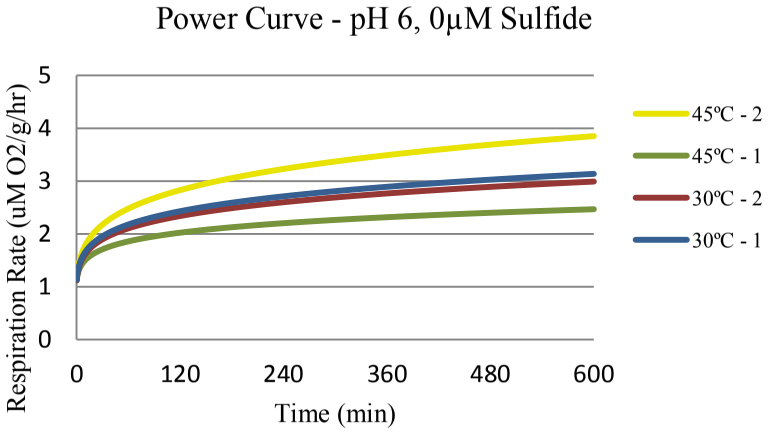

These graphs show the best fit power curves for the pH, sulfide, and combined treatments. Replicates correspond to the values in **Table 2**. In the combined curve, the predicted value is 16.02 µmol $O_2 \bullet g^{-1} \bullet h^{-1}$derived in equation 0b, representing the theoretical respiration rate at 45°C if sulfide and pH effects were additive.

congener of *P. sulfincola* also found on the Juan de Fuca Ridge). The authors determined that *P. palmiformis* has a total sulfide binding capacity of 1550 µmol/L of mixed body fluids (vascular blood and coelomic fluid). In the absence of similar data on *P. sulfincola*, we used these values to constrain the volume specific binding capacity. To estimate the proportion of body fluid found in *P. sulfincola*, we weighed and homogenized a nominally sized *P. sulfincola*, centrifuged the homogenate at 18,000 x g to pellet cellular debris and decanted the supernatant. The cellular debris was resuspended in 100 µL 1x PBS and centrifuged at 18,000 x g. The supernatant was decantanted and the remaining pellet was weighed. Via subtraction from the weight of the intact worm, we estimate that *P. sulfincola* is ~ 80% body fluid, and that a typical worm contains approximately 100 µL of mixed body fluid (vascular blood, coelomic fluid, which also contains sulfide binding proteins, and other intercellular fluids). This percentage estimate is consistent with the results of another study by (35), which examined polychaete wet and dry weights. Based on these observations, we determined that an average *P. sulfincola* can bind a total of 155 nmol of sulfide before saturating their capacity.

Moreover, sulfide binding kinetics of *P. palmiformis* total body fluid across a dialysis membrane revealed an apparent K_m of 290 µmol • L^{-1} (30). *In vitro*, Martineu et al. 1997 (30) determined that *P. palmiformis* appeared to reach 50% capacity within 2 hours, and saturation within 5 hours. Upon saturation, any hydrogen sulfide diffusing into the worm must be dealt with via oxidation or other detoxification pathways (of course, bound sulfide must ultimately be expelled or oxidized, though this can occur at a later time).

Sulfide Uptake

The equation used to calculate permeate flux J (mol • cm^{-2} • h^{-1}) through a system is Fick's First Law of diffusion.

$$J = -PA(C^{(o)} - C^{(i)}) \qquad [1]$$

C is concentration (mol • cm^{-3}) outside (o) and inside (i) the system; A is permeable surface area (cm^2); P is the permeability coefficient of the tissue (cm • h^{-1}). To calculate uptake

rate prior to binding capacity saturation in our system we assume $C^{(i)} = 0$, an environmental H_2S concentration of 250 µmol (and thus $C^{(o)} = 250$ nmol •cm^{-3}). To calculate flux with these assumptions requires that we A) best estimate the worm body surface area, and B) consider flux of H_2S and HS^-, two chemical species of sulfide that vary as a function of pH.

There are two main external body tissues to solve for surface area (A) in *P. sulfincola*: the body wall epithelium and the gills. To estimate body wall surface area ($A_{(bw)}$) in a worm with 100µL of mixed body fluid we measured a body length (without branchiae) of 1.4cm and a broadest width at 0.4cm. Approximating the shape of worm to be that of a cone, we find that $A_{(bw)}$= 0.89 cm^2. While the gill branchiae surface area ($A_{(g)}$) are more difficult to approximate, SEM and TEM images of *Paralvinella grasslei* have been used to determine a surface area of 47 $cm^2 \bullet g^{-1}$ wet weight (36). Accordingly, our 100µL worm had a total mass of 0.130g, resulting in $A_{(g)}$ = 6.1 cm^2. Thus, 87% of the surface area of exchange in *P. sulfincola* lies in the gill brachiae.

Because pH affects the speciation and permeability of sulfide, and our analyses considers diffusion at the two pHs used in these treatments (pH 6 and pH 8). At pH 6, 94% of sulfide exists as highly membrane permeable H_2S, whereas at pH 8, 85% sulfide exists as the less membrane permeable HS^-. While no direct measurements of sulfide permeability have been done in paralvinellids,, such measurements exist for *Urechis caupo*, an echiuran worm endemic to sulfidic mudflats. This worm was found to have a body wall sulfide permeability coefficient ($P_{(bw)}$) of 0.15 at pH 6.0, and 0.068 at pH 8.0 (11). *U. caupo* lacks external gills, and therefore there is no similar permeability coefficient for gill surfaces. However, we can estimate that the thickness of the *P. sulfincola* gill filaments are approximately only 2-3µm, as empirically estimated for other paralvinellid species (36) and therefore could assume a higher sulfide permeability than epidermal tissue. An alternate value we can use would be the *U. caupo* hindgut – which is close in thickness to gill tissue, and the echiuran respiratory exchange surface. Herein we assume our tissue is comparable with a partially inflated hindgut. If so, and accounting for the speciation at each pH, the ($P_{(g)}$) at pH 6.0 would be 0.75, and 0.14 at pH 8.0 (11).

With our new constraints, our flux equation becomes

$$J = -(P_{(bw)} \bullet A_{(bw)} + P_{(g)} \bullet A_{(g)}) \bullet C^{(o)} \qquad [2]$$

Assuming more conservative gill permeability, we estimate flux as:

At pH 6.0 → $J = -(0.15 \bullet 0.89 + 0.15 \bullet 6.1) \bullet 250 = \mathbf{-262}$ (nmol • h^{-1}) [3a]

At pH 8.0 → $J = -(0.068 \bullet 0.89 + 0.068 \bullet 6.1) \bullet 250 = \mathbf{-119}$ (nmol • h^{-1}) [3b]

If we assume a more permeable gill, we estimate flux as:

At pH 6.0 → $J = -(0.15 \bullet 0.89 + 0.75 \bullet 6.1) \bullet 250 = \mathbf{-1177}$ (nmol • h^{-1}) [4a]

At pH 8.0 → $J = -(0.068 \bullet 0.89 + 0.14 \bullet 6.1) \bullet 250 = \mathbf{-229}$ (nmol • h^{-1}) [4b]

Despite the estimated differences in sulfide flux at pH 6, in both cases sulfide flux is significantly higher than at pH 8.0. Indeed, assuming a more permeable gill, we estimate a five-fold greater rate in sulfide influx at pH 6 versus pH 8. Returning to our sulfide binding capacity value of 155 nmol, we calculate that at 250 μmol sulfide and pH 8.0 (disregarding any sulfide detoxification), *P. sulfincola* would exceed its binding capacity conservatively in 78 minutes with the more conservative permeability estimate, and 41 minutes assuming more permeable gills. When the pH is lowered to 6.0, sulfide binding capacity is exceeded in 35 minutes assuming more permeable gills, or just 8 minutes assuming more permeable gills. Furthermore, note that these rates may significantly outpace the K_m of the binding reaction, meaning that not all of the incoming sulfide may be immediately bound, increasing coelomic concentrations of free (unbound) sulfide. Using the 5h saturation value obtained from *in vitro* studies on *P. palmiformis* (30), we can estimate the percentage of incoming sulfide bound per hour. Conservatively, at pH 8.0, 26% of the incoming sulfide can be bound within the first hour. That number drops to 11.7%*hr^{-1} when considering the rate of sulfide uptake at pH 6.0. These percentages are lower still if we accept the parameters of equations 4a and 4b.

Intracellular buffering capacity and proton elimination

Maintaining a non-carbonate buffering pool allows an organism to maintain pH_i homeostasis during periods of stress. Conversely, if the non-carbonate buffering pool is depleted,

the animal may not be able to continue to eliminate incoming protons. To determine the state of the non-carbonate buffering pool of *P. sulfincola*, we tested its intracellular buffering capacity ***(β)*** – defined as the amount of base needed to change the pH_i of the sample by 1 pH unit/gram tissue – by comparing homogenized whole worms previously maintained under stress conditions to untreated control worms. **Figure 3.2** demonstrates that there was no significant difference between worms exposed to low pH and high sulfide and both unexposed and untreated samples. Thus, it is unlikely that the experimental respiration rate differential observed for *P. sulfincola* maintained at high sulfide and low pH were due to the inability of the organism to maintain intracellular pH, as these data suggest that buffering capacity had not been compromised at any of the treatments presented here.

Figure 3.2: Non-carbonate intracellular buffering capacity

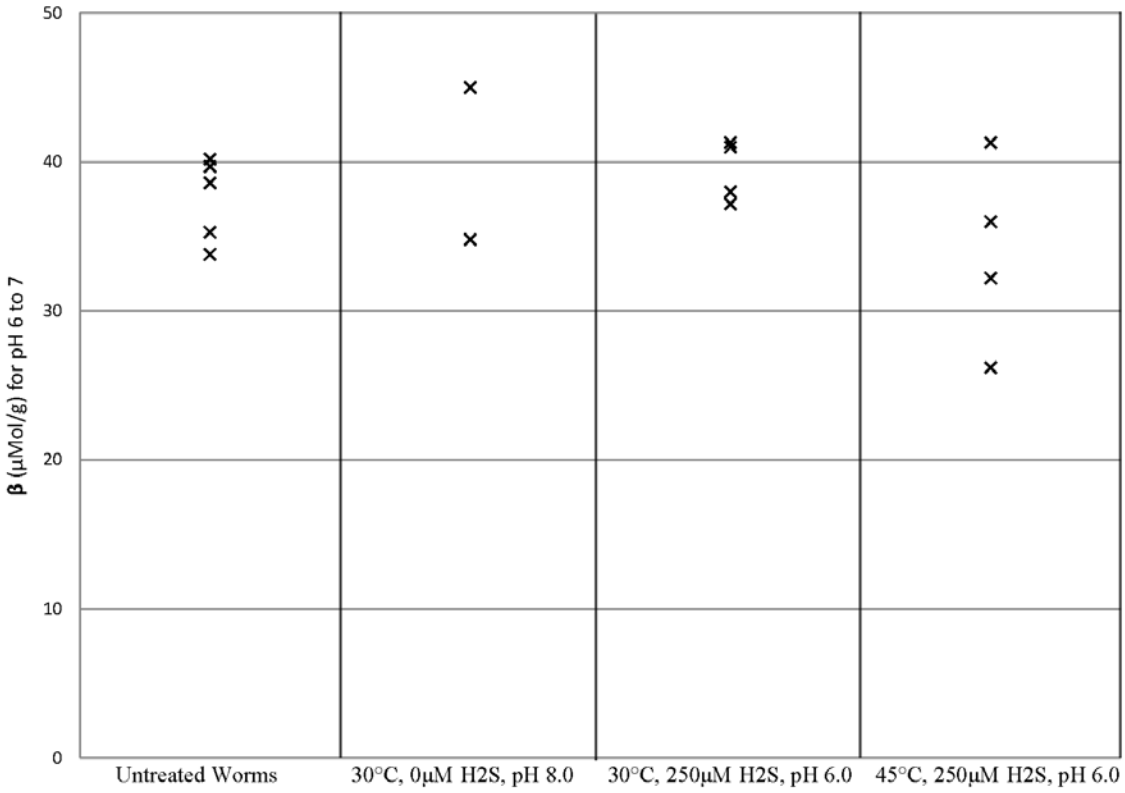

This graph demonstrates the non-bicarbonate intracellular buffering capacity by measuring β ($\mu mol*g^{-1}$) for the linear range of pH 6 to 7. Higher values indicated a larger buffering pool.

While the non-bicarbonate buffering capacity suggests that the worms can maintain internal pH under stress conditions, there is a metabolic cost to buffering involved in the exchange of ions during periods of low pH and elevated sulfide. This is due to the fact that to maintain pH_i, the organism must actively work against an H+ gradient, use ATPase pumps rather than simply ion channels. While empirically identifying the contribution of specific H^+/Na^+, Na^+/K^+, and K^+/H^+ ATP-ase antiporters is beyond of the scope of these analyses, we can derive a range of aerobic respiration rates for our system using previously published calculations. Comparing these ranges to our observed aerobic respiration rates allows us to determine if the increases in respiration observed are due either in part or whole to pH_i buffering.

Based on the relation between the proton elimination rate (μequiv g^{-1} h^{-1}) and H_2S uptake rate (μmol ΣH_2S g^{-1} h^{-1}) derived for *Riftia pachyptila* (***y*** = –0.826+7.629***x***) in Figure 2A of (37), we can put boundaries on the rate of proton elimination, and therefore aerobic respiration necessary to maintain pH_i in *Paralvinella sulfincola.* **Table 3.3** includes the values we have derived from our sulfide uptake estimation, combined with the proton equivalent rate for *R. pachyptila* at 250μM sulfide, giving us the proton equivalent ranges for *P. sulfincola* at pH 6 and pH 8 with 250μM.

Table 3.3 - Proton Equivalent Rates

				Low	**High**
Tissue Permeability	**pH**	**Sulfide uptake rate (μmol g^{-1} h^{-1})**	**Proton Elim. Rate (μequiv g^{-1} h^{-1})**	**O_2 Respiration Rate Range (μmol g^{-1} h^{-1})**	
Conservative	6	2017.4	15.39	0.83	2.48
	8	916.3	6.99	0.38	1.13
Permeable	6	9062.9	69.14	3.72	11.15
	8	1763.3	13.45	0.72	2.17

We know that ATPases exchange between 1-3 protons/ATP (38) and that 6.2 ATP are produced/oxygen molecule. Including these calculations into our table, combined with the two estimates of sulfide permeability and we get 4 oxygen respiration rate ranges – a conservative and

permeable range for both pH tested. These ranges represent the net increase of oxygen consumption required by the organism to compensate for the influx of protons under multistress conditions. At pH 8, we find a conservative range of 0.38 – 1.13 μmol g^{-1} h^{-1}, and a permeable range estimated at 0.72 – 2.17 μmol g^{-1} h^{-1}. At pH 6 under conservative conditions, the range is 0.83 – 2.48 13 μmol g^{-1} h^{-1}, but the permeability model shows a range of 3.72 – 11.15 μmol g^{-1} h^{-1}. While the upper boundary of this is high – it assumes a highly permeable membrane with a set of ATPases that exchange only 1 proton/ATP – it still does not account for 100% of the respiration increase observed in either 30°C replicate, and especially at 45°C.

Unbound Sulfide

If an organism has exceeded its sulfide binding capacity but continues to uptake sulfide, internal levels of free sulfide will increase. To determine if pH played a role in concentrations of total unbound sulfide within our *Paralvinella sulfincola*, free sulfide levels were measured in twelve experimentally treated worms. Internal unbound sulfide levels in worms subjected to 250μM sulfide, pH 8.0 and 45°C were compared to levels in worms maintained at 250μM sulfide and pH 6.0 at both 30°C and 45°C. Our results can be found in **Figure 3.3**. Determination of each sulfide concentration per gram tissue was determined by comparing spectra readings at 670nm to an untreated worm standard curve. ANOVA analysis of our treatments found an F-value of 6.9 and a null hypothesis probability of 0.015, indicating significantly elevated levels of sulfide for worms maintained at pH 6.0 compared to those maintained at pH 8.0 (p <0.05).

Constraining rates of sulfide detoxification

Hydrogen sulfide has been shown to inhibit 90% of Cytochrome c oxidase (COX) activity at concentrations as low as 5μM (22). Thus, it is imperative that organisms successfully sequester (through binding) and detoxify the sulfide (through oxidation or elimination). The first step of most common pathways of sulfide detoxification is the oxidation of hydrogen sulfide to thiosulfate (S_2O_3). Stoichiometrically, this means that three O_2 molecules are needed to oxidize four H_2S. At pH 8.0, based on equations 3b and 4b, an individual worm would need to increase its

Figure 3.3: Unbound Sulfide Concentration

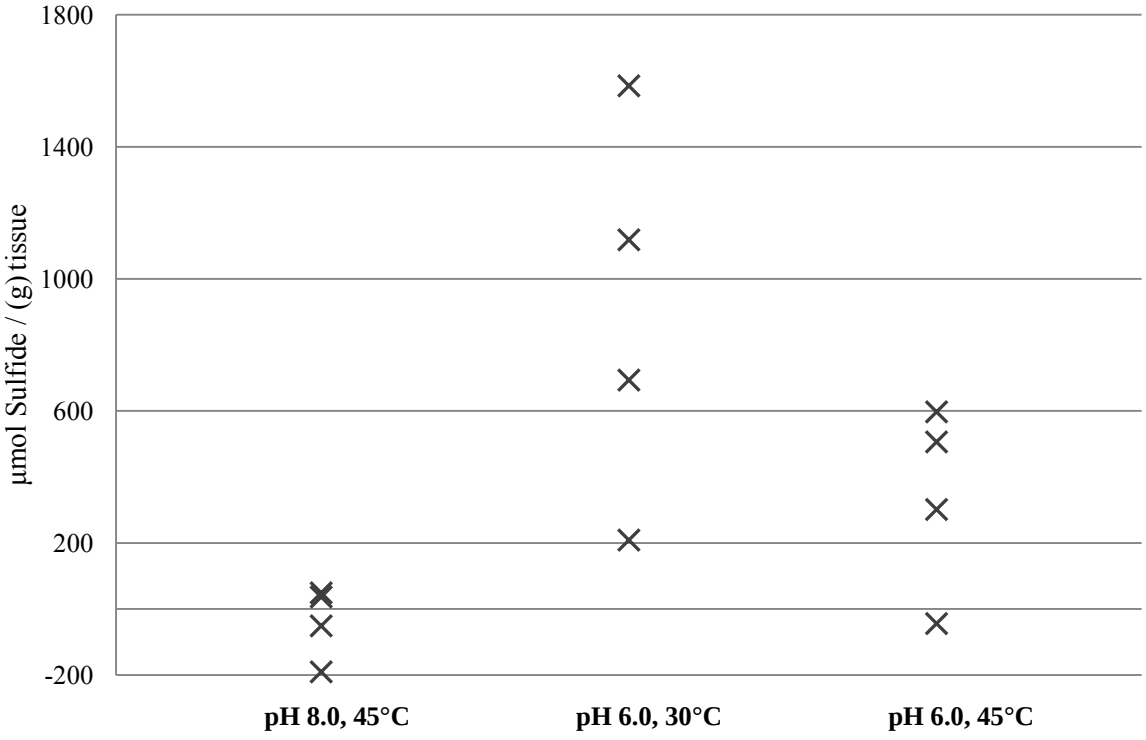

This graph shows the concentration of unbound sulfide within the coelom of *P. sulfincola* in µmol/g. Each X represents an individual replicates; 4 replicates were analyzed per treatment on a spectrophotometer at 670nm, and quantified using a standard curve built from untreated samples and known concentrations of sulfide.

oxygen uptake rate by between 0.69-1.32 µmol • g^{-1} • hr^{-1}. At pH 6.0, based on equations 3a and 4a, the worm needs to increase its oxygen uptake rate by 1.52-6.79 µmol • g^{-1} • hr^{-1}.

For all organisms, there is a maximal rate at which sulfide can be oxidized or bound. In *P. sulfincola,* the rate of total sulfide detoxification was calculated in (39). There, they found the rate of detoxification is, as expected, dependent on the concentration of exposure. Starting with 200µmols of sulfide, they calculated an average rate of detoxification to be 1.51 µmol•min^{-1}•g^{-1} protein. Substituting this value into the Table 3 of Martineu and Juniper (1997) (39), we find that *P. sulfincola* detoxifies ~.034 µmol/ min^{-1}• g^{-1} wet weight tissue, which, in our 0.130g example

worm, translates to a sulfide detoxification rate of 245 nmols/hr. Note this value is conservative, because our treatment included 250μmol sulfide, so it is likely that under these conditions *P. sulfincola* would have a slightly faster detoxification rate.

Our calculation of at least 245 nmols/hr suggests that *P. sulfincola* is effectively able to detoxify at a rate greater than influx when the pH is 8.0, using either permeability coefficient. However, at pH 6.0, it is conservatively (from equation 3a) getting a net influx of 17nmols/hr. If we assume higher permeability of gills (equation 4a), this net influx jumps to a catastrophic 945 nmols/hr even at max detoxification rate -likely higher if we adjust up the permeability of gill tissue. Because the volume of the worm is only 100uL, the concentration of hydrogen sulfide at pH 6.0 increases 170 μM, in the conservative case, reaching equilibrium with the environmental concentration of 250 μM in less than 90 minutes. Following values from equation 4a, this time drops to approximately 15 minutes.

Discussion

To survive periods of stress, organisms must maintain homeostasis at a variety of different conditions. The objective of these experiments was to determine if the temporal extent and magnitude of a multi-stress effect arising from exposure to decreased pH, increased H_2S and increased temperature. To investigate the response of the worms to these stressors, we measured aerobic respiration rates in *P. sulfincola* during each treatment. We also performed intracellular buffering capacity analysis, free sulfide quantification, and derived a number of constraints from the literature to constrain a model of sulfide and H^+ input and elimination under each condition set.

With these data, we were able to determine that there was indeed a combinatory effect on the *P. sulfincola* aerobic respiration rate when the pH was low and the sulfide level elevated. This is highly relevant to the life history of these organisms, as the aforementioned factors can co-vary *in situ* (e.g. increases in the proportion of vent fluid in the habitable zone will concurrently

decrease pH, increase H_2S and increase temperature (40). However, these factors do not always co-vary, (e.g.) temperature can increase through conductive heating (41). These experiments provide the first *in vivo* response data for *P. sulfincola* to single stressors pH and sulfide, as well as their combined effect; the data herein provide the first glimpse into how these factors influence oxygen uptake and respiration. *In situ*, oxygen levels decrease concurrently with increasing temperature and sulfidity. Thus our observed increases in oxygen respiration rates in the combined treatment could be an adaptive response to surviving periods of thermal stress, which are often accompanied by periods of low oxygen concentration. In addition to increasing respiration rates, alvinellids are known for having extremely effective oxygen binding proteins (e.g. hemoglobin) (42). This evolved efficiency is necessary adaptation to the surviving the dynamic vent environment because both high temperature and high sulfide concentration limits oxygen availability.

pH

When an organism is exposed to a low pH, it must actively preserve intracellular pH (pH_i) to maintain functional cellular processes. To this end, a number of buffering processes can occur within the cell (43) including bicarbonate and non-bicarbonate buffering, H^+/K^+ antiporter exchanges, H^+-ATPases, and other methods (31). In our system, when the pH was lowered from 8.0 to 6.0, we observed an average increase from 1.13 to 3.46 μmol $O_2 \bullet g^{-1} \bullet h^{-1}$, a 3-fold increase in respiration. While we were not able to produce a full time series on the pH only treatments due to technical limitations on board ship, we were able to measure a steady rate of respiration for more than 4 hours, which suggests that the organism had reached homeostasis. Additionally, we found no significant differences in the non-carbonate intracellular buffering capacity between samples maintained under even the most challenging treatment. This supports the conclusion that the elevated respiratory rates in *P. sulfincola* are due to effects of both a low pH and high H_2S.

Sulfide

To constrain our model with input and dissipation rates of sulfide, we first calculated the capacity of the sulfide binding pool within the worm using numbers determined on the sister species, *Paralvinella palmiformis* (30). Next, we gauged the rates of input across the epithelia and the gill tissue using equations and empirically derived calculations of diffusion constants found in (11). To model sulfide detoxification, we used the amount of oxygen required to convert sulfide to thiosulfate, a common detoxification pathway in marine invertebrates (11). In our sulfide only sample, we saw an increase from 1.13 to 3.39 μmol $O_2 \bullet g^{-1} \bullet h^{-1}$, also a 3-fold increase in respiration. Importantly, these values were also steady after several hours, indicating that the animals in this condition had also reached homeostasis.

Multistressor effects

If pH and H_2S affected *P. sulfincola* similarly when combined, we should have expected to see a roughly 6-fold increase, before temperature was added. However, even in the 30°C combined treatment, we observed a respiration rate of 23 μmol $O_2 \bullet g^{-1} \bullet h^{-1}$, after 10 hours, roughly a 20-fold increase. This is due to two fundamental cross-reactive problems between elevated sulfide and low pH. First, as demonstrated in **Table 3.3,** in the presence of hydrogen sulfide, the organism must eliminate a larger quantity of H^+ ions due to the thiosulfate (and further end products) detoxification pathway. Depending on the permeability of the epithelia, this increase could be between 2-5x greater. In addition, pH affects the speciation of sulfide. At pH 6, it is 94% H_2S, in contrast to HS^- which is dominate at pH 8. H_2S is more permeable across the epithelial membrane, and thus, the uptake, and therefore sulfide detoxification pathways increase 2-5x (based on equations 3a and 4a) in combination with lowered pH. Taken together, this could account for anywhere from a 4-10 fold increase from respiration rate increases due to elevated H_2S or lower pH alone. From baseline this accounts for a 12-30 fold increase. Thus, our observed 20-fold increase could in fact be due to these two combinatory factors.

Toxicity Effects

The calculations done here suggest that the rise in respiration rate cannot be solely due to sulfide detoxification pathways. Although our model suggests that the animal could provide enough oxygen to detoxify sulfide, even under low pH conditions, we cannot be certain of the rate of detoxification. Additionally, our measurements of unbound sulfide demonstrate that there is a significant increase of internal sulfide under multistress conditions. If environmental sulfide concentrations reach toxic levels, and our model show that the binding capacity of *P. sulfincola* would be filled within 2 hours at 250μM sulfide, than we would expect to see Cytochrome c poisoning, and depolarization in the mitochondria (21, 23).

There are many additional sulfide toxicity effects that could occur at high levels of sulfide including oxidative damage to RNA and DNA (44), decreased cell proliferation (45) and a decrease of the antioxidant glutathione pool (46). However, one toxic effect due to sulfide poisoning we do not observe in our system is the inhibition of enzymes involved in aerobic metabolism (47). If this were to occur, we would expect to see respiration levels drop dramatically, as internal sulfide levels rose. Instead, the levels continued to rise steadily during the multistress treatment, indicating ongoing aerobic respiration. Sulfide-tolerant organisms have been shown to utilize mitochondrial sulfide oxidation as an important mechanism for reducing sulfide toxicity (48), which may explain this continual increase in respiration, as levels of sulfide continue to rise within the organism.

Conclusions

It is interesting to note that although the oxygen uptake rate is not fully or even partially inhibited in the presence of high concentrations of sulfide. We assert that the organism has an acute tolerance range that includes surviving a confluence of all three factors (pH, sulfide, and temperature), but that long-term survival under these conditions may not be possible. This is due to the speciation and permeability of sulfide at pH 6.0, increasing the influx faster than the binding and detoxifying mechanisms within the worm. Additionally, it may also be possible that

the *P. sulfincola* strategy may be able to build internal levels of sulfide, waiting for a period of low sulfide along with normoxia to oxidize sulfide, and remove it from the coelom. The priapulid worm *Halicryptus spinulosus* can survive long periods anaerobically, even with very high concentrations of internal sulfide (49). Determining which of these processes are occurring is beyond of the scope of this study.

This research highlights the necessity to contextualize the correlative effects of environmental stresses that occur within an organism. While *P. sulfincola* did not physiologically exhibit signs of duress during exposure to just decreased pH or increased sulfide, when a confluence of all three factors occurs, respiration rates increase beyond additive effects. Determining whether the organism will reach equilibrium in time or eventually succumb to an unsustainable increasing respiration rate is the natural next progression for this research. While multi-stressor effects have been investigated in other organisms e.g. the mudflat worm *Urechis caupo* (12), to date no studies have examined multi-stressor effects in an organism with an exemplary adaptive capacity such as *P. sulfincola*, allowing it to quickly respond to environmental stress in a dynamic environment. *P. sulfincola*, as shown here and previously, is ideal for characterizing physiological response to a multiple-stress event due to its pronounced chemo- and thermotolerance (6). Understanding the multi-stressor in this way allows for frame of reference for ascertaining the effect of climate change and ocean acidification on organisms with lower adaptive capacities. Ultimately, our findings demonstrate the importance of understanding the emergent effects of a multiple-stress event and ultimately reflect the limitations of an organism to maintain homeostasis over a range of environmentally relevant conditions.

REFERENCES

1. Van Dover C. The ecology of deep-sea hydrothermal vents: Princeton Univ Pr; 2000.

2. Tunnicliffe V, Desbruyeres D, Jollivet D, Laubier L. Systematic and Ecological Characteristics of *Paralvinella sulfincola* Desbruyeres and Laubier, a New Polychaete (Family Alvinellidae) from Northeast Pacific Hydrothermal Vents. Can J Zool. 1993 Feb;71(2):286-97.

3. Sarrazin J, Levesque C, Juniper S, Tivey M. Mosaic community dynamics on Juan de Fuca Ridge sulphide edifices: substratum, temperature and implications for trophic structure. CBM-Cahiers de Biologie Marine. 2002;43(3-4):275-9.

4. Juniper SK, Martineu P. Alvinellids and sulfides at hydrothermal vents of the eastern Pacific: a review. American Zoologist. 1995;35(2):174-85.

5. Lee RW. Thermal tolerances of deep-sea hydrothermal vent animals from the Northeast Pacific. Biol Bull. 2003 Oct;205(2):98-101.

6. Girguis PR, Lee RW. Thermal preference and tolerance of alvinellids. Science. 2006 Apr 14;312(5771):231.

7. Bris N, Gaill F. How does the annelid *Alvinella pompejana* deal with an extreme hydrothermal environment? Life in Extreme Environments. 2007:315-39.

8. Chevaldonné P, Fisher C, Childress J, Desbruyères D, Jollivet D, Zal F, et al. Thermotolerance and the'Pompeii worms'. Marine Ecology Progress Series. 2000;208:293-5.

9. Cary SC, Shank T, Stein J. Worms bask in extreme temperatures. Nature (London). 1998;391(6667):545-6.

10. Girguis PR, Childress JJ. Metabolite uptake, stoichiometry and chemoautotrophic function of the hydrothermal vent tubeworm *Riftia pachyptila*: responses to environmental variations in substrate concentrations and temperature. J Exp Biol. 2006 Sep;209(Pt 18):3516-28.

11. Julian D, Arp AJ. Sulfide permeability in the marine invertebrate *Urechis caupo*. Journal of Comparative Physiology B: Biochemical, Systemic, and Environmental Physiology. 1992;162(1):59-67.

12. Julian D, Chang M, Judd J, Arp A. Influence of environmental factors on burrow irrigation and oxygen consumption in the mudflat invertebrate *Urechis caupo*. Marine Biology. 2001;139(1):163-73.

13. Christensen AB, Nguyen HD, Byrne M. Thermotolerance and the effects of hypercapnia on the metabolic rate of the ophiuroid *Ophionereis schayeri*: Inferences for survivorship in a changing ocean. Journal of Experimental Marine Biology and Ecology. 2011.

14. Pörtner HO. Ecosystem effects of ocean acidification in times of ocean warming: a physiologist's view. Effects of ocean acidification on marine ecosystems. 2008;373:203-17.

15. Abele D, Heise K, Portner H, Puntarulo S. Temperature-dependence of mitochondrial function and production of reactive oxygen species in the intertidal mud clam *Mya arenaria.* J Exp Biol. 2002;205(13):1831-41.

16. Abele D, Puntarulo S. Formation of reactive species and induction of antioxidant defence systems in polar and temperate marine invertebrates and fish. Comp Biochem Physiol A Mol Integr Physiol. 2004 Aug;138(4):405-15.

17. Dahlhoff E, O'Brien J, Somero G, Vetter R. Temperature effects on mitochondria from hydrothermal vent invertebrates: evidence for adaptation to elevated and variable habitat temperatures. Physiological zoology. 1991;64(6):1490-508.

18. O'Brien J, Dahlhoff E, Somero G. Thermal resistance of mitochondrial respiration: hydrophobic interactions of membrane proteins may limit thermal resistance. Physiological zoology. 1991;64(6):1509-26.

19. Reipschl, Auml A, Ouml H. Metabolic depression during environmental stress: the role of extracellular versus intracellular pH in *Sipunculus nudus*. J Exp Biol. 1996;199(8):1801.

20. Khan A, Schuler M, Prior M, Yong S, Coppock R, Florence L, et al. Effects of hydrogen sulfide exposure on lung mitochondrial respiratory chain enzymes in rats. Toxicology and applied pharmacology. 1990;103(3):482-90.

21. Dorman DC, Moulin FJM, McManus BE, Mahle KC, James RA, Struve MF. Cytochrome oxidase inhibition induced by acute hydrogen sulfide inhalation: correlation with tissue sulfide concentrations in the rat brain, liver, lung, and nasal epithelium. Toxicological Sciences. 2002;65(1):18.

22. Powell MA, Arp AJ. Hydrogen sulfide oxidation by abundant nonhemoglobin heme compounds in marine invertebrates from sulfide rich habitats. Journal of Experimental Zoology. 1989;249(2):121-32.

23. Julian D, April KL, Patel S, Stein JR, Wohlgemuth SE. Mitochondrial depolarization following hydrogen sulfide exposure in erythrocytes from a sulfide-tolerant marine invertebrate. J Exp Biol. 2005;208(21):4109.

24. Beauchamp RO, Jr., Bus JS, Popp JA, Boreiko CJ, Andjelkovich DA. A critical review of the literature on hydrogen sulfide toxicity. Crit Rev Toxicol. 1984;13(1):25-97.

25. Jacques AG. The Kinetics of Penetration : Xii. Hydrogen Sulfide. J Gen Physiol. 1936 Jan 20;19(3):397-418.

26. Gillooly JF, Brown JH, West GB, Savage VM, Charnov EL. Effects of size and temperature on metabolic rate. Science. 2001;293(5538):2248.

27. Castellini MA, Somero GN. Buffering capacity of vertebrate muscle: correlations with potentials for anaerobic function. Journal of Comparative Physiology. 1981;143(2):191-8.

28. Seibel BA, Thuesen EV, Childress JJ, Gorodezky LA. Decline in pelagic cephalopod metabolism with habitat depth reflects differences in locomotory efficiency. The Biological Bulletin. 1997;192(2):262.

29. Cline JD. Spectrophotometric determination of hydrogen sulfide in natural waters. Limnology and Oceanography. 1969;14(3):454-8.

30. Martineu P, Juniper SK, Fisher CR, Massoth GJ. Sulfide binding in the body fluids of hydrothermal vent alvinellid polychaetes. Physiol Zool. 1997 Sep-Oct;70(5):578-88.

31. Hochachka PW, Somero GN. Biochemical adaptation: mechanism and process in physiological evolution: Oxford University Press, USA; 2002.

32. Khan M, Ahmed S, Salazar A, Gurumendi J, Khan A, Vargas M, et al. Effect of temperature on heavy metal toxicity to earthworm *Lumbricus terrestris* (Annelida: Oligochaeta). Environmental toxicology. 2007;22(5):487-94.

33. Flores JF, Fisher CR, Carney SL, Green BN, Freytag JK, Schaeffer SW, et al. Sulfide binding is mediated by zinc ions discovered in the crystal structure of a hydrothermal vent tubeworm hemoglobin. Proceedings of the National Academy of Sciences of the United States of America. 2005;102(8):2713.

34. Arp AJ, Childres JJ, Vetter RD. The sulphide-binding protein in the blood of the vestimentiferan tube-worm, *Riftia pachyptila*, is the extracellular haemoglobin. J Exp Biol. 1987;128(1):139.

35. Ricciardi A, Bourget E. Weight-to-weight conversion factors for marine benthic macroinvertebrates. Marine Ecology Progress Series. 1998;163:245-51.

36. Jouin C, Gaill F. Gills of hydrothermal vent annelids: structure, ultrastructure and functional implications in two alvinellid species. Progress in oceanography. 1990;24(1-4):59-69.

37. Girguis PR, Childress JJ, Freytag JK, Klose K, Stuber R. Effects of metabolite uptake on proton-equivalent elimination by two species of deep-sea vestimentiferan tubeworm, *Riftia pachyptila* and *Lamellibrachia cf luymesi:* proton elimination is a necessary adaptation to sulfide-oxidizing chemoautotrophic symbionts. J Exp Biol. 2002 Oct;205(Pt 19):3055-66.

38. Steinmetz PR, Andersen OS. Electrogenic proton transport in epithelial membranes. Journal of Membrane Biology. 1982;65(3):155-74.

39. Martineu P, Juniper SK. Comparison of the benzyl viologen and bimane HPLC assays for the determination of sulfide oxidizing capability in the tissues of hydrothermal vent and non-vent polychaetes. Canadian Journal of Zoology. 1997;75(10):1618-27.

40. Johnson KS, Childress JJ, Beehler CL. Short-term temperature variability in the Rose Garden hydrothermal vent field: an unstable deep-sea environment. Deep Sea Research Part A Oceanographic Research Papers. 1988;35(10-11):1711-21.

41. Johnson HP, Tivey MA, Bjorklund TA, Salmi MS, Canales JP, Detrick RS, et al. Hydrothermal circulation within the Endeavour Segment, Juan de Fuca Ridge. Geochem Geophys Geosyst. 2010;11.

42. Hourdez S, Lallier F. Adaptations to hypoxia in hydrothermal-vent and cold-seep invertebrates. Reviews in Environmental Science and Biotechnology. 2007;6(1):143-59.

43. Seibel BA, Walsh PJ. Potential impacts of CO2 injection on deep-sea biota. Science. 2001;294(5541):319.

44. Joyner-Matos J, Predmore BL, Stein JR, Leeuwenburgh C, Julian D. Hydrogen sulfide induces oxidative damage to RNA and DNA in a sulfide-tolerant marine invertebrate. Physiological and biochemical zoology: PBZ. 2009;83(2):356.

45. Hance JM, Andrzejewski JE, Predmore BL, Dunlap KJ, Misiak KL, Julian D. Cytotoxicity from sulfide exposure in a sulfide-tolerant marine invertebrate. Journal of Experimental Marine Biology and Ecology. 2008;359(2):102-9.

46. Truong DH, Eghbal MA, Hindmarsh W, Roth SH, O'Brien PJ. Molecular Mechanisms of Hydrogen Sulfide Toxicity. Drug metabolism reviews. 2006;38(4):733-44.

47. Bagarinao T. Sulfide as an environmental factor and toxicant: tolerance and adaptations in aquatic organisms. Aquatic Toxicology (Amsterdam). 1992;24(1-2):21-62.

48. Grieshaber MK, Völkel S. Animal adaptations for tolerance and exploitation of poisonous sulfide. Annual review of physiology. 1998;60(1):33-53.

49. Oeschger R, Vetter RD. Sulfide detoxification and tolerance in *Halicryptus spinulosus* (Priapulida): a multiple strategy. Marine ecology progress series Oldendorf. 1992;86(2):167-79.

Chapter 4

Differential expression of antioxidant genes during thermal stress in *Paralvinella sulfincola*

Abstract

Short-term adaptive response to fluctuations in temperature is a vital facet of organismal survival, especially in the dynamic environment of hydrothermal vents. While many studies have focused on the expression of molecular chaperones to thermal stress, few have explored the biological response to the oxidative stress linked to rising temperatures. Our experiments focus on exploring this link and the gene expression of a suite of antioxidant responses in *Paralvinella sulfincola*, a thermotolerant hydrothermal vent annelid. *P. sulfincola* were experimentally maintained for a 10 hour time series at 45°C and for a 3 hour time series at 50°C, with a control group maintained for 10 hours at 30°C. We used quantitative PCR to measure the relative gene expression of superoxide dismutase (SOD), catalase (CAT), glutathione peroxidase 1 (GPX1) and 4 (GPX4), and glutathione reductase (GSR), using beta-actin (ACTB) as a reference gene. At 45°C, we found a consistent, but not statistically significant, increase in expression of each gene over the first 3 hours, followed by a return to control (30°C) levels by 10 hours. There was no consistent upregulation of antioxidant genes over 3 hours of 50°C, suggesting either physiological dysfunction or metabolic depression. We posit the observed differences between our treatment temperatures reflect a sustainable (45°C) versus acute (50°C) response to thermal stress.

Keywords: qPCR, *Paralvinella sulfincola,* oxidative stress, thermal stress

Introduction

The ability of an organism to survive stress hinges on its capacity to readily adapt to the full dynamic range of environmental conditions it faces. In many systems, temperature is the most widely fluctuating factor, and gene response to thermal shifts, especially by ectotherms, are essential for the organism to maintain optimal cellular function (1). Phenotypic responses to heat stress such as avoidance behavior (2-3), respiratory and metabolic shifts (4-7), and even decreased fecundity (8) have been characterized. In addition, activity for a group of molecular chaperone proteins known as heat shock proteins have been very well studied (5, 9-10).

Recently, a link between heat stress and oxidative stress has been demonstrated in eukaryotes (11-14). As reviewed in chapter two, reactive oxygen species (ROS), also referred to as free radicals, are molecules with one unpaired electron, derived from the reduction of molecular oxygen. These include, among others, the superoxide radical (O_2^-), hydrogen peroxide (H_2O_2), and most dangerously reactive, the hydroxyl radical ($HO^\bullet$) (for review: (15). While a number of cellular processes (i.e. respiration, signal transduction, and oxidative reactions) create ROS through normal function, increased temperatures increase metabolic demand on tissue, inducing a state of functional tissue hypoxia (16). In response, mitochondria increase respiration rates to meet increased metabolic demands and thus increase the production of ROS, creating twice as many oxidative radicals for every 10°C increase in temperature (13, 17-18).

Cells are well-equipped to deal with the production of free radicals. Metabolites and enzymes involved in reducing reactive oxygen species are broadly called antioxidants. In mitochondria, O_2^- is converted to H_2O_2 either spontaneously, or through the enzymatic intermediate found in the cytosol – Superoxide dismutase Cu-Zn (SOD). Hydrogen peroxide is uncharged, and therefore diffuses freely through cellular membranes. If not enzymatically reduced, H_2O_2 can become the highly reactive $HO^\bullet$ radical via Fenton-catalyzed reduction (19). Thus, a number of antioxidant enzymes further reduce hydrogen peroxide before Fenton reactions occur. Catalase (CAT) are heme-containing enzymes that catalyze the reaction $2H_2O_2 \rightarrow 2H_2O +$

O_2. Found in the peroxisome, catalase is a cell signaling enzyme when oxidative stress levels are low, but actively reduces H_20_2 during periods of oxidative stress (15, 20-21).

Equally important to oxidative defense is glutathione (L-γ-glutamyl-L-cysteinylglycine, GSH), a tripeptide thiol and the primary nonprotein antioxidant in metazoans (22). Mammalian studies have shown this molecule to abundant (intracellularly in mM concentrations), ubiquitously expressed throughout tissues and cellular structures, and important in reducing hydrogen peroxide as well as other toxic compounds (23-25). Glutathione is a principal component of the mitochondrial oxidant defense; however, it is manufactured in the cytoplasm and transported via dicarboxylate and 2-oxoglutarate carriers (26). Glutathione reduces H_2O_2 to H_2O by creating a disulfide bridge with a second GSH molecule to form glutathione disulfide (GSSG), the oxidized version of GSH. This reaction is catalyzed by the enzyme family glutathione peroxidase (GPX 1.11.1.9). GSSG is recycled back to the reduced form of GSH by glutathione reductase (GSR, EC 1.8.1.7).

The gene GPX1, first discovered by Mills in 1957 (27), codes for a selenoenzyme commonly found in cytosol which can be secreted from the cell during periods of thermal stress (28-29). GPX1 is part of a family of six glutathione peroxidases found first in mammals, and one of four that use a selenocysteine as an active site. These selenoproteins catalyze the reduction of hydrogen peroxide by oxidizing 2 GSH thiols using a disulfide bridge to form GSSG (23, 29-30), GPX4, like GPX1, also codes for a selenoprotein utilized during periods of thermal stress; however, this protein product is membrane bound in the mitochondria (29). GPX4, also known as hydroperoxide glutathione peroxidase, is a signaling molecule known for its important role in antioxidant stress response (31-32). Glutathione peroxidases catalyze the glutathione reaction, and thus, maintenance of a functional pool cannot be understated during periods of oxidative stress (21, 33). Glutathione reductase (GSR) is a flavoenzyme that reduces GSSG to GSH by oxidizing NADPH to NADP+ (23), allowing 2 GSH to reduce additional H_2O_2.

Enzyme assay (14, 34-36), microarray (37-39) and quantitative proteomics (including our results from chapter 2) experiments have previously observed (mostly) increased response in the activity of SOD, CAT, GPX, and GSR during and after thermal stress episodes. However, very few studies to date have precisely characterized the response of antioxidant gene expression over time in relation to thermal stress (40-41). Furthermore, no study to date has characterized expression of these genes in a highly thermal tolerant organism. Our study organism is *Paralvinella sulfincola*, a highly thermotolerant hydrothermal vent endemic annelid. Further description of the environment and life history of this organism can be found in chapters one and two. In this study, we analyze the gene expression of five important antioxidants in response to thermal stress: SOD (Cu-Zn), CAT, GPX1, GPX4, and GSR. We subject *P. sulfincola* to a time series at two challenging thermal regimes in this study: one near their chronic survival limit, and one above this point, but within their acute survival range. The expression of each of these genes is compared to that of a control group of worms maintained well within their normal thermal range. The goal of the experiment is to understand antioxidant gene responses to thermal stress in both acute and chronic treatments in a highly thermal tolerant organism.

Methods

Animal Collection and Experimental Design

Paralvinella sulfincola were collected from hydrothermal vents in the Main Endeavour field located along the Juan de Fuca Ridge (47°57'N, 129°5'W) at a depth of 2,200m during the R/V *Atlantis* cruise 15-67 in July 2010. Collection method, processing, and system design are described in chapter two and three (Methods-*Animal Collection and System Design*). Five to six *P. sulfincola* were placed into each high pressure chamber, and acclimated overnight at 27.5 MPa, 0 μM sulfide, pH 8.0, 30°C. Control animals were kept continuously at 30°C throughout the duration of the experiment. Experimental chambers were increased to and isothermally maintained at either 45°C (1, 2, 3, 10hrs) or 50°C (1, 2, 3hrs). We did not maintain any samples at

50°C longer than 3 hours because survival is reduced to zero after 6 hours of treatment. At the conclusion of each trail, our biological replicates for each experimental treatment and the control (30°C, 10hr) were selected - a total of 32 *P. sulfincola*. These animals were flash frozen for molecular processing.

Extraction and Reverse Transcription

Total RNA was isolated from *Paralvinella sulfincola* gill tissue (50-100mg) using Trizol RT (MRC Gene, Cincinnati, OH) in a modified single step RNA extraction method (42-43). To remove genomic DNA contamination, the total RNA was treated with TURBO DNA-free (Ambion, Austin, TX). The DNase-treatment was verified using the Qubit dsDNA HS Assay (Invitrogen, Carlsbad, CA) as per manufacturer's instructions. DNA was below the limit of detection (10pg/µl). The treated RNA product was normalized to 1.75µg and used as template in a reverse transcription (RT) reaction using random hexamers with the SuperScript VILO cDNA synthesis kit (Invitrogen, Carlsbad, CA).

Reference gene selection

Essential to conducting effective comparative qPCR assays is the process of normalizing data to correct and control for differences in RNA extraction, cDNA synthesis and amplification efficiencies, and technical variation (44-45). Difficulties always arise when choosing a normalization method to account for technical variation between samples. The qPCR data can be normalized against sample size, total RNA concentration or genomic DNA. However, the use of reference genes as an internal control is highly advantageous as they have been exposed to the same treatment as the target genes and represent the cumulative error of the entire process (46). The ideal reference gene is expected to maintain stable expression between experimental groups due to the fundamental function it plays in the cell (47). Studies have pointed to the difficulties of using well known reference genes during experimental treatments such as stress response studies due to expression change of some reference proteins (48-49). Unfortunately, a universal reference gene that is stably expressed in all tissues and across different treatments does not exist (50).

It is therefore vital to have outside validation of a reference gene to be used in a quantitative PCR experiment. We used the proteomics dataset as an experimentally verified source from which to choose our reference gene. After listing the normalized quantity and probability of differential expression (Pr(DE)) of all proteins detected in our MS/MS database for *Paralvinella sulfincola* and its congener *Paralvinella palmiformis* from chapter 2, we chose *β*-Actin (ACTB) as our reference gene for three reasons. First, ACTB is well characterized as a reference gene choice in prior qPCR studies, so its advantages and disadvantages are already discussed in literature. Second, it was highly expressed as a protein across all temperature treatments (*P. sulfincola* – 2nd of 1419; *P. palmiformis* – 1st of 1419). Finally, it was also one of the most evenly expressed proteins in both species, that is to say it exhibited the least amount of differential expression under thermal stress (*P. sulfincola* – Pr(DE) 0.0031, 1416th of 1419; *P. palmiformis* – Pr(DE) 0.0219, 1415th of 1419). Although this validation method uses protein expression and not gene expression levels, it is the best external test possible for a reference gene in *P. sulfincola.*

Primer design and verification

Our previously constructed Expressed Sequence Tag (EST) *P. sulfincola* transcriptome library (chapter two Methods) was used to design primers for both our reference gene (beta-actin – ACTB) and our experimental genes. Primer sequences are listed in **Table 4.1**. All primers used in this study were designed and built by PrimerDesign Ltd (Southampton, UK), except for ACTB, which was designed using online free software Primer 3 (http://biotools.umassmed.edu/bioapps/primer3_www.cgi) (51). Specificity of the primers was verified both with a local Blastn (52) against the EST library, and on the NCBI n/r database also using Blastn. A positive control PCR was run on each primer pair with *P. sulfincola* template DNA to optimize the amplification and verify a product of the expected size on a subsequent gel when compared to a 100bp DNA ladder (Invitrogen, Carlsbad, CA).

Table 4.1: Primer sequences

Gene Name	Symbol	Isotig #	EC	Size (bp)	Sense/Antisense Primers
Glutathione Peroxidase-1 cytosolic	GPX1	29428	1.11.1.9	109	GCAAGAACCTGGCGATAATGG
					ATTGATGTTGACCCTCTCTGTTAG
Glutathione Peroxidase 4	GPX4	06856		96	TGCCTTCTTCCACTGGTCTT
					CTTACTGCTGCTGGTTTTATATCG
Glutathione Reductase	GSR	17409	1.8.1.7	129	ACTGGGTCATTTTCATCCTGTAA
					GAGCACTGTCTTAGGTAACTTCA
Catalase	CAT	20024	1.11.1.6	123	GTTTGAACACATCGGAAAGAAGA
					TCGTCTGTATAGAACTTGATAGCA
Superoxide Dismutase (Cu-Zn)	SOD	11194	1.15.1.1	120	TATGCTGACTGACCCACTGAT
					GATAACTTGCTGTCTGGATAGGAT
Beta-Actin	ACTB	02281		150	TGTTGATAGAATGATGAAAGAAATGAC
					CGTTGACAGTGATGCCAAAAT
Glutathione Synthase	GSS	05202	6.4.2.3	86	AGTAAGTGTTAAGATGGATGGATGT
					AGTAGTCTTTGGCTTGGTTCAC

Each experimental gene and our reference gene were tested using these primer pairs. Isotig # refers to the location of the sequence in our EST library. EC is the enzyme commission number (if applicable). Glutathione Synthase was ultimately excluded from our RT-PCR experiments.

qPCR primer controls

Primer pair efficiency was assessed using a relative standard curve method (design described in detail in the Applied Biosystems technical note (53)). Briefly, we pooled cDNA from a representative from each treatment to ensure representation of all genes. We then performed a four-fold dilution series [1, 1:4, 1:16, 1:64, 1:256, 1:1024, 1:4096] to ensure that the efficiency of the primers were precise across a sufficient working range (approximately a 12 cycle qPCR range). Thus, Ct values from approximately 18-30 were verified through our dilution series. Each primer pair was assayed in triplicate over the entire dilution series. Results of primer efficiency and significance can be found in **Table 4.2**. Precision of the primers was determined to be strong in all primer sets (all $R^2 > 0.98$). However, the efficiency of Glutathione Synthase (GSS) was found to be out of the acceptable efficiency range of 80% to 120% (54). To avoid primer bias therefore, GSS was excluded from further qPCR studies to avoid primer bias. In addition, each primer pair was additionally tested to confer a single product using dissociation (melt) curve analysis (a gradual denaturation from 55°C to 95°C is continually monitored; a single peak signifies a single PCR product). All remaining primer pairs were found to contain a single melting peak. Finally, a no-template control (NTC), in which no cDNA is added to the reaction mix, was run for each primer set under identical conditions to verify no amplification due to contamination or primer dimers.

Table 4.2: Primer efficiencies

Gene	Std Curve Slope	R^2	Eff. (%)
GPX1	Y = -3.539*LOG(X) + 39.39	0.995	105.4
GPX4	Y = -3.186*LOG(X) + 40.95	0.992	106
GSR	Y = -2.931*LOG(X) + 43.74	0.981	119.4
CAT	Y = -3.256*LOG(X) + 43.97	0.982	102.8
SOD	Y = -3.273*LOG(X) + 41.23	0.998	102.1
B-Actin	Y = -3.539*LOG(X) + 39.39	0.998	91.7
GSS	Y = -3.539*LOG(X) + 39.39	0.993	**130.4**

Efficiencies of each primer pair used in our data set are listed here. Slope equations were used to normalize for primer efficiency differences across an unknown range of initial RNA concentrations in our experimental samples. We considered Primer Efficiency% between 80and 120 to be reliable as demonstrated in ((54):Table 3). GSS was outside this range and was excluded from further experimentation.

qPCR assay design

Each 20µl reaction was set up using Quanta PerfeCTa SYBR Green FastMix (Gaithersburg, MD) with Low ROX – a passive reference dye. Experimental primers were added to a final concentration of 300nM. All real time PCR experiments were completed using a Mx3005P thermal cycler (Strategene, Santa Clara, CA). Each biological sample was analyzed over three technical replicates to allow for statistical analysis. The samples were initially denatured for 3 minutes at 95°C, and then 40 cycles were completed with a 2-step thermal profile of 15 seconds 95°C denaturation, 60 seconds annealing and elongation at 60°C. The threshold cycle (Ct) value was automatically selected by the software for each plate. A subsequent melt curve from 55°C to 95°C was also completed for each experimental replicate to verify the fidelity of the reaction.

There are two methods for relative quantification of samples in RT-PCR: the comparative Ct (ΔΔCt) method (55) and the relative standard curve method (54). We chose to analyze our data using the relative standard curve because it accounts for differences in efficiency values and

starting RNA concentrations by using mathematical corrections based on the relative slopes of the primers. Although this method is more involved in the analysis, it allows for accurate comparisons even at very low expression level differences between genes (53).

Data analysis

To determine expression level differences in antioxidant genes between control and treatment temperatures, a series of normalization calculations were performed. We followed methods described in Applied Biosystems (53). The Ct values for each of three technical replicates were averaged and a standard deviation was calculated for each biological sample. Then an internal ratio of experimental Ct / ACTB Ct was calculated and a standard deviation of the quotient was determined. Next for each experimental treatments, the four biological replicates were averaged and their standard deviation quotients were pooled. A second ratio was determined for each gene comparing the expression under thermal stress to the 30°C control, and a second order standard deviation was determined for this quotient. This final average and standard deviation, along with the variation found in our reference gene (ACTB), were used to build our figure plots. In addition, we performed an unpaired T-test on between experimentally treated biological replicates (prior to pooling standard error) between comparing experimental response to control (45°C or 50°C versus 30°C) and between each other (45°C versus 50°C), assuming unequal variance (Welch's T-test) (56).

Results

Our experiments maintained *P. sulfincola* at two treatment temperatures (45°C and 50°C) for 10 hours each. All worms survived the 45°C treatment for the duration of the experiment. There was 100% survival up to 3 hours in 50°C, however there was 33% (2 of 6) mortality by 4 hours, and 100% (6 of 6) mortality by 6 the six hour treatment. This is consistent with previous literature (57-58) as well as our own previous findings (**Figure 2.1**). Thus these temperatures

allow for a comparison in *P. sulfincola* between a chronic survival (45°C) and acute survival (50°C).

We examined the gene expression response of 5 genes (**Table 4.1**) that code for the transcription of antioxidants or enzymes that act on antioxidants. The two purposes of this experiment were to identify any gene expression shifts during thermal stress over a short time frame that differ significantly from our control sample (45°C or 50°C versus 30°C) and to compare responses between chronic and acute thermal profiles (45°C versus 50°C). In addition, I evaluated these data in relation to our proteomic dataset developed in chapter two, to determine if any of the shifts correspond to or conflict with our previous findings. To that end, **Table 4.3** extracts Pr(DE) values for GPX1, GPX4, SOD, and GSR from our proteomic data in chapter two. If gene expression matches protein response in our experiment, we would expect to see an upregulation of GPX1 and GSR, and no significant expression change in SOD and GPX4. We did not detect CAT in our protein dataset, and therefore cannot make a prediction for this gene. Based on our previous results (**Figure 2.1**) we chose 30°C as a biologically relevant control. It is a temperature well within the range of thermal tolerance for *P. sulfincola*, and because of its utility in comparing results to previous proteomic work conducted at the same temperature.

Table 4.3: Proteomic Response

Gene Name	Isotig #	Pr (DE)
Glutathione Reductase	17409	0.9999
Glutathione Peroxidase 1	29428	0.9888
Glutathione Peroxidase 4	06856	0.0810
Superoxide Dismutase	11194	0.0281

Pr(DE) means probability of differential expression, from our proteomic analysis. The Pr(DE) values are built from values obtained in chapter two.

Table 4.4 shows the response fold change in all five experimental treatments compared to control treatment, with standard deviation of the pooled samples reported for each treatment. It also lists the gene expression shifts between experimental time points. **Figures 4.1-4.5**, cross-referenced to their appropriate gene in **Table 4.4**, show a graphical representation of the gene expression fold changes for each gene. The graphs represent fold change ratio of experimental expression over control, with an average value and pooled standard error determined for each time point at 45°C and 50°C. The standard deviation of the 30°C control sample for each gene is represented by a grey bar across all treatments. While we observe pronounced fold change in many treatments are present in our data set, the two-tailed unpaired Welch's T-test for unequal sample variation only found one significant ($p<0.05$) expression difference between an experimental treatment and control–downregulation of CAT after 10 hours at 45°C. Additionally, no significant fold differences were determined between experimental treatments (45°C versus 50°C). It is still informative, however, to analyze observed expression fold changes in our data.

In general, at 45°C, there appears to be a consistent trend for increased expression of each antioxidant until the 3 hour time point, followed by a return to control levels or even downregulation at 10 hours (**Table 4.4**). GPX1 expression (**Figure 4.1**) increases between hour 1 (0.826 ± 0.228) and hour 3 (1.740 ± 0.235), but returns to the original level (0.907 ± 0.115) by 10 hours. GPX4 expression (**Figure 4.2)** at 45°C follows the same pattern to a greater magnitude. GPX4 appears to be downregulated at 1 hour (0.394 ± 0.072), and then dramatically upregulated at 2 hours (4.047 ± 0.653), maintained at 3 hours (4.060 ± 0.593), and again returns to the first expression level (0.515 ± 0.080) by 10 hours. GSR follows the same pattern, but the data is less reliable because the Ct values of GSR were consistently lower than the other genes, suggesting that this is a low-abundance gene over all treatments. SOD showed the most dramatic response of all genes, although again internal variance kept the p-value slightly above 0.05. SOD expression increased from 0.897 (± 0.343) at 1hour to 13.654 (± 1.446) at 3 hours and returns to 0.370 (± 0.049) by 10 hours. Finally, CAT showed the only significant change of the experiment,

Table 4.4: Gene expression fold change of experimental treatments

	45°C							50°C					30°C	
	1h	**2h**	**3h**	**10h**	**1→2**	**2 →3**	**3→10**	**1h**	**2h**	**3h**	**1 → 2**	**2 → 3**	**--**	**Fig. #**
GPX1	0.826	1.240	1.740	0.907	1.502	1.403	0.521	1.467	0.804	1.562	0.548	1.942	1.000	**4.1**
SD	0.228	0.156	0.235	0.115				0.255	0.101	0.418			0.135	
GPX4	0.394	4.047	4.060	0.515	10.283	1.003	0.127	1.311	1.853	1.350	1.414	0.729	1.000	**4.2**
SD	0.072	0.653	0.593	0.080				0.206	0.205	1.317			0.144	
GSR	0.486	0.968	1.255	0.732	1.991	1.296	0.583	1.077	0.483	0.303	0.449	0.628	1.000	**4.3**
SD	0.182	0.209	0.263	0.154				0.286	0.130	0.203			0.283	
SOD	0.897	1.722	13.654	0.370	1.920	7.929	0.027	1.200	3.291	1.020	2.742	0.310	1.000	**4.4**
SD	0.343	0.232	1.446	0.049				0.202	0.263	0.229			0.106	
CAT	0.962	1.690	1.817	**0.459**	1.757	1.075	0.253	1.456	0.799	0.614	0.549	0.768	1.000	**4.5**
SD	0.218	0.196	0.508	0.079				0.297	0.191	0.315			0.097	

This table shows the ratio of expression of four pooled experimental samples to four pooled control samples (1h, 2h, 3h, 10h). Pooled standard deviation is reported. Bold number indicates significant fold-change ($p<0.05$) in relation to control (30°C). In addition, ratio of fold change within the experimental treatments is shown. This is the fold change when going from one time point to the next (i.e. Δ 2h/1h). Figure # refers to the appropriate graphical representation of expression fold change for each gene.

Figure 4.1: Glutathione peroxidase 1 gene response

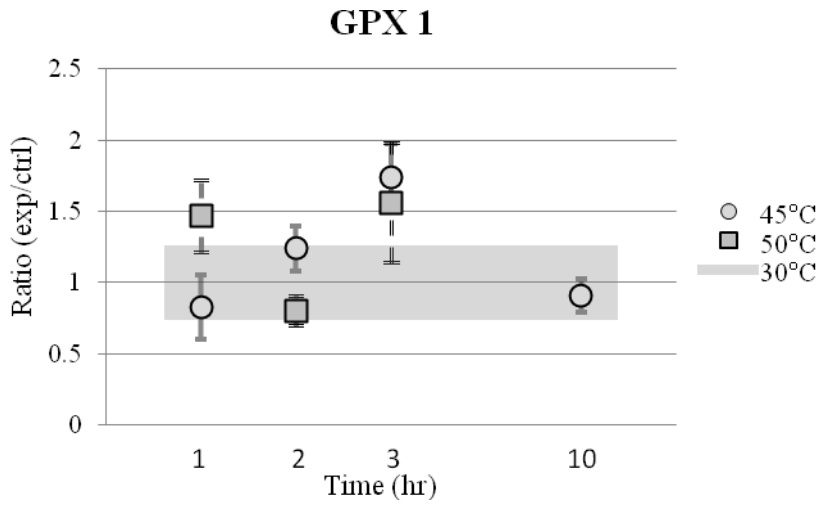

Figure 4.2: Glutathione peroxidase 4 gene response

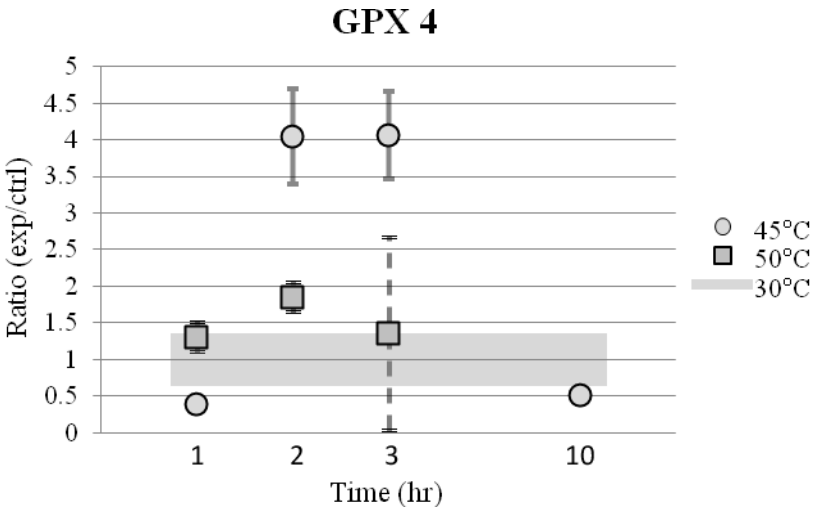

Figure 4.3: GSR expression

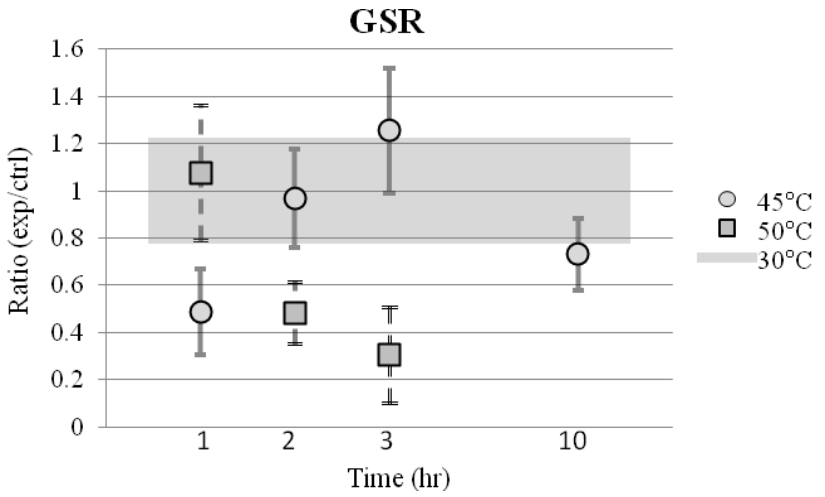

Figure 4.4: SOD expression

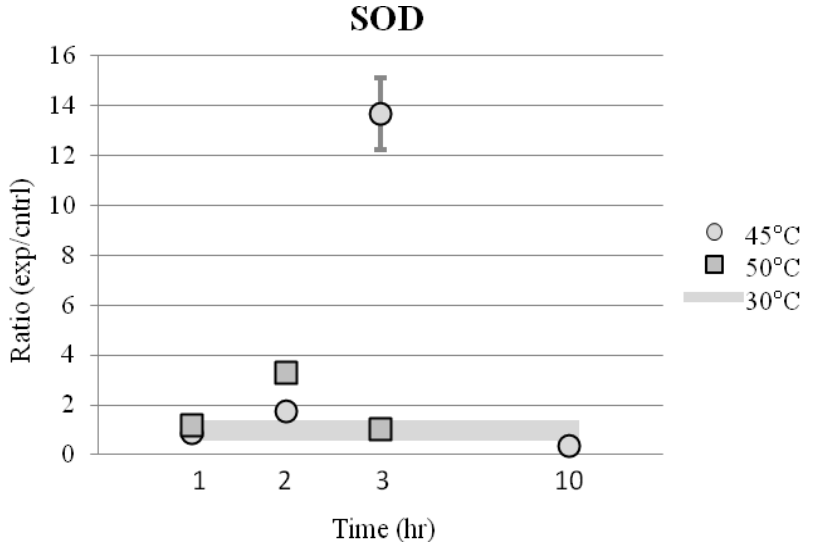

Figure 4.5- CAT expression

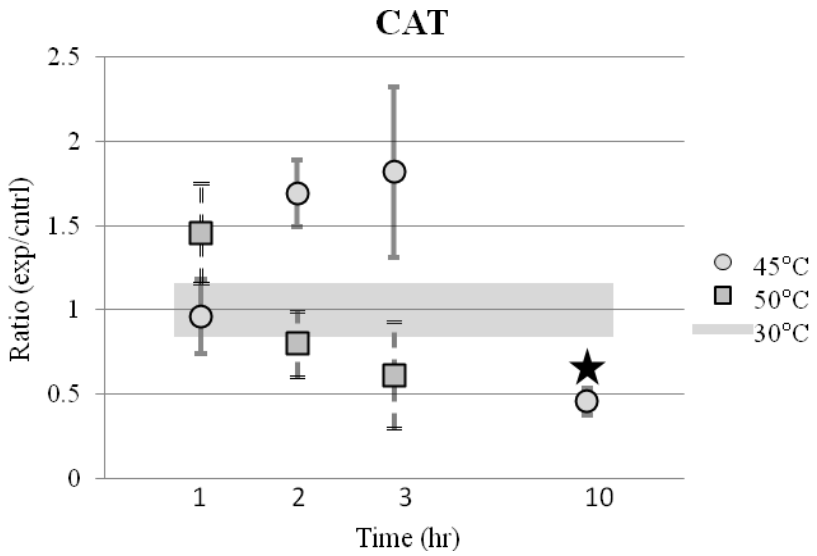

Figures 4.1-4.5 show the fold change over time for each of five antioxidant genes between *P. sulfincola* maintained at 30ºC and those at elevated temperatures (45ºC and 50ºC). The star represents a significant decrease in expression compared to the control (30°C) value.

comparing 10hr treatment (0.459 ± 0.079) to control values 1 (± 0.097). It followed the same increase until 3 hour treatment (1.817 ± 0.508) as the rest of the genes demonstrated. There is no discernible pattern at 50°C. Expression of GPX1 and GPX4 are inversely related, GSR and CAT are downregulated by 3 hours, and SOD shows a spike at 2 hours (3.291 ± 0.263), while 1 and 3 hour treatments closely represent the control (1.200 ± 0.202, 1.020 ± 0.106 respectively).

Discussion

The purpose of our experiment was to measure gene expression response to acute oxidative stress in the highly thermotolerant *Paralvinella sulfincola*. When an organism undergoes periods of thermal stress, a number of cellular metabolic shifts occur including the increase of both exogenous and endogenous sources of ROS that must be managed to avoid oxidative damage to DNA, RNA, or lipids. A suite of antioxidant responses have been identified that combat this increase in oxidative stress (15, 18, 22). A significant body of literature has discussed the effects of superoxide dismutase, catalase, and glutathione cycling on ROS formation and propagation. However, our study represents the first experimental data of antioxidant gene responses within a highly thermotolerant organism. In addition, it is one of only a few experiments that explore antioxidant gene response over a time series of continual thermal treatment, due to the preference for microarray study of thermal response, and the limitations and expense that accompany that technology.

Our data demonstrate that *Paralvinella sulfincola* respond differently at 45°C than they do at 50°C. There appears to be a universal, coordinated regulation of antioxidant gene expression at 45°C, while there appears to lack any pattern of expression in response to 50°C (**Table 4.4**). 45°C was chosen as a temperature that approaches but not surpass the chronic lethal maximum (CL_{Max}) in *P. sulfincola* ((58), **Figure 2.1**). Thus, it is likely that the animal is maintaining stable metabolic function. There is still a thermal stress applied, and the antioxidant machinery is engaged, but the response is systematic and temporary; gene expression peaked at 3

hours in all experimental tests, and then shifted down to or even below control expression at 10 hours. This is not observed at 50°C, however, a temperature above the CL_{Max} but below the acute critical thermal tolerance maximum (CT_{Max}). We do not have a 50°C time point at 10 hours because there is no *P. sulfincola* survival after 6 hours at 50°C. Still, our data may point to metabolic dysfunction occurring within the first three hours of treatment at 50°C.

Our gene expression experiment contributes to the recent, but growing pool of data concerning the response of antioxidant responses to thermal stress. Because a majority of heat stress experiments have focused on expression levels of molecular chaperones, antioxidant gene response studies have not emerged until recently. Previous research has suggested that RNA transcription may decrease as part of a global metabolic depression (7, 59). At 50°C , worm's decreased expression of 4 of the 5 antioxidant genes measured from 2hr → 3 hr; in fact, two genes are downregulated at 3 hours, as compared to control (GSR and CAT) . Thus, *P. sulfincola* may indeed be reducing their metabolism at 50°C as a method for survival as long as possible or until the stress is removed (through reducing the amount of endogenous ROS created during heat stress). We will however, need to conduct further tests of enzymatic activity and metabolic gene expression on our acutely stressed (50°C) organisms to assess if this is the case. Additionally, while our trends are promising, we acknowledge that individual variations still account for a large portion of the total variance, causing there to be little in the way of statistically significant trends. Because further collections are not feasible from a vent environment, we will incorporate additional reference genes to reduce levels of error in further iterations of this analysis. Previous studies have identified α-tubulin and ubiquitin as alternate choices for reference genes, as they vary little in response to temperature (60).

In a study of expression responses in the pacific oyster *Crassostrea gigas* (40), the authors compared a control group (13°C) to a sub-CL_{Max} temperature (25°C) continuously for 24 days, sampling six times within the time period. They did identify a glutathione peroxidase which was significantly upregulated at 3 and 7 days which then returned to control expression for

the remainder of the experiment. However, in a separate study of deep sea shrimp (*Rimicaris exoculata*, not thermotolerant), glutathione peroxidase was found to be slightly downregulated with increasing temperature (41). Our 45°C data is consistent with the oyster dataset, albeit on a shorter timescale of hours, not days. This type of response indicates an below the CL_{Max}, *P. sulfincola* can react to a stress, regulate the amount of mRNA pool needed for protein translation, and then return to homeostatic levels after the response period is complete.

It is important to note, however, that a larger mRNA pool does not always translate to a larger protein pool. This is evidenced by the fact that even though all five antioxidant genes were upregulated at 3 hours of 45°C, they do not consistently match our proteomic findings from chapter 2 (**Table 4.3**). Our proteomic data showed an increase in GPX1 and GSR but no change in SOD and GPX4 (Catalase was not found in our proteomic dataset). Thus it is important to keep in mind that RNA expression pools may be replacing damaged nucleotide messages, or providing material for the continual production and use of a protein. This would mean that the flux in the system was high, but that the absolute value of each protein would remain steady.

Ultimately, our findings of the differential gene expression response in an extremely thermotolerant metazoan can be used to inform models in other systems. We demonstrated a difference in the production of antioxidants between a population of chronically stressed versus an acutely stressed group. While expression levels are all relative, it is the trend that is important. If an organism is to survive in its environment continually, it must be able to reach equilibrium with its surroundings. This concept is especially important when viewed in the context of climate change. As global temperatures increase, organisms (especially marine) will face thermal regimes outside of their evolved tolerance ranges. Determining at what temperature in sensitive, keystone species (e.g. corals) expression profiles switch from adaptive response (resembling *P. sulfincola* 45°C treatment) to metabolic depression (resembling *P. sulfincola* 50°C treatment) will be an important step towards understanding the effects that global warming will have on marine life.

We hope this research will inform further antioxidant response studies on a range of systems from sensitive (coral bleaching) to robust (hydrothermal vent endemic) organisms.

REFERENCES

1. Hochachka PW, Somero GN. Biochemical adaptation: mechanism and process in physiological evolution: Oxford University Press, USA; 2002.

2. Hendersen RW, Graham JA. Avoidance of heat by rats: Effects of thermal context on rapidity of extinction 1, 2. Learning and Motivation. 1979;10(3):351-63.

3. Wittenburg N, Baumeister R. Thermal avoidance in *Caenorhabditis elegans*: an approach to the study of nociception. Proc Natl Acad Sci U S A. 1999 Aug 31;96(18):10477-82.

4. Wilmore DW, Long JM, Mason Jr AD, Skreen RW, Pruitt Jr BA. Catecholamines: mediator of the hypermetabolic response to thermal injury. Annals of surgery. 1974;180(4):653.

5. Feder ME, Hofmann GE. Heat-shock proteins, molecular chaperones, and the stress response: evolutionary and ecological physiology. Annu Rev Physiol. 1999;61:243-82.

6. Anestis A, Lazou A, Portner HO, Michaelidis B. Behavioral, metabolic, and molecular stress responses of marine bivalve *Mytilus galloprovincialis* during long-term acclimation at increasing ambient temperature. Am J Physiol Regul Integr Comp Physiol. 2007 Aug;293(2):R911-21.

7. Boutet I, Tanguy A, Le Guen D, Piccino P, Hourdez S, Legendre P, et al. Global depression in gene expression as a response to rapid thermal changes in vent mussels. Proceedings of the Royal Society B: Biological Sciences. 2009;276(1670):3071.

8. Biggers BG, Geisert R, Wetteman R, Buchanan D. Effect of heat stress on early embryonic development in the beef cow. J Anim Sci. 1987;64(5):1512.

9. Lindquist S. The heat-shock response. Annu Rev Biochem. 1986;55:1151-91.

10. Daugaard M, Rohde M, Jaattela M. The heat shock protein 70 family: Highly homologous proteins with overlapping and distinct functions. FEBS Lett. 2007 Jul 31;581(19):3702-10.

11. Abele D, Heise K, Portner H, Puntarulo S. Temperature-dependence of mitochondrial function and production of reactive oxygen species in the intertidal mud clam *Mya arenaria*. J Exp Biol. 2002;205(13):1831-41.

12. Heise K, Puntarulo S, Portner HO, Abele D. Production of reactive oxygen species by isolated mitochondria of the Antarctic bivalve *Laternula elliptica* (King and Broderip) under heat stress. Comp Biochem Physiol C Toxicol Pharmacol. 2003 Jan;134(1):79-90.

13. Keller M, Sommer AM, Portner HO, Abele D. Seasonality of energetic functioning and production of reactive oxygen species by lugworm (*Arenicola marina*) mitochondria exposed to acute temperature changes. J Exp Biol. 2004 Jun;207(Pt 14):2529-38.

14. Park H, Ahn I, Park K, Hyun S. Response of antioxidant defence systems to thermal stress in the Antarctic clam *Laternula elliptica*. Antarctic Science. 2008;20(06):521-6.

15. Lesser MP. Oxidative stress in marine environments: biochemistry and physiological ecology. Annu Rev Physiol. 2006;68:253-78.

16. Portner HO. Climate variations and the physiological basis of temperature dependent biogeography: systemic to molecular hierarchy of thermal tolerance in animals. Comp Biochem Physiol A Mol Integr Physiol. 2002 Aug;132(4):739-61.

17. Abele D, Puntarulo S. Formation of reactive species and induction of antioxidant defence systems in polar and temperate marine invertebrates and fish. Comp Biochem Physiol A Mol Integr Physiol. 2004 Aug;138(4):405-15.

18. Starkov AA. Protein-mediated energy-dissipating pathways in mitochondria. Chem Biol Interact. 2006 May 15;161(1):57-68.

19. Halliwell B, Gutteridge JMC. Free radicals in biology and medicine: Clarendon Press Oxford; 1989.

20. Bonekamp NA, Völkl A, Fahimi HD, Schrader M. Reactive oxygen species and peroxisomes: struggling for balance. Biofactors. 2009;35(4):346-55.

21. Michiels C, Raes M, Toussaint O, Remacle J. Importance of SE-glutathione peroxidase, catalase, and CU/ZN-SOD for cell survival against oxidative stress. Free Radical Biology and Medicine. [doi: 10.1016/0891-5849(94)90079-5]. 1994;17(3):235-48.

22. Hayes JD, McLellan LI. Glutathione and glutathione-dependent enzymes represent a co-ordinately regulated defence against oxidative stress. Free radical research. 1999;31(4):273-300.

23. Dringen R. Metabolism and functions of glutathione in brain. Prog Neurobiol. 2000 Dec;62(6):649-71.

24. Pastore A, Federici G, Bertini E, Piemonte F. Analysis of glutathione: implication in redox and detoxification. Clin Chim Acta. 2003 Jul 1;333(1):19-39.

25. Andreyev AY, Kushnareva YE, Starkov AA. Mitochondrial metabolism of reactive oxygen species. Biochemistry (Mosc). 2005 Feb;70(2):200-14.

26. Chen Z, Lash LH. Evidence for mitochondrial uptake of glutathione by dicarboxylate and 2-oxoglutarate carriers. J Pharmacol Exp Ther. 1998 May;285(2):608-18.

27. Mills GC. Hemoglobin catabolism. I. Glutathione peroxidase, an erythrocyte enzyme which protects hemoglobin from oxidative breakdown. J Biol Chem. 1957 Nov;229(1):189-97.

28. Flohe L, Gunzler WA, Schock HH. Glutathione peroxidase: a selenoenzyme. FEBS Lett. 1973 May 15;32(1):132-4.

29. Herbette S, Roeckel-Drevet P, Drevet JR. Seleno-independent glutathione peroxidases. More than simple antioxidant scavengers. FEBS J. 2007 May;274(9):2163-80.

30. Chance B, Sies H, Boveris A. Hydroperoxide metabolism in mammalian organs. Physiol Rev. 1979 Jul;59(3):527-605.

31. Seiler A, Schneider M, Forster H, Roth S, Wirth EK, Culmsee C, et al. Glutathione peroxidase 4 senses and translates oxidative stress into 12/15-lipoxygenase dependent- and AIF-mediated cell death. Cell Metab. 2008 Sep;8(3):237-48.

32. Yant LJ, Ran Q, Rao L, Van Remmen H, Shibatani T, Belter JG, et al. The selenoprotein GPX4 is essential for mouse development and protects from radiation and oxidative damage insults. Free Radical Biology and Medicine. 2003;34(4):496-502.

33. Mittler R. Oxidative stress, antioxidants and stress tolerance. Trends in plant science. 2002;7(9):405-10.

34. Heise K, Puntarulo S, Nikinmaa M, Abele D, Pörtner HO. Oxidative stress during stressful heat exposure and recovery in the North Sea eelpout *Zoarces viviparus* L. J Exp Biol. 2006;209(2):353.

35. Parihar MS, Javeri T, Hemnani T, Dubey AK, Prakash P. Responses of superoxide dismutase, glutathione peroxidase and reduced glutathione antioxidant defenses in gills of the freshwater catfish (*Heteropneustes fossilis*) to short-term elevated temperature. Journal of Thermal Biology. 1997;22(2):151-6.

36. Ding H, Zhou B, Liu L, Cheng S. Oxidative stress and metallothionein expression in the liver of rats with severe thermal injury. Burns. 2002;28(3):215-21.

37. Lockwood BL, Sanders JG, Somero GN. Transcriptomic responses to heat stress in invasive and native blue mussels (genus *Mytilus*): molecular correlates of invasive success. J Exp Biol. 2010;213(20):3548.

38. Enjalbert B, Nantel A, Whiteway M. Stress-induced gene expression in *Candida albicans*: absence of a general stress response. Molecular biology of the cell. 2003;14(4):1460.

39. Desalvo M, Voolstra C, Sunagawa S, Schwarz J, Stillman J, Coffroth MA, et al. Differential gene expression during thermal stress and bleaching in the Caribbean coral *Montastraea faveolata*. Molecular ecology. 2008;17(17):3952.

40. Meistertzheim AL, Tanguy A, Moraga D, Thebault MT. Identification of differentially expressed genes of the Pacific oyster *Crassostrea gigas* exposed to prolonged thermal stress. FEBS J. 2007 Dec;274(24):6392-402.

41. Cottin D, Shillito B, Chertemps T, Tanguy A, Léger N, Ravaux J. Identification of differentially expressed genes in the hydrothermal vent shrimp *Rimicaris exoculata* exposed to heat stress. Marine Genomics. 2010;3:71-8.

42. Chomczynski P, Sacchi N. Single-step method of RNA isolation by acid guanidinium thiocyanate-phenol-chloroform extraction. Analytical biochemistry. 1987;162(1):156-9.

43. Simms D, Cizdziel PE, Chomczynski P. TRIzol: A new reagent for optimal single-step isolation of RNA. Focus. 1993;15(4):99-102.

44. Bustin SA. Absolute quantification of mRNA using real-time reverse transcription polymerase chain reaction assays. J Mol Endocrinol. 2000 Oct;25(2):169-93.

45. Bustin SA. Quantification of mRNA using real-time reverse transcription PCR (RT-PCR): trends and problems. J Mol Endocrinol. 2002 Aug;29(1):23-39.

46. Huggett J, Dheda K, Bustin S, Zumla A. Real-time RT-PCR normalisation; strategies and considerations. Genes Immun. 2005 Jun;6(4):279-84.

47. Ransbotyn V, Reusch TBH. Housekeeping gene selection for quantitative real-time PCR assays in the seagrass *Zostera marina* subjected to heat stress. Limnology and Oceanography: Methods. 2006;4:367-73.

48. Suzuki T, Higgins PJ, Crawford DR. Control selection for RNA quantitation. Biotechniques. 2000 Aug;29(2):332-7.

49. Nicot N, Hausman JF, Hoffmann L, Evers D. Housekeeping gene selection for real-time RT-PCR normalization in potato during biotic and abiotic stress. J Exp Bot. 2005 Nov;56(421):2907-14.

50. Haller F, Kulle B, Schwager S, Gunawan B, Heydebreck A, Sultmann H, et al. Equivalence test in quantitative reverse transcription polymerase chain reaction: confirmation of reference genes suitable for normalization. Analytical biochemistry. 2004;335(1):1-9.

51. Rozen S, Skaletsky H. Primer3 on the WWW for general users and for biologist programmers. Methods Mol Biol. 2000;132(3):365-86.

52. Altschul SF, Gish W, Miller W, Myers EW, Lipman DJ. Basic local alignment search tool. J Mol Biol. 1990 Oct 5;215(3):403-10.

53. Biosystems A. Guide to Performing Relative Quantitation of Gene Expression Using Real-Time Quantitative PCR. Applied Biosystems. 2008.

54. Pfaffl MW. A new mathematical model for relative quantification in real-time RT–PCR. Nucleic acids research. 2001;29(9):e45.

55. Livak KJ, Schmittgen TD. Analysis of relative gene expression data using real-time quantitative PCR and the 2-ΔΔ CT method. Methods. 2001;25(4):402-8.

56. Welch BL. The generalization of "Student's" problem when several different population variances are involved. Biometrika. 1947 January 1, 1947;34(1-2):28-35.

57. Lee RW. Thermal tolerances of deep-sea hydrothermal vent animals from the Northeast Pacific. Biol Bull. 2003 Oct;205(2):98-101.

58. Girguis PR, Lee RW. Thermal preference and tolerance of alvinellids. Science. 2006 Apr 14;312(5771):231.

59. Storey KB, Storey JM. Metabolic rate depression in animals: transcriptional and translational controls. Biol Rev Camb Philos Soc. 2004 Feb;79(1):207-33.

60. Pantile R, Webster N. Strict thermal threshold identified by quantitative PCR in the sponge *Rhopaloeides odorabile*. Marine Ecology Progress Series. 2011;431:97-105.

Chapter 5

Conclusions

Stress (n): Constraining force or influence: as a state resulting in one of bodily or mental tension resulting from factors that tend to alter an existent equilibrium (1).

Every living being experiences stress, and to survive, every living being has evolved tolerances to environmental stressors. The most universal abiotic influence is temperature, and thus, thermotolerance, adaptations and response to thermal variation, is a fundamental factor shaping evolution. In fact, the most highly conserved protein by far is the molecular chaperone Heat Shock Protein 70kDa, responsible for correctly folding proteins during periods of thermal and other stress (2). Evolved mechanisms of thermotolerance including antifreeze proteins in notothenioid fish (3), cryptobiosis in tardigrades (4), and additional hyperthermostable proteins in extremophilic archaea (5), allow many organisms to inhabit a wide variety of stressful thermal environments, from < -2°C to > 120°C.

Since the first modern thermal physiology experiments conducted nearly 100 years ago on anesthetized goldfish (6), we have learned a great deal about the physiological and biochemical limits to thermal ranges in both eukaryotes and prokaryotes. While prokaryotes are able to maintain growth at temperatures well over 100°C, sustained eukaryotic thermal tolerance has repeatedly found a limit below 50°C. As discussed in chapter 1, although authors have offered many reasons for this eukaryotic limit including protein misfolding, mitochondrial dysfunction, oxidative damage, and membrane instability, the exact causes remain unclear. To

date, almost all studies have looked at thermotolerance and causes of thermal stress in mesotolerant eukaryotes. However, to determine the precise physiological and biochemical limiters, it is imperative to study an organism whose upper thermal limit approaches that of all eukaryotes. Recent studies of *Paralvinella sulfincola* have found just that, a thermophilic hydrothermal vent polychaete which demonstrates a sustained survival range from 4 to >45°C and acute survival up to 60°C (7-8). This study system is made even more attractive because of the existence of a mesotolerant congener, *P. palmiformis,* which inhabits the same environment and has a sustained upper limit of approximately 39°C with acute tolerance to < 45°C (**Figure 2.1**). Utilizing the comparative power of this system, the primary goal of my thesis was to identify and understand the fundamental limits to eukaryotic thermotolerance.

I participated in a series of cruises on the *R/V* Atlantis from 2007 to 2010 to collect the samples and conduct the necessary experiments for this project. The organisms were recovered alive using the *DSV Alvin*, and all experiments were conducted onboard using a flow-through high pressure respirometry system (**Figure 2.6**) that maintained the worms in at *in situ* pressure. All together a total of 1366 worms were experimentally treated, varying the parameters of temperature, pH, sulfide concentration, and duration. A portion of these experiments included concurrent measurements of aerobic respiration rate using a dissolved oxygen probe. Further molecular analyses included a transcriptomic library built *via* pyrosequencing, a LC-MS/MS comparative proteomic database, enzymatic assays, and quantitative PCR. These investigations around thermotolerance in *Paralvinella sulfincola* built a thesis that centers on oxidative stress, synergistic stressors, and antioxidant response.

Chapter two focused on comparing the proteomic profile of *Paralvinella sulfincola* to *Paralvinella palmiformis* under a variety of thermal regimes. Many systems showed a significant regulation with increasing temperature. In *P. palmiformis* heat shock proteins were predictably upregulated; notably, this was not found to be the case in *P. sulfincola*. This was due to the fact that *P. sulfincola* maintained high levels of heat shock proteins across their thermal range. I posit

that this is a crucial element of their thermotolerance, because *P. sulfincola* do not experience a lag time of gene expression and translation to produce necessary heat shock proteins if their environment changes. Because the worms reside nearest to the hot vent effluent (9) and vent currents can shift quickly and unpredictably (10), this adaptation is central to their cellular stress response. However, the analysis does support the previously stated theory that oxidative stress is linked to thermal stress (11-13). As the temperature increased, both species showed differential expression of antioxidant (specifically glutathione) cycling.

The second investigation, reported in chapter three, focused on understanding the interplay between temperature, pH and sulfide on oxygen respiration rates in *P. sulfincola.* Animals living on and around vents experience multiple concurrent abiotic stresses including acidic pH as low as 2.8 and high levels of sulfide concentrations (10, 14). By varying temperature, pH, and sulfide, I was able to examine the unaccompanied and combinatory effects of these three influences. Predictably, respiration differences between temperatures (30 and 45°C) matched previously determined Q_{10} values (15). The results showed a comparable increase in aerobic respiration (~3x) in response to individual shifts in acidic pH (8.0 →6.0) or sulfide concentration (0-250μM). However, when both pH and sulfide stresses were applied, the result was not simply additive in effect, it was a 20-fold increase in respiration rate. To explain this result, I determined intracellular non-bicarbonate buffering capacity and internal concentrations of sulfide at different treatments in *P. sulfincola*, and I matched these data with known values of H^+/ATP exchanges, sulfide uptake and detoxification rates. I determined that the cause of this discrepancy was an emergent synergistic effect, known as a multistress effect, for two primary reasons. First, lower pH altered the dominant species of sulfide in seawater from HS^- to the more permeable, more toxic species H_2S. Second, the increase in internal sulfide increases the amount of H^+ ions that must be exchanged due to the sulfide detoxification pathway, increasing the ATP and therefore aerobic respiratory cost to the animal. Accounting for these shifts, our value was within the predicted range.

Finally, chapter four expounded on the findings in chapter two by investigating the antioxidant gene response to thermal stress in *P. sulfincola*, to understand regulation at the RNA level. This was the first chapter to compare the effects of a chronic thermal stress (45°C - below the chronic lethal max; CL_{Max} (16)) to an acute stress (50°C - between the CL_{Max} and the critical thermal max; CT_{Max} (17)). I used a time series to detail the regulation over time of five antioxidant genes (superoxide dismutase - SOD, catalase - CAT, glutathione peroxidase 1 - GPX1, glutathione peroxidase 4 - GPX4, and glutathione reductase - GSR). Using relative quantification qPCR normalized to beta-actin (ACTB), I determined that there was a similar inducible upregulation (albeit lacking statistical significance to $p < 0.05$) of all five genes. This contrasted with the profile at 50°C which showed no correlative regulation. This gene expression data supports the observation that *P. sulfincola* is beyond its sustainable thermal limit by 50°C, because at that treatment, it lacks the capability to respond appropriately to oxidative stress by upregulating antioxidant genes.

From this research, the first to quantify global protein and antioxidant responses to temperature in an extremely thermotolerant eukaryote, three primary conclusions can be reached – 1) pronounced thermal tolerance in *P. sulfincola* is likely enabled by its constitutive expression of heat shock proteins and limited by its ability to quickly and appropriately respond to the commensurate increase in oxidative stress, 2) this thermal tolerance limit is likely negatively affected by synergistic multistress effects, and 3) antioxidant gene expression response differs significantly between chronically and acutely stressed treatments, supporting the theory that oxidative stress is limiting in this system. These findings are applicable to other current areas of stress tolerance response: climate change and ocean acidification. Comparisons between sensitive (i.e. corals) and thermotolerant (*P. sulfincola*) eukaryotes can provide insight into what biomolecular responses are lacking in vulnerable systems. The development of appropriate metrics (e.g. antioxidant gene expression profiles) to determine if a sensitive organism has exceeded its CL_{Max} will allow for an accurate appraisal of ecosystem health and sustainability.

Knowledge of emergent multistress effects can inform research on ocean acidification, a growing triple threat to marine life of increased CO_2, increased temperature and decreased pH. Finally, I suggest that oxidative stress response be more carefully studied across a broad spectrum of eukaryotes, as it may ultimately be a limiting stress across many eukaryotic species.

REFERENCES

1. Merriam-Webster Inc. The Merriam-Webster dictionary. Springfield, Mass.: Merriam-Webster; 2005.

2. Daugaard M, Rohde M, Jäättelä M. The heat shock protein 70 family: highly homologous proteins with overlapping and distinct functions. FEBS letters. 2007;581(19):3702-10.

3. Davies PL, Hew CL. Biochemistry of fish antifreeze proteins. The FASEB Journal. 1990;4(8):2460.

4. Reuner A, Hengherr S, Mali B, Förster F, Arndt D, Reinhardt R, et al. Stress response in tardigrades: differential gene expression of molecular chaperones. Cell Stress and Chaperones. 2010;15(4):423-30.

5. Unsworth LD, Van Der Oost J, Koutsopoulos S. Hyperthermophilic enzymes- stability, activity and implementation strategies for high temperature applications. FEBS Journal. 2007;274(16):4044-56.

6. Ege R, Krogh A. On the relation between the temperature and the respiratory exchange in fishes. Internationale Revue der Gesamten Hydrobiologie und Hydrographie. 1914;7(1):48-55.

7. Lee RW. Thermal tolerances of deep-sea hydrothermal vent animals from the Northeast Pacific. Biol Bull. 2003 Oct;205(2):98-101.

8. Girguis PR, Lee RW. Thermal preference and tolerance of alvinellids. Science. 2006 Apr 14;312(5771):231.

9. Sarrazin J, Levesque C, Juniper S, Tivey M. Mosaic community dynamics on Juan de Fuca Ridge sulphide edifices: substratum, temperature and implications for trophic structure. CBM-Cahiers de Biologie Marine. 2002;43(3-4):275-9.

10. Lowell RP, Rona PA, Von Herzen RP. Seafloor hydrothermal systems. Journal of geophysical research. 1995;100(B1):327-52.

11. Abele D, Heise K, Portner H, Puntarulo S. Temperature-dependence of mitochondrial function and production of reactive oxygen species in the intertidal mud clam *Mya arenaria*. J Exp Biol. 2002;205(13):1831-41.

12. Heise K, Puntarulo S, Portner HO, Abele D. Production of reactive oxygen species by isolated mitochondria of the Antarctic bivalve *Laternula elliptica* (King and Broderip) under heat stress. Comp Biochem Physiol C Toxicol Pharmacol. 2003 Jan;134(1):79-90.

13. Keller M, Sommer AM, Portner HO, Abele D. Seasonality of energetic functioning and production of reactive oxygen species by lugworm (*Arenicola marina*) mitochondria exposed to acute temperature changes. J Exp Biol. 2004 Jun;207(Pt 14):2529-38.

14. Douville E, Charlou J, Oelkers E, Bienvenu P, Jove Colon C, Donval J, et al. The Rainbow vent fluids (36 14'N, MAR): the influence of ultramafic rocks and phase separation on trace metal content in Mid-Atlantic Ridge hydrothermal fluids. Chemical Geology. 2002;184(1-2):37-48.

15. Khan M, Ahmed S, Salazar A, Gurumendi J, Khan A, Vargas M, et al. Effect of temperature on heavy metal toxicity to earthworm *Lumbricus terrestris* (Annelida: Oligochaeta). Environmental toxicology. 2007;22(5):487-94.

16. Beitinger TL, Bennett WA, McCauley RW. Temperature tolerances of North American freshwater fishes exposed to dynamic changes in temperature. Environmental Biology of Fishes. 2000;58(3):237-75.

17. Lutterschmidt WI, Hutchison VH. The critical thermal maximum: history and critique. Canadian Journal of Zoology. 1997;75(10):1561-74.